

1992  
1992

**Equivalence of Some System Identification  
Methods That Use Finite Hankel Matrices**

by

**Su-Zu Juang**

A Thesis submitted to  
the Faculty of  
the Graduate School of Engineering and Applied Sciences of  
the George Washington University  
in partial satisfaction of the requirements for the degree of  
Master of Science

May 1992

Thesis directed by  
Dr. Robert H. Tolson



## *Abstract*

This thesis provides a theoretical and experimental comparison between a number of time domain multiple-input multiple-output modal identification methods that are based on the Hankel matrix, specifically, the Eigensystem Realization Algorithm (ERA), Ibrahim Time Domain (ITD) or Multiple-Reference Time Domain (MRTD), and Modified Multiple-Reference Time Domain (MMRTD) methods. In order to accomplish this, basic concepts in system realization theory are reviewed. These include state space representation, discrete-time and continuous-time representations, the Markov parameters, the Hankel matrix, and the observability and controllability grammians. The two published realizations of the ERA method are shown to converge to the input-normal and internally balanced realizations when the Hankel matrix size tends to infinity. An output-normal realization of the ERA is derived as the third natural realization based on the singular value decomposition and it is shown that the three realizations are theoretically identical. The MRTD and MMRTD methods are presented. Real-valued realizations of the MRTD and MMRTD methods, which are traditionally formulated in the complex modal space, are derived. The relationship between the ERA, MRTD, and MMRTD realizations are found. The MRTD and MMRTD realizations are shown to be the same as the output-normal and input-normal realizations of the ERA, respectively. Transformation matrices to convert from one realization to another are formulated. Examples using simulated and actual experimental data are presented to verify these findings and to examine computational differences between methods that are theoretically identical. The simulated system has closely spaced frequencies and mode shapes. Both noise free and noise contaminated cases

are tested. The experimental data are obtained from a flexible structure (HMB-2R). Using double precision MATLAB on an IBM 386 personal computer, the theoretically identical methods are shown to be numerically identical for the cases considered to 11 significant digits.

## TABLE OF CONTENTS

<b>1. Introduction</b>	<b>1</b>
1.1 Overview.....	1
1.2 Thesis Outline.....	3
<b>2. Mathematical Preliminaries</b>	<b>5</b>
2.1 The State Space Representation. ....	5
2.2 Discrete and Continuous Models of a Dynamic System. ....	6
2.2.1 Continuous-Time Models.....	6
2.2.2 Conversion from Continuous to Discrete-Time State Space Model.....	8
2.2.3 Conversion from Discrete to Continuous-Time State Space Model.....	9
2.3 Markov Parameters.....	11
2.3.1 Sampled Response to Impulse Input .....	13
2.3.2 Sampled Response to Unit Pulse Input (Markov Parameters).....	14
2.3.3 Free Decay Response .....	15
2.4 Infinite Hankel Matrix.....	16
2.5 Controllability and Observability Grammians .....	17
2.6 Finite Hankel Matrix.....	18
<b>3. System Realization using Eigensystem Realization Algorithm</b>	<b>21</b>
3.1 Minimal-Dimensional Realizations of the ERA Method by Singular Value Decomposition (SVD).....	21
3.2 Input-Normal Realization of ERA .....	24
3.3 Internally Balanced Realization of ERA.....	26
3.4 Output-Normal Realization of ERA.....	29
3.5 Summary Table .....	31
<b>4. Multiple-Reference Time Domain Method</b>	<b>34</b>
4.1 The Hankel Matrix for MRTD Method.....	35
4.2 MRTD Minimal Realization.....	37
4.2.1 Traditional Development.....	37

4.2.2	Real-Valued Realization of MRTD.....	42
4.3	Modified Multiple-Reference Time Domain (MMRTD).....	47
4.3.1	Traditional Development.....	47
4.3.2	Real-Valued Realization of MMRTD.....	51
<b>5.</b>	<b>Coordinate Transformation Matrices between Different Equivalent Realizations</b>	<b>55</b>
5.1	Relationship between ERA and MRTD Realizations.....	55
5.2	Relationship between ERA and MMRTD Realizations.....	57
5.3	Transformation Matrices between three Realizations of the ERA.....	58
5.4	Summary Graphics.....	59
<b>6.</b>	<b>Numerical Results</b>	<b>61</b>
6.1	Simulation Results.....	62
6.1.1	Noise-free Results.....	63
6.1.2	Noise-contaminated Results.....	69
6.2	Test Data.....	74
<b>7.</b>	<b>Summary and Conclusions</b>	<b>98</b>
7.1	Summary.....	98
7.2	Conclusions.....	100
	<b>Appendix A: General Response of Linear System by Modal Analysis</b>	<b>102</b>
	<b>Appendix B: The Generalized Inverse</b>	<b>107</b>
B.1	Definition of the (Moore-Penrose) Generalized Inverse.....	107
B.2	The Singular Value Decomposition as a Method to Calculate the Generalized Inverse.....	107
B.3	Least Squares Solution and the Generalized Inverse.....	109
	<b>Appendix C: Real Realization from Complex Realization</b>	<b>111</b>
C.1	Single Input Two Output System with Two Modes.....	111
C.2	Single-Input Multiple-Output (SIMO) System with Multiple Modes.....	113
C.3	Multiple-Input Multiple-Output (MIMO) System with Multiple Modes.....	116

## List of Acronyms

<b>ERA</b>	Eigensystem Realization Algorithm
<b>ITD</b>	Ibrahim Time Domain
<b>MRTD</b>	Multiple-Reference Time Domain
<b>MMRTD</b>	Modified Multiple-Reference Time Domain
<b>INF</b>	Input-Normal Form
<b>IBF</b>	Internally Balanced Form
<b>ONF</b>	Output-Normal Form
<b>SIMO</b>	Single-Input Multiple-Output
<b>MIMO</b>	Multiple-Input Multiple-Output
<b>PSD</b>	Power Spectral Density
<b>HMB-2R</b>	Hybrid Model Build 2 Rigid

## List of Symbols

$A$	system matrix by ERA
$B$	input matrix by ERA
$C$	output matrix by ERA
$c_d$	damping matrix
$D$	direct transmission matrix
$E$	system matrix by MRTD
$E_m$	system matrix by MMRTD
$E_{uv}^T \equiv [I_{u \times u}, 0_{u \times (v-1)u}]$	block selection matrix
$F$	input matrix by MRTD
$F_m$	input matrix by MMRTD
$G$	output matrix by MRTD
$G_m$	output matrix by MMRTD
$H(k)$	Hankel matrix
$I_n$	identity matrix of order $n$
$k$	stiffness matrix
$\ell$	number of outputs
$L, L_m, L_c$	complex valued modal participation matrices
$L_r$	real valued modal participation matrix
$m$	number of inputs
$N$	number of modes
$n$	system order
$P$	left singular vector matrix
$P_n$	truncated left singular vector matrix

$Q$	right singular vector matrix
$Q_r$	truncated right singular vector matrix
$q(t)$	position function in generalized coordinates
$\dot{q}(t)$	velocity function in generalized coordinates
$\ddot{q}(t)$	acceleration function in generalized coordinates
$r$	number of time shifts in column direction
$s$	number of time shifts in row direction
$u(k)$	input vector
$V_r, V_{ri}, V_{ro}, V_{rb}$	finite observability matrices
$V_s, V_{si}, V_{so}, V_{sb}$	finite controllability matrices
$W_o$	infinite observability matrix
$W_c$	infinite controllability matrix
$\hat{W}_{ot}$	observability grammian
$\hat{W}_{ct}$	controllability grammian
$x(k)$	state vector in generalized coordinates
$Y(k)$	Markov parameter
$y(k)$	output vector
$z(k)$	state vector in transformed coordinates
$z_r$	discrete-time eigenvalue of the $r$ -th mode
$\alpha_1, \alpha_2, \alpha_3$	constant matrices
$\eta(t)$	position function in transformed coordinates
$\dot{\eta}(t)$	velocity function in transformed coordinates
$\ddot{\eta}(t)$	acceleration function in transformed coordinates
$\lambda_r = \sigma_r + j\omega_r$	continuous-time eigenvalue of the $r$ -th mode
$\sigma_r$	real part of $\lambda_r$ , $\sigma_r = -\zeta_r \omega_{nr}$
$\omega_{nr}$	natural frequency of the $r$ -th mode
$\omega_r$	damped frequency of the $r$ -th mode

$\zeta_r$	damping factor of the $r$ -th mode
$\Delta t$	sampling time interval
$\Lambda$	eigenvalue matrix (diagonal matrix)
$\Sigma$	singular value matrix
$\Sigma_n$	truncated singular value matrix
$\Psi, \Psi_m, \Psi_c$	complex valued mode shape matrices
$\Psi_r$	real valued mode shape matrix

# Chapter 1

## Introduction

### 1.1 Overview

The basic objective of system identification is to develop a mathematical model of a physical system by observing its input-output relationship. System identification models can be used for many purposes, e.g., system analysis or controller design. In practice, one is often limited to linear models. Fortunately, many physical systems can be approximated by linear equations. There are several models that can be used to describe the input-output characteristics of a linear system. In modern linear system theory, the continuous-time state space model is used. A state space model consists of the system matrix, input matrix, and output matrix.<sup>1</sup> For a linear system, the state space matrices are not unique in the sense that equivalent sets of state space matrices describe the same input-output relationship. The process of finding a state space model for a linear system is known as realization.<sup>1</sup> The system considered here is linear, time-invariant with stable modes. The state space matrices are required for several controller design methods, but they can also be used to determine the modal parameters of the system such as natural frequencies, damping factors, and mode shapes.<sup>1</sup>

In the past, many methods for determining the state space model of a linear system from measured outputs were developed. Important principles of realization theory were developed in Refs. 2 & 3. Ref. 4 developed a method to determine a state space model

using the Hankel matrix for the case of no measurement noise. The Hankel matrix is a special matrix of Markov parameters or pulse response samples. A state space model of the smallest possible dimension is called a minimal state space model and the process of finding a minimal state space model is called minimum realization. The problem of minimal realizations were studied in Refs. 5-7. For the treatment of noisy data, Ref. 8 proposed the use of the singular value decomposition in combination with Ref. 4. The singular value decomposition technique has been found very effective in dealing with noisy data as suggested in Refs. 9-11. The Eigensystem Realization Algorithm (ERA)<sup>12-14</sup> is a generalization of Ref. 4 based on a generalized Hankel matrix in combination with the singular value decomposition technique.

The methods discussed above were developed in the context of first-order differential equations. During this same time, structural dynamists were developing modal identification methods to determine the frequencies and mode shapes based on the second-order equations of dynamics. Some of the modal parameter identification techniques were also based on the Hankel matrix. In particular, they are the Ibrahim Time Domain (ITD),<sup>14-17</sup> Multiple-Reference Time Domain (MRTD),<sup>17</sup> and Modified Multiple-Reference Time Domain (MMRTD) methods.<sup>17</sup> These methods assume a solution in the form of complex mode shapes and complex frequencies, and then formulate the modal parameter identification as an eigenvalue problem. The MMRTD method is a modified version of MRTD to reduce required computer memory storage for certain problems. Free decay data or pulse response data are usually used for system identification by these methods.

It is the purpose of this thesis to provide a theoretical and experimental comparison between the MRTD and MMRTD methods and the various realizations of the ERA algorithm. This is motivated by the fact that despite their apparent differences, the mathematics of the MRTD and MMRTD methods and the ERA are related in that they both

use the singular value decomposition and the Hankel matrix in their formulation. It will be shown in this thesis that the MRTD and MMRTD methods are mathematically identical to certain realizations of the ERA. The apparent differences occur between the three methods because the MRTD and MMRTD methods are traditionally formulated in complex modal space, while the ERA is formulated in the state space format of modern control theory. Therefore, the difference between the three methods are not fundamental. The thesis will first provide a detailed formulation of the MRTD, MMRTD, and ERA algorithms. Next, the MRTD and MMRTD formulations will be shown to be equivalent to certain forms of the ERA. Relationship between MRTD, MMRTD, and various versions of the ERA will be established. Furthermore, the various versions of the ERA are also equivalent to each other. The ERA, MRTD, and MMRTD methods produce different but equivalent realizations. Numerical examples will be provided to illustrate any numerical difference between the methods. Free decay data is used to identify the system using different system identification methods. The numerical examples include those using simulated data with closely spaced frequencies and mode shapes and test data from an actual large flexible structure (HMB-2R).<sup>18</sup>

## **1.2 Thesis Outline**

The remainder of the thesis is organized as follows.

Chapter 2 will present some basic mathematics and definitions which include the state space equations, the Markov parameter, conversion from continuous-time (discrete-time) to discrete-time (continuous-time) state space model, and the controllability and observability grammians.

Chapter 3 will derive the three realizations of the ERA based on different ways of selecting the controllability and observability matrices. It will be shown that under certain limit conditions, these realizations of the ERA converge to the input-normal, output-normal, and internally-balanced realizations.

Chapter 4 will derive the realizations of the MRTD and MMRTD methods. These methods are normally formulated to compute the modal parameters such as damped frequencies, damping factors, mode shapes, and modal participation factor matrix. In this thesis, certain relations established in the MRTD and MMRTD formulations are further developed to provide real-valued state space model representations for these methods. This is done so that their comparison with the ERA realizations can be made.

Chapter 5 will establish the theoretical relationship between the realizations of the ERA, MRTD, and MMRTD methods.

Chapter 6 will illustrate the numerical relationship between the realizations of the ERA, MRTD, and MMRTD methods by examples using simulated and test data.

Chapter 7 is a summary of the basic results and conclusions.

## Chapter 2

### **Mathematical Preliminaries**

This chapter presents a brief review of the basic concepts in system realization theory. The state space representation of a linear system both in discrete and continuous time are reviewed. The Markov parameters, the Hankel matrix, and the observability and controllability grammians are presented. These basic concepts will be used in later chapters to provide a theoretical comparison between various time-domain state space realization methods.

#### **2.1 The State Space Representation**

State space theory describes the time behavior of physical systems in a mathematical manner. In particular, the state space approach is useful because:<sup>19,20</sup>

- 1) State space provides an organized approach to the analysis of linear systems in many areas (engineering, economics, ecology, etc...).
- 2) Multiple-input multiple-output systems can be treated conceptually the same as single-input single-output systems.
- 3) Problems formulated by state space methods can easily be programmed on a computer.
- 4) High-order linear systems can be analyzed.

- 5) State space theory is the foundation for further studies in nonlinear systems, stochastic systems, and optimal control.

## 2.2 Discrete and Continuous Models of a Dynamic System

The state space method requires that the description of a dynamical system be reformulated into the form of  $n$  first-order descriptions called the normal form. Dynamic systems are normally described by continuous-time second order differential equations. Experimental data are generally taken at discrete times. The following sections develop the relationship between a second-order dynamic system and the first-order equations, then relate the continuous-time system to the discrete-time system.

### 2.2.1 Continuous-Time Models

The equations of motion for a linear time invariant dynamic system in second-order form are<sup>14,21</sup>

$$m\ddot{q}(t) + c_d\dot{q}(t) + kq(t) = F_f u(t) \quad (2.1)$$

where  $m$ ,  $c_d$  and  $k$  denote constant system mass, damping, and stiffness matrices, respectively. Generally, the output quantities are linear functions of position, velocity, and acceleration.<sup>14,21</sup> In this case, the output equation can be written as

$$y(t) = \alpha_1 q(t) + \alpha_2 \dot{q}(t) + \alpha_3 \ddot{q}(t)$$

$$= [\alpha_1 - \alpha_3 m^{-1} k] q(t) + [\alpha_2 - \alpha_3 m^{-1} c_d] \dot{q}(t) + \alpha_3 m^{-1} F_f u(t)$$

where  $\alpha_1$ ,  $\alpha_2$ , and  $\alpha_3$  are matrices. The second-order equations given in Eq. (2.1) together with the output equation can be written in first-order form as

$$\begin{aligned} \dot{x}(t) &= A_c x(t) + B_c u(t) \\ y(t) &= C x(t) + D u(t) \end{aligned} \quad (2.2)$$

where

$$\begin{aligned} x(t) &= \begin{bmatrix} q(t) \\ \dot{q}(t) \end{bmatrix}, \quad A_c = \begin{bmatrix} 0 & I \\ -m^{-1}k & -m^{-1}c_d \end{bmatrix}, \quad B_c = \begin{bmatrix} 0 \\ m^{-1}F_f \end{bmatrix} \\ C &= [\alpha_1 - \alpha_3 m^{-1}k \quad \alpha_2 - \alpha_3 m^{-1}c_d], \quad D = \alpha_3 m^{-1}F_f \end{aligned} \quad (2.3)$$

and  $x$  is a  $n$ -dimensional state vector,  $u$  is a  $m$ -dimensional input vector and  $y$  is a  $\ell$ -dimensional output or measurement vector at time  $t$ .  $A_c$  is the continuous-time system matrix which represents the system dynamics.  $B_c$  is the continuous-time input matrix of dimensions  $n \times m$ .  $C$  is the output matrix of dimensions  $\ell \times n$  and  $D$  is a direct transmission term of dimensions  $\ell \times m$  where  $n$  is the number of orders,  $m$  is the number of inputs, and  $\ell$  is the number of outputs of the system. This is the continuous-time state space description of the system given in Eq. (2.1). The general response of a linear system by modal analysis is discussed in Appendix A.

## 2.2.2 Conversion from Continuous to Discrete-Time State Space Model

Although the dynamics are continuous, the data are usually collected at discrete, uniformly spaced times. A discrete representation of the continuous-time system can be used to describe the system response at discrete-time samples. In this section, the relationship between continuous and discrete-time models is described. Starting from any initial condition  $x(t_0)$ , the general solution for  $x(t)$  at any time  $t$  for any input  $u(t)$  is<sup>1,14,21</sup>

$$x(t) = e^{A_c(t-t_0)}x(t_0) + \int_{t_0}^t e^{A_c(t-\tau)}B_c u(\tau)d\tau$$

To convert to discrete time the change in  $x(t)$  from one time step to the next, we let  $t_0 = k\Delta t$  and  $t = (k+1)\Delta t$  in the above equation where the discrete sampling time intervals are defined as  $0, \Delta t, 2\Delta t, \dots$

$$x[(k+1)\Delta t] = e^{A_c\Delta t}x(k\Delta t) + \int_{k\Delta t}^{(k+1)\Delta t} e^{A_c[(k+1)\Delta t-\tau]}B_c u(\tau)d\tau$$

Let  $x(k)$  denote  $x(k\Delta t)$ , and  $x(k+1)$  denote  $x((k+1)\Delta t)$ . Assume that the input  $u(k\Delta t) = u(k)$  is held constant over the time interval from  $k\Delta t$  to  $(k+1)\Delta t$ . Therefore, Eq. (2.2) can be written at every time step as

$$\begin{aligned}x(k+1) &= Ax(k) + Bu(k) \\ y(k) &= Cx(k) + Du(k)\end{aligned}\tag{2.4}$$

where

$$A = e^{A_c\Delta t} \quad , \quad B = \int_0^{\Delta t} e^{A_c\tau}d\tau B_c\tag{2.5}$$

and  $A$  is the discrete-time system matrix which represents the system dynamics.  $B$  is the discrete-time input matrix of dimensions  $n \times m$ .  $C$  and  $D$  are the same as in the continuous-time representation given in Eq. (2.2). Therefore, Eq. (2.4) is a discrete-time state space equation with a sampling interval  $\Delta t$  for the continuous-time dynamic system in Eq. (2.2).

### 2.2.3 Conversion from Discrete to Continuous-Time State Space Model

If one uses sampled data, a realized system matrix  $A$  is in discrete-time, it must be converted to a continuous-time state matrix for comparison with the original dynamic system. For the case that  $A$  can be diagonalized by a matrix  $T$ <sup>1,14,21</sup>

$$T^{-1}AT = \Lambda = \text{diag}(z_1, z_2, \dots, z_n)$$

$\Lambda$  can be written as

$$\Lambda = e^{\text{diag}\left(\frac{\ln z_1}{\Delta t}, \frac{\ln z_2}{\Delta t}, \dots, \frac{\ln z_n}{\Delta t}\right)\Delta t}$$

Recall that  $A = e^{A_c \Delta t}$ , then

$$\Lambda = T^{-1}AT = T^{-1}\left(e^{A_c \Delta t}\right)T = e^{(T^{-1}A_c T)\Delta t}$$

Hence,

$$e^{(T^{-1}A_c T)\Delta t} = e^{\text{diag}\left(\frac{\ln z_1}{\Delta t}, \frac{\ln z_2}{\Delta t}, \dots, \frac{\ln z_n}{\Delta t}\right)\Delta t}$$

Therefore, a continuous-time system matrix can be obtained from

$$A_c = T \left[ \text{diag} \left( \frac{\ln z_1}{\Delta t}, \frac{\ln z_2}{\Delta t}, \dots, \frac{\ln z_n}{\Delta t} \right) \right] T^{-1} \quad (2.6)$$

The relationship between the eigenvalues  $z_r$  of the discrete-time system and the eigenvalues  $\lambda_r$  of the continuous-time system are<sup>1,17,21</sup>

$$\begin{aligned} \lambda_r &= \sigma_r \pm j\omega_r = \frac{\ln z_r}{\Delta t} \\ &= \text{Re} \left( \frac{\ln z_r}{\Delta t} \right) + j \left\{ \text{Im} \left( \frac{\ln z_r}{\Delta t} \right) \pm \frac{2i\pi}{\Delta t} \right\} \end{aligned} \quad (2.7)$$

where  $r = 1, 2, 3, \dots, n$ ;  $i = 0, 1, 2, \dots$ . In the identification of structures, the real parts of the eigenvalues are the modal damping factors characterizing the decay rates of the modal oscillations, and the imaginary parts are the modal frequencies.

To convert the discrete  $B$  to a continuous  $B_c$ , the following equation is used<sup>21</sup>

$$B_c = (A - I)^{-1} A_c B \quad (2.8)$$

To show Eq. (2.8), write  $A = e^{A_c \Delta t}$  as a convergent power series

$$A = e^{A_c \Delta t} = I + A_c(\Delta t) + \frac{A_c^2(\Delta t)^2}{2!} + \frac{A_c^3(\Delta t)^3}{3!} + \dots$$

Therefore,

$$A - I = A_c(\Delta t) + \frac{A_c^2(\Delta t)^2}{2!} + \frac{A_c^3(\Delta t)^3}{3!} + \dots$$

Hence

$$(A - I)B_c = A_c B_c(\Delta t) + \frac{A_c^2 B_c(\Delta t)^2}{2!} + \frac{A_c^3 B_c(\Delta t)^3}{3!} + \dots \quad (2.9)$$

Integrate the second equation in Eq. (2.5) term by term, and pre-multiply by  $A_c$ .

$$A_c B = A_c B_c (\Delta t) + \frac{A_c^2 B_c (\Delta t)^2}{2!} + \frac{A_c^3 B_c (\Delta t)^3}{3!} + \dots \quad (2.10)$$

Comparing Eq. (2.9) and Eq. (2.10), it can be seen that  $(A - I)B_c = A_c B$ . Therefore,  $B_c = (A - I)^{-1} A_c B$ . Thus, to convert from discrete-time to continuous-time use Eqs. (2.6) and (2.8). The eigenvalues are converted using Eq. (2.7).

### 2.3 Markov Parameters

In linear system identification, the Markov parameters play a very important role. The Markov parameters will be briefly described in this section. For a system with  $\ell$  outputs and  $m$  inputs, the sampled pulse response functions, known as the Markov parameters, associated with the discrete state space matrices  $(A, B, C, D)$  are defined to be<sup>21</sup>

$$\begin{aligned} Y(-1) &= D \\ Y(k) &= CA^k B \quad k = 0, 1, 2, \dots \end{aligned} \quad (2.11)$$

$Y(k)$  is a  $\ell \times m$  pulse response matrix whose columns are the pulse responses due to the  $m$  inputs.

The state space matrices  $A, B, C,$  and  $D$  are not unique for a given system since the state vector is coordinate-dependent. For example, let the state vector be transformed by any non-singular coordinate transformation matrix  $T$ <sup>1,14</sup>

$$z(k) = T^{-1}x(k) \quad (2.12)$$

Then Eqs. (2.4) can be written as

$$z(k+1) = T^{-1}ATz(k) + T^{-1}Bu(k)$$

$$y(k) = CTz(k) + Du(k)$$

which is a state space description  $(T^{-1}AT, T^{-1}B, CT, D)$  relating  $u(k)$  and  $y(k)$  by a new state vector  $z(k)$ . However, the system Markov parameters computed using these state space equations are the same as before,

$$Y(k) = CT(T^{-1}AT)^k T^{-1}B = CA^k B \quad (2.13)$$

*Even though there are an infinite number of state-space representations that produce the same input-output mapping, the Markov parameters are unique for a given linear system.*<sup>1</sup>

A state space description  $A$ ,  $B$ , and  $C$  can be put in the complex modal coordinates by the transformation matrix  $T^*$  that diagonalizes  $A$ ,

$$\Lambda = (T^*)^{-1}AT^*$$

and

$$\Psi = CT^* \quad , \quad L = (T^*)^{-1}B$$

where  $\Psi$  is an  $\ell \times n$  complex mode shape matrix,  $L$  is an  $n \times m$  complex modal participation matrix, and  $n$  is the order of the system. Assuming a real, continuous-time, damped, oscillatory, stable system, the eigenvalues will appear as complex conjugate pairs so that  $\Lambda$  can be written as a  $2 \times 2$  block diagonal matrix

$$\Lambda = \text{diag}(e^{\lambda_1 \Delta t}, e^{\lambda_2 \Delta t}, \dots, e^{\lambda_{2N} \Delta t})$$

$$= \begin{bmatrix} \begin{bmatrix} e^{\lambda_1 \Delta t} & 0 \\ 0 & e^{\lambda_1^* \Delta t} \end{bmatrix} & & & \\ & \begin{bmatrix} e^{\lambda_2 \Delta t} & 0 \\ 0 & e^{\lambda_2^* \Delta t} \end{bmatrix} & & \\ & & \dots & \\ & & & \begin{bmatrix} e^{\lambda_{2N} \Delta t} & 0 \\ 0 & e^{\lambda_{2N}^* \Delta t} \end{bmatrix} \end{bmatrix}$$

where  $\lambda_1, \lambda_2, \lambda_3, \dots, \lambda_{2N}$  are the eigenvalues of the continuous-time system matrix  $A_c$ ,  $\lambda_r = \sigma_r + j\omega_r$  is the complex frequency of the  $r$ -th mode,  $r = 1, 2, \dots, n$ , and  $\sigma_r$  and  $\omega_r$  are the real and imaginary parts of  $\lambda_r$ , respectively. The blank spaces denote the zero elements and the superscript \* denotes the complex conjugate. Therefore, the Markov parameters  $Y(k)$  can also be written as

$$Y(k) = \Psi \Lambda^k L \quad (2.14)$$

The Markov parameters take different forms depending on the system and the input.

### 2.3.1 Sampled Response to Impulse Input

Let an impulse input denoted by  $\delta(0)$  be applied to the system given by

$$\dot{x}(t) = A_c x(t) + B_c u(t)$$

$$y(t) = Cx(t) + Du(t)$$

Starting from zero initial conditions,  $x(0) = 0$ , the response is denoted by  $y(k\Delta t)$ ,  $k = 0, 1, 2, \dots$ , and measured at discrete-time intervals  $k\Delta t$  beginning with  $y(0) = y(0^+)$  immediately after the impulse has been applied to the system. The sampled response by the impulse input is<sup>1,21</sup>

$$\begin{aligned} y(k\Delta t) &= Ce^{A_c k\Delta t} x(0) + Ce^{A_c k\Delta t} \int_0^{k\Delta t} e^{-A_c \tau} B_c u(\tau) d\tau + Du(k\Delta t) \\ &= C(e^{A_c k\Delta t}) B_c = Y(k) \end{aligned}$$

Since  $A^k = e^{A_c k\Delta t}$ . Therefore,

$$Y(k) = CA^k B_c \quad k = 0, 1, 2, 3, \dots \quad (2.15)$$

where  $A$  is the discrete-time system matrix corresponding to the sampling period  $\Delta t$ ,  $B_c$  is the continuous-time input matrix, and  $C$  is the output matrix which is the same for both discrete and continuous-time cases. The parameters  $CA^k B_c$  in Eq. (2.15) are not precisely the Markov parameters of the system as described in Eq. (2.13) in Section 2.3, but they have the same form as the Markov parameters.

### 2.3.2 Sampled Response to Unit Pulse Input (Markov Parameters)

Similar to the impulse response of a continuous system, we have the unit pulse response of a discrete system. Let a unit pulse input be applied to the system given by Eq. (2.4)

$$\begin{aligned} x(k+1) &= Ax(k) + Bu(k) \\ y(k) &= Cx(k) + Du(k) \end{aligned}$$

where the unit pulse input is defined as<sup>21</sup>

$$u(k\Delta t) = \begin{cases} 1 & , \quad k = 0 \\ 0 & , \quad k = 1, 2, 3, \dots \end{cases} \quad (2.16)$$

with a zero-order hold on the input to maintain the input values during each sampling interval. The response is measured at discrete sampling intervals, and denoted by  $y(k\Delta t)$ ,  $k = 0, 1, 2, 3, \dots$ , with zero initial conditions. Therefore, the response of the discrete-time system is<sup>21</sup>

$$y(0) = D$$

$$y((k+1)\Delta t) = CA^k B = Y(k) \quad k = 0, 1, 2, 3, \dots \quad (2.17)$$

where  $A$ ,  $B$ , and  $C$  are the system discrete-time matrices. Thus, the parameters  $CA^k B$  are the discrete-time Markov parameters of the system.

### 2.3.3 Free Decay Response

System identification methods can also use free decay response to identify a system. Consider the free response of the system given in Eq. (2.1), from a non-zero initial condition with no forcing function, the sampled response is<sup>21</sup>

$$y(k\Delta t) = CA^k x(0) = Y(k) \quad k = 0, 1, 2, 3, \dots \quad (2.18)$$

If free decay data from several different initial conditions  $x_1(0)$ ,  $x_2(0)$ ,  $\dots$  are available, then the data can be combined as

$$\begin{aligned} [y_1(k\Delta t), y_2(k\Delta t), \dots] &= [CA^k x_1(0), CA^k x_2(0), \dots] \\ &= CA^k [x_1(0), x_2(0), \dots] \end{aligned}$$

Again,  $Y(k)$  in Eq. (2.18) are not the Markov parameters of the system but they have the same structure as the Markov parameters. An identification procedure applied to the above sequence produces a realization of  $A$ ,  $C$ , and the initial condition  $x(0)$ . Of course, the input matrix  $B$  can not be determined from free decay data alone.

## 2.4 Infinite Hankel Matrix

For later connection with controllability and observability grammians, we consider an infinite Hankel matrix formed by an infinite sequence of Markov parameters as<sup>13</sup>

$$H = \begin{bmatrix} Y(0) & Y(1) & \dots & Y(s-1) & \dots \\ Y(1) & Y(2) & \dots & Y(s) & \dots \\ \vdots & \vdots & \ddots & \vdots & \\ Y(r-1) & Y(r) & \dots & Y(r+s-2) & \\ \vdots & \vdots & & & \ddots \end{bmatrix} \quad (2.19)$$

Define

$$W_o = \begin{bmatrix} C \\ CA \\ \vdots \\ CA^{r-1} \\ \vdots \end{bmatrix}$$

and

$$W_c = [B, AB, \dots, A^{s-1}B, \dots] \quad (2.20)$$

Equation (2.19) becomes

$$H = W_o W_c \quad (2.21)$$

For a system of order  $n$ , if  $W_o$  is of rank  $n$ , the system is said to be *observable*<sup>1</sup>. Similarly, if  $W_c$  is of rank  $n$ , the system is said to be *controllable*<sup>1</sup>. From Eq. (2.21), the rank of the Hankel matrix is equal to the order of a controllable, observable system. The Hankel matrix  $H$ , which is made of Markov parameters, is independent of coordinate system, but  $W_o$  and  $W_c$  are not. *In fact, the fundamental difference between the methods to be discussed depend on how  $H$  is decomposed into  $W_o$  and  $W_c$ .*

## 2.5 Controllability and Observability Grammians

If the system is stable, *the discrete controllability and observability grammians*<sup>1,13</sup> are defined respectively as

$$\hat{W}_{ct} = \sum_{k=0}^{\infty} A^k B B^T (A^T)^k$$

and

$$(2.22)$$

$$\hat{W}_{ot} = \sum_{k=0}^{\infty} (A^T)^k C^T C A^k$$

From the discrete controllability and observability grammians definitions given in Eqs. (2.22) and Eq. (2.20), it can be shown that

$$\hat{W}_{ct} = W_c W_c^T$$

and

$$\hat{W}_{ot} = W_o^T W_o \tag{2.23}$$

Recall that there are an infinite number of realizations that describe a given system of the form given in Eq. (2.13). These realizations are equivalent in the sense that they represent the same system but in different coordinates. *There are three special coordinate systems known as internally balanced, input-normal, and output-normal. The realization  $(A, B, C)$  is said to be internally balanced if and only if  $\hat{W}_{ct} = \hat{W}_{ot} = \Sigma$ . The realization is said to be input-normal if and only if  $\hat{W}_{ct} = I$  and  $\hat{W}_{ot} = \Sigma^2$ ; and output-normal if and only if  $\hat{W}_{ct} = \Sigma^2$ ,  $\hat{W}_{ot} = I$ ,<sup>1,22,23</sup> where  $\Sigma$  is an diagonal matrix and  $I$  is the identity matrix. The relationship between  $\Sigma$  and the Hankel matrix of a system will be discussed in Section 3.1.*

## 2.6 Finite Hankel Matrix

In practice, one must work with finite-dimensional matrices. In this section, the finite Hankel matrix is introduced. The *finite Hankel matrix* is defined as<sup>1</sup>

$$H(k) = \begin{bmatrix} Y(k) & Y(k+1) & \cdots & Y(k+s-1) \\ Y(k+1) & Y(k+2) & \cdots & Y(k+s) \\ \vdots & \vdots & & \vdots \\ Y(k+r-1) & Y(k+r) & \cdots & Y(k+r+s-2) \end{bmatrix}$$

Since  $Y(k) = CA^k B$ , then  $H(k)$  can be expressed as

$$H(k) = V_r A^k W_s \quad (2.24)$$

where

$$V_r = \begin{bmatrix} C \\ CA \\ \vdots \\ CA^{r-1} \end{bmatrix} \quad W_s = [B, AB, \dots, A^{s-1}B] \quad (2.25)$$

$r$  and  $s$  are the sampling time shifts in the column and row directions, respectively.  $V_r$  is the observability matrix of dimensions  $lr \times n$ , and  $W_s$  is the controllability matrix of dimensions  $n \times ms$ . From Eq. (2.23), the order of the system is equal to the rank of the Hankel matrix for a system which is both controllable and observable. In the presence of noise, the Hankel matrix tends to be full rank. From Eqs. (2.20), and (2.25), the observability and controllability matrices from the infinite Hankel matrix and finite Hankel matrix can be related by

$$W_o = \begin{bmatrix} C \\ CA \\ \vdots \\ CA^{r-1} \\ CA^r \\ \vdots \\ CA^{2r-1} \\ CA^{2r} \\ \vdots \end{bmatrix} = \begin{bmatrix} V_r \\ V_r A^r \\ V_r A^{2r} \\ \vdots \end{bmatrix} \quad (2.26)$$

and

$$\begin{aligned} W_c &= [B \quad AB \quad \dots \quad A^{s-1}B \quad A^s B \quad \dots \quad A^{2s-1}B \quad A^{2s}B \quad \dots] \\ &= [W_s \quad A^s W_s \quad A^{2s} W_s \quad \dots] \end{aligned} \quad (2.27)$$

and then the controllability and observability grammians<sup>13</sup> defined in Section 2.5 can be written as

$$\begin{aligned} \hat{W}_{ct} &= W_c W_c^T \\ &= W_s W_s^T + (A^s)^T W_s W_s^T (A^s)^T + (A^{2s})^T W_s W_s^T (A^{2s})^T + \dots \end{aligned} \quad (2.28)$$

and

$$\begin{aligned} \hat{W}_{ot} &= W_o^T W_o \\ &= V_r^T V_r + (A^r)^T V_r^T V_r (A^r)^T + (A^{2r})^T V_r^T V_r (A^{2r})^T + \dots \end{aligned}$$

This relationship will later be used to show that certain realizations convert to input-normal, output-normal, and internally balanced forms.

## Chapter 3

# **System Realization using Eigensystem Realization Algorithm**

This chapter presents the development of the Eigensystem Realization Algorithm (ERA). Realization refers to finding a state space description of a linear system from input-output data or free decay data. For an asymptotically stable system, these realizations are shown to convert to the input-normal and internally balanced realizations when the Hankel matrix size tends to infinity. An output-normal realization of the ERA is also derived.

### **3.1 Minimal-Dimensional Realizations of the ERA Method by Singular Value Decomposition (SVD)**

In the noise free case, a realization with the least possible dimensions is called a minimal or irreducible realization. The dimension of the system refers to the dimension of the state vector  $x(k)$  or the size of the system matrix  $A$ . In this section, the relation between three natural realizations of the ERA and the input-normal, internally balanced, and output-normal realizations are derived. The ERA algorithm uses the singular value decomposition of a finite-Hankel matrix to determine a system model.<sup>12-14</sup> The singular value decomposition technique can be used to determine the order of the system. From the singular value decomposition of  $H(0)$ ,<sup>1</sup>

$$H(0) = P\Sigma Q^T = P_n \Sigma_n Q_n^T \quad (3.1)$$

where the size of the Hankel matrix  $H(0)$  is  $lr \times ms$ , and  $P$  and  $Q$  are orthonormal matrices with  $lr$  and  $ms$  rows, respectively.  $\Sigma$  is a diagonal matrix of the singular values of  $H(0)$ . If the rank of  $H(0)$  is  $n$ , then the singular value matrix  $\Sigma$  will contain only  $n$  positive singular values, and the remaining singular values are zero. In this case, the matrices  $P_n$  and  $Q_n$  are formed by the first  $n$  columns of  $P$  and  $Q$  corresponding to  $n$  positive singular values and  $\Sigma_n$  is the singular value matrix formed by  $n$  positive singular values of  $\Sigma$ . Since  $H(0) = V_r W_s$ , the rank of  $H(0)$  cannot exceed the rank of  $V_r$  or  $W_s$  where  $V_r$  and  $W_s$  are the observability and controllability matrices, respectively. The rank of  $H(0)$  is the minimum of the rank of the controllability space and observability space. In the noise-free case, the order of the system is equal to the rank of the Hankel matrix  $H(0)$  assuming  $H(0)$  is sufficiently large.

In practical problems with noise, there will be no zero singular values. In this case, the larger singular values are assumed to represent the signal and the smaller singular values are assumed to present the noise. To obtain a minimum realization only a certain number of the singular values are retained, say  $n$ . In this case, one can write

$$H(0) \approx P_n \Sigma_n Q_n^T = V_r W_s \quad (3.2)$$

$H(0)$  is known, but  $V_r$  and  $W_s$  are unknown. Equation. (3.2) suggests three natural ways of selecting  $V_r$  and  $W_s$ , resulting in three different realizations of the system

1.  $V_{ri} = P_n \Sigma_n$  ,  $W_{si} = Q_n^T$

This will be shown to produce the input-normal form (INF)

$$2. \quad V_{rb} = P_n \Sigma_n^{1/2}, \quad W_{sb} = \Sigma_n^{1/2} Q_n^T$$

This will be shown to produce the internally balanced form (IBF)

$$3. \quad V_{ro} = P_n, \quad W_{so} = \Sigma_n Q_n^T$$

This will be shown to produce the output-normal form (ONF)

From Eq. (2.24), regardless of choice,

$$H(1) = V_r A W_s \quad (3.3)$$

where  $V_r$  is the observability matrix formed by matrices  $A$  and  $C$ , and  $W_s$  is the controllability matrix formed by matrices  $A$  and  $B$ . By choice  $V_r$  is of full column rank and  $W_s$  is of full row rank, thus  $V_r^+ V_r = I_n$  and  $W_s W_s^+ = I_n$ .  $I_n$  is an identity matrix with order  $n$  and the superscript "+" denotes the pseudo-inverse. The pseudo-inverse is discussed in appendix B. Therefore, premultiplying Eq. (3.3) by  $V_r$  and also postmultiplying Eq. (3.3) by  $W_s$  yields

$$A = V_r^+ H(1) W_s^+ \quad (3.4)$$

For any integer number  $u$  and  $v$ , define a  $u \times uv$  selection matrix  $E_{uv}^T$  consisting of identity and null matrices. The selection matrix is convenient for notational purposes but are not needed for computational purposes.

$$E_{uv}^T \equiv [I_{u \times u}, \quad 0_{u \times (v-1)u}] \quad (3.5)$$

From Eq. (3.2), and also from the first partitions of Eq. (2.25) in Chapter 2, the  $C$  and  $B$  matrices also selected with this choice of  $V_r$  and  $W_s$ , respectively, are

$$C = E_{tr}^T V_r \quad \text{and} \quad B = W_s E_{ms} \quad (3.6)$$

where  $E_{tr}$  and  $E_{ms}$  are defined in section 3.1 on page 23.

### 3.2 Input-Normal Realization of ERA

In the first paper on ERA,<sup>12</sup> the realization of the ERA was represented in the input-normal form. In that paper, the singular value decomposition of  $H(0)$  is written as

$$H(0) \approx P_n \Sigma_n Q_n^T = [P_n \Sigma_n] [Q_n^T] \equiv [V_{ri}] [W_{si}] \quad (3.7)$$

where we have  $V_{ri} = P_n \Sigma_n$  and  $W_{si} = Q_n^T$ . Therefore, from Eq. (3.4)

$$A_i = V_{ri}^+ H(1) W_{si}^+ \quad (3.8)$$

From Eq. (3.2), and the first partitions of Eq. (2.25), the  $C_i$  and  $B_i$  matrices also selected with this choice of  $V_{ri}$  and  $W_{si}$ , respectively, are

$$C_i = E_{tr}^T V_{ri} \quad \text{and} \quad B_i = W_{si} E_{ms} \quad (3.9)$$

Since the columns of  $P_n$  and  $Q_n$  are orthonormal, the pseudoinverse of  $V_{ri}$  and  $W_{si}$  can be obtained as

$$V_{ri}^+ = [V_{ri}^T V_{ri}]^{-1} (V_{ri}^T) = [\Sigma_n P_n^T P_n \Sigma_n]^{-1} (\Sigma_n P_n^T) = \Sigma_n^{-1} P_n^T$$

and

$$W_{si}^+ = W_{si}^T [W_{si} W_{si}^T]^{-1} = Q_n [Q_n^T Q_n]^{-1} = Q_n$$

Therefore, a minimal realization  $[A_i, B_i, C_i]$  is

$$\begin{aligned} A_i &= \Sigma_n^{-1} P_n^T H(1) Q_n \\ B_i &= Q_n^T E_{ms} \end{aligned} \quad (3.10)$$

$$C_i = E_{lr}^T P_n \Sigma_n$$

To see that this is an input-normal realization, note that  $V_{ri} = P_n \Sigma_n$  and  $W_{si} = Q_n^T$ . Also, the columns of  $P_n$  and  $Q_n$  are orthonormal, i.e.,  $P_n^T P_n$  and  $Q_n^T Q_n$  are identity matrices. Therefore,

$$\begin{aligned} V_{ri}^T V_{ri} &= \Sigma_n P_n^T P_n \Sigma_n = \Sigma_n^2 \\ W_{si} W_{si}^T &= Q_n^T Q_n = I_n \end{aligned} \quad (3.11)$$

Substituting Eq. (3.11) into Eq. (2.28) given in Chapter 2, the observability and controllability grammians of Eq. (2.28) result in

$$\hat{W}_{oi} = \Sigma_n^2 + (A_i^r)^T \Sigma_n^2 (A_i^r) + (A_i^{2r})^T \Sigma_n^2 (A_i^{2r}) + \dots$$

and

$$\hat{W}_{ci} = I_n + (A_i^s) I_n (A_i^s)^T + (A_i^{2s}) I_n (A_i^{2s})^T + \dots \quad (3.12)$$

If the system is asymptotically stable, the magnitudes of all the eigenvalues of  $A_i$  are less than one,  $(|\lambda_i(A_i)| < 1)$ .<sup>1,13</sup> Therefore, when  $r$  and  $s$  tend to infinity, for an asymptotically stable system, Eq. (3.12) yields

$$\lim_{r \rightarrow \infty, s \rightarrow \infty} \hat{W}_{ot} = \lim_{r \rightarrow \infty, s \rightarrow \infty} \Sigma_n^2 = \Sigma_\infty^2$$

$$\lim_{r \rightarrow \infty, s \rightarrow \infty} \hat{W}_{ct} = \lim_{r \rightarrow \infty, s \rightarrow \infty} I_n = I_n$$

Thus, this realization of the ERA converges to the input-normal realization when  $r$  and  $s$  tend to infinity.

### 3.3 Internally Balanced Realization of ERA

In later papers of ERA,<sup>13,14</sup> another realization of the ERA was selected because it resulted in an internally balanced system. The internally balanced realization is also discussed in Ref. 9. The Hankel matrix in Eq. (3.3) can also be written as

$$H(1) = V_{rb} A_b W_{sb} \quad (3.13)$$

where  $V_{rb}$  is the observability matrix formed by internally balanced matrices  $A_b$  and  $C_b$ , and  $W_{sb}$  is the controllability matrix formed by internally balanced matrices  $A_b$  and  $B_b$ . To derived this realization, write

$$H(0) = P_n \Sigma_n Q_n^T = \left[ P_n \Sigma_n^{1/2} \right] \left[ \Sigma_n^{1/2} Q_n^T \right] \equiv [V_{rb}] [W_{sb}] \quad (3.14)$$

where  $P_n$ ,  $\Sigma_n$ ,  $Q_n$ , and  $n$  are the same as before in Eq. (3.2), and  $V_{rb} = P_n \Sigma_n^{1/2}$  and  $W_{sb} = \Sigma_n^{1/2} Q_n^T$ . Therefore, from Eq. (3.13) using the same steps in Section 3.1, we obtain

$$A_b = V_{rb}^+ H(1) W_{sb}^+$$

and

$$C_b = E_{tr}^T V_{rb} \quad \text{and} \quad B_b = W_{sb} E_{ms}$$

where  $E_{tr}^T$  and  $E_{ms}$  are selection matrices. Because the columns of  $P_n$  and  $Q_n$  are orthonormal, the pseudoinverse of  $V_{rb}$  and  $W_{sb}$  can be obtained as

$$\begin{aligned} V_{rb}^+ &= [V_{rb}^T V_{rb}]^{-1} (V_{rb}^T) = \left[ \Sigma_n^{1/2} P_n^T P_n \Sigma_n^{1/2} \right]^{-1} \left( \Sigma_n^{1/2} P_n^T \right) \\ &= \Sigma_n^{-1/2} P_n^T \end{aligned}$$

and

$$\begin{aligned} W_{sb}^+ &= (W_{sb}^T) [W_{sb} W_{sb}^T]^{-1} = \left( Q_n \Sigma_n^{1/2} \right) \left[ \Sigma_n^{1/2} Q_n^T Q_n \Sigma_n^{1/2} \right]^{-1} \\ &= Q_n \Sigma_n^{-1/2} \end{aligned}$$

Therefore, an internally balanced minimal realization  $[A_b, B_b, C_b]$  is

$$\begin{aligned} A_b &= \Sigma_n^{-1/2} P_n^T H(1) Q_n \Sigma_n^{-1/2} \\ B_b &= \Sigma_n^{1/2} Q_n^T E_{ms} \end{aligned} \tag{3.15}$$

$$C_b = E_{tr}^T P_n \Sigma_n^{1/2}$$

The above realization is an internally balanced realization, since  $V_{rb} = P_n \Sigma_n^{1/2}$  and  $W_{sb} = \Sigma_n^{1/2} Q_n^T$ , and  $P_n^T P_n$  and  $Q_n^T Q_n$  are identity matrices, hence

$$V_{rb}^T V_{rb} = \Sigma_n^{1/2} P_n^T P_n \Sigma_n^{1/2} = \Sigma_n$$

and

$$W_{sb}W_{sb}^T = \Sigma_n^{1/2} Q_n^T Q_n \Sigma_n^{1/2} = \Sigma_n \quad (3.16)$$

Substituting Eq. (3.16), into Eq. (2.28) in Chapter 2, the observability and controllability grammians can be shown to be

$$\begin{aligned} \hat{W}_{ot} &= W_o^T W_o \\ &= V_{rb}^T V_{rb} + (A_b^r)^T V_{rb}^T V_{rb} (A_b^r) + (A_b^{2r})^T V_{rb}^T V_{rb} (A_b^{2r}) + \dots \\ &= \Sigma_n + (A_b^r)^T \Sigma_n (A_b^r) + (A_b^{2r})^T \Sigma_n (A_b^{2r}) + \dots \end{aligned} \quad (3.17)$$

and

$$\begin{aligned} \hat{W}_{ct} &= W_c W_c^T \\ &= W_{sb} W_{sb}^T + (A_b^s) W_{sb} W_{sb}^T (A_b^s)^T + (A_b^{2s}) W_{sb} W_{sb}^T (A_b^{2s})^T + \dots \\ &= \Sigma_n + (A_b^s) \Sigma_n (A_b^s)^T + (A_b^{2s}) \Sigma_n (A_b^{2s})^T + \dots \end{aligned} \quad (3.18)$$

Again, for an asymptotically stable system, when  $r$  and  $s$  approach infinity, Eqs. (3.17) and (3.18) result in<sup>13</sup>

$$\lim_{r \rightarrow \infty, s \rightarrow \infty} \hat{W}_{ot} = \lim_{r \rightarrow \infty, s \rightarrow \infty} \Sigma_n = \Sigma_\infty$$

and

$$\lim_{r \rightarrow \infty, s \rightarrow \infty} \hat{W}_{ct} = \lim_{r \rightarrow \infty, s \rightarrow \infty} \Sigma_n = \Sigma_\infty$$

*Therefore, this realization of the ERA converges to the internally balanced realization when  $r$  and  $s$  tend to infinity.*<sup>13</sup>

### 3.4 Output-Normal Realization of ERA

In this section, the output-normal realization is derived. This form is different from the two above realizations of the ERA and has not been published previously. In this case, the Hankel matrix in Eq. (3.3) can be expressed as

$$H(1) = V_{ro} A_o W_{so} \quad (3.19)$$

where  $V_{ro}$  and  $W_{so}$  are the observability and controllability matrices formed by output-normal matrices  $A_o$  and  $C_o$ , and  $A_o$  and  $B_o$ , respectively. Write  $H(0)$  as

$$H(0) \approx P_n \Sigma_n Q_n^T = [P_n] [\Sigma_n Q_n^T] \equiv [V_{ro}] [W_{so}]$$

where  $V_{ro} = P_n$  and  $W_{so} = \Sigma_n Q_n^T$ . Therefore

$$A_o = V_{ro}^+ H(1) W_{so}^+$$

and

$$C_o = E_{tr}^T V_{ro} \quad \text{and} \quad B_o = W_{so} E_{ms}$$

where  $E_{tr}^T$  and  $E_{ms}$  are selection matrices. Since the columns of  $P_n$  and  $Q_n$  are orthonormal, the pseudoinverse of  $V_{ro}$  and  $W_{so}$  can be obtained

$$\begin{aligned} V_{ro}^+ &= [V_{ro}^T V_{ro}]^{-1} (V_{ro}^T) = [P_n^T P_n]^{-1} (P_n^T) \\ &= P_n^T \end{aligned}$$

and likewise

$$\begin{aligned}
W_{so}^+ &= (W_{so}^T)[W_{so}W_{so}^T]^{-1} = (Q_n\Sigma_n)[\Sigma_n Q_n^T Q_n \Sigma_n]^{-1} \\
&= Q_n \Sigma_n^{-1}
\end{aligned}$$

Again, a minimal realization  $[A_o, B_o, C_o]$  can be found as

$$A_o = P_n^T H(1) Q_n \Sigma_n^{-1}$$

$$B_o = \Sigma_n Q_n^T E_{ms} \tag{3.20}$$

$$C_o = E_{lr}^T P_n$$

To prove that this is an output-normal realization, since  $V_{ro} = P_n$ ,  $W_{so} = \Sigma_n Q_n^T$ , and  $P_n^T P_n$  and  $Q_n^T Q_n$  are identity matrices, therefore

$$V_{ro}^T V_{ro} = P_n^T P_n = I_n$$

and

$$W_{so} W_{so}^T = \Sigma_n Q_n^T Q_n \Sigma_n = \Sigma_n^2$$

Therefore, for an asymptotically stable system, when  $r$  and  $s$  approach infinity, the observability and controllability grammians are

$$\begin{aligned}
\lim_{r \rightarrow \infty, s \rightarrow \infty} \hat{W}_{or} &= \lim_{r \rightarrow \infty, s \rightarrow \infty} (W_o^T W_o) \\
&= \lim_{r \rightarrow \infty, s \rightarrow \infty} \left[ V_{ro}^T V_{ro} + (A_o^r)^T V_{ro}^T V_{ro} (A_o^r) + (A_o^{2r})^T V_{ro}^T V_{ro} (A_o^{2r}) + \dots \right]
\end{aligned}$$

$$\begin{aligned}
&= \lim_{r \rightarrow \infty, s \rightarrow \infty} \left[ I_n + (A_o^r)^T I_n (A_o^r) + (A_o^{2r})^T I_n (A_o^{2r}) + \dots \right] \\
&= I_n
\end{aligned}$$

and

$$\begin{aligned}
\lim_{r \rightarrow \infty, s \rightarrow \infty} \hat{W}_{ot} &= \lim_{r \rightarrow \infty, s \rightarrow \infty} (W_c W_c^T) \\
&= \lim_{r \rightarrow \infty, s \rightarrow \infty} \left[ W_{so} W_{so}^T + (A_o^s) W_{so} W_{so}^T (A_o^s)^T + (A_o^{2s}) W_{so} W_{so}^T (A_o^{2s})^T + \dots \right] \\
&= \lim_{r \rightarrow \infty, s \rightarrow \infty} \left[ \Sigma_n^2 + (A_o^s) \Sigma_n^2 (A_o^s)^T + (A_o^{2s}) \Sigma_n^2 (A_o^{2s})^T + \dots \right] \\
&= \Sigma_\infty^2
\end{aligned}$$

*Thus, this realization converges to the output-normal realization when  $r$  and  $s$  tend to infinity.*

### 3.5 Summary Table

In previous sections, we showed that if the system is stable, the three realizations :  $[A_i, B_i, C_i]$ ,  $[A_b, B_b, C_b]$ , and  $[A_o, B_o, C_o]$  by the ERA method converge to the input-normal, internally balanced, and output-normal realizations, respectively when the number of rows and columns of the Hankel matrix  $H(0)$  tend to infinity. The three realizations are summarized in the following Table 1.

Table 1: The three realizations of ERA

ERA Realizations	System matrix $A$	Input matrix $B$	Output matrix $C$
input-normal	$A_i = \Sigma_n^{-1} P_n^T H(1) Q_n$	$B_i = Q_n^T E_{ms}$	$C_i = E_{tr}^T P_n \Sigma_n$
internally balanced	$A_b = \Sigma_n^{-1/2} P_n^T H(1) Q_n \Sigma_n^{-1/2}$	$B_b = \Sigma_n^{1/2} Q_n^T E_{ms}$	$C_b = E_{tr}^T P_n \Sigma_n^{1/2}$
output-normal	$A_o = P_n^T H(1) Q_n \Sigma_n^{-1}$	$B_o = \Sigma_n Q_n^T E_{ms}$	$C_o = E_{tr}^T P_n$

The steps in the deriving of ERA method for system identification are summarized below :

- 1) Form the Hankel matrices  $H(0)$  and  $H(1)$ .
- 2) Obtain the singular value decomposition matrices  $[P, \Sigma, Q]$  of  $H(0)$ .
- 3) Select the order of the system by truncating  $P, \Sigma,$  and  $Q$  to  $P_n, \Sigma_n,$  and  $Q_n$ . To do this, the singular values are first normalized and the ratios between each singular value and the largest one are computed. Singular values with ratio less than a certain value, say  $\frac{1}{1000}$ , are truncated. This is a trial and error procedure and problem dependent.
- 4) Choose the observability matrix  $V_r$  and controllability matrix  $W_s$  from the decomposition of  $H(0)$  according to the form desired.
- 5) Compute the  $A$  matrix from premultiplying Eq. (3.3) by  $V_r^+$  and postmultiplying Eq. (3.3) by  $W_s^+$ .
- 6) Obtain the  $B$  and  $C$  matrices from Eq. (2.25) in Chapter 2 with selection matrices  $E_{tr}^T$  and  $E_{ms}$ , and with the choice  $V_r$  and  $W_s$ .

To use ERA, depending on which realization is desired, the equations in Table 1 can be directly applied.

In Chapter 5, it will be shown that the three realizations of the ERA are mathematically equivalent and they will give the same mode shapes, and complex frequencies. It will be also shown that one realization of the ERA can be transformed to the another by a transformation matrix. In the next chapter, the real-valued realization  $[E, F, G]$  of the MRTD method, and the real-valued realization  $[E_m, F_m, G_m]$  of the MMRTD method will be derived. Later, it will be shown that these are in fact the output-normal and input-normal realizations, respectively.

## Chapter 4

### Multiple-Reference Time Domain Method

In this chapter two real realizations  $[E, F, G]$  and  $[E_m, F_m, G_m]$  of the MRTD and MMRTD methods, respectively are derived. Both MRTD and MMRTD use the singular value decomposition of the Hankel matrix  $H(0)$  to compute their minimal realizations<sup>17</sup>. Both methods have always been presented in complex modal space and formulate the realization problem as an eigenvalue problem. Therefore, the mathematics looks somewhat different from the ERA formulation. *However, it will be shown that the MRTD and MMRTD methods produce the same realizations as the output-normal and input-normal realizations of the ERA.* The difference between MRTD and MMRTD methods is that depending on the dimensions of the Hankel matrix one method requires less computer memory storage. Section 4.1 will discuss the Hankel matrix expressed in terms of complex modal parameters for the MRTD and MMRTD methods. Section 4.2 derives a complex realization  $[\Lambda, L, \Psi]$  of the MRTD method in complex modal coordinates, and an equivalent real realization  $[E, F, G]$  of the MRTD method in output-normal coordinates. Section 4.3 will derive the complex realization  $[\Lambda, L_m, \Psi_m]$  in complex modal coordinates by the MMRTD method, and an equivalent real realization  $[E_m, F_m, G_m]$  of the MMRTD method in input-normal coordinates.

## 4.1 The Hankel Matrix for MRTD Method

As shown in Section 2.3, for a system with  $\ell$  outputs and  $m$  inputs, the sampled pulse response function can be written as<sup>17</sup>

$$Y(k) = \Psi \Lambda^k L \quad (4.1)$$

where

$$\Lambda = \text{diag}(e^{\lambda_1 \Delta t}, e^{\lambda_2 \Delta t}, \dots, e^{\lambda_n \Delta t}) \quad (4.2)$$

and  $n$  denotes the order of the system. In general,  $Y(k)$  is an  $\ell \times m$  matrix whose  $i - j$ th element is the response at time  $t = k\Delta t$  of the  $i$ -th output due to a unit pulse applied at the  $j$ -th input. Therefore, the  $\ell r \times ms$  finite-Hankel matrix can be rewritten as

$$\begin{aligned} H(k) &= \begin{bmatrix} \Psi \Lambda^k L & \Psi \Lambda^{k+1} L & \dots & \Psi \Lambda^{k+s-1} L \\ \Psi \Lambda^{k+1} L & \Psi \Lambda^{k+2} L & \dots & \Psi \Lambda^{k+s} L \\ \vdots & \vdots & & \vdots \\ \Psi \Lambda^{k+r-1} L & \Psi \Lambda^{k+r} L & \dots & \Psi \Lambda^{k+r+s-2} L \end{bmatrix} \\ &= \begin{bmatrix} \Psi \\ \Psi \Lambda \\ \vdots \\ \Psi \Lambda^{r-1} \end{bmatrix} \Lambda^k [L, \Lambda L, \dots, \Lambda^{s-1} L] \end{aligned} \quad (4.3)$$

Define an  $\ell r \times n$  matrix  $\bar{\Psi}$

$$\bar{\Psi} = \begin{bmatrix} \Psi \\ \Psi \Lambda \\ \vdots \\ \Psi \Lambda^{r-1} \end{bmatrix} \quad (4.4)$$

and an  $n \times ms$  matrix  $\bar{L}$

$$\bar{L} = [L, \Lambda L, \dots, \Lambda^{s-1} L] \quad (4.5)$$

Equation (4.3) becomes

$$H(k) = \bar{\Psi} \Lambda^k \bar{L} \quad \text{or} \quad H(0) = \bar{\Psi} \bar{L} \quad (4.6)$$

Similarly, the one sampling time shifted Hankel matrix  $H(k+1)$  is

$$H(k+1) = \bar{\Psi} \Lambda^{k+1} \bar{L} \quad \text{or} \quad H(1) = \bar{\Psi} \Lambda \bar{L} \quad (4.7)$$

As shown in Section 2.6, the order of the system is equal to the rank of the Hankel matrix  $H(0)$ , (or  $H(1)$ ). In the original Ibrahim time domain (ITD) method,<sup>14-17</sup> the eigenvalues, mode shapes, and modal participations were determined by a least squares and eigenvalues solution between Eqs. (4.6) and (4.7). This is rewritten here as follows. Premultiply Eq. (4.6) by the generalized inverse  $\bar{\Psi}^+$  of the  $\bar{\Psi}$  matrix,

$$\bar{\Psi}^+ H(0) = \bar{L} \quad (4.8)$$

since  $\bar{\Psi}$  is of full column rank. Substituting Eq. (4.8) into Eq. (4.7) yields

$$H(1) = \bar{\Psi} \Lambda \bar{\Psi}^+ H(0) \quad (4.9)$$

To obtain the eigenvalue problem, postmultiply Eq. (4.9) by the generalized inverse of  $\bar{\Psi}^+ H(0)$ . Note that  $\bar{\Psi}^+ H(0)$  is in general not a square matrix, but, it is of full row rank.

$$H(1) (\bar{\Psi}^+ H(0))^+ = \bar{\Psi} \Lambda \quad (4.10)$$

Since  $(\bar{\Psi}^+ H(0))^+ = H^+(0) \bar{\Psi}$  (Appendix A), Eq. (4.10) becomes

$$E_{ITD} \bar{\Psi} = \bar{\Psi} \Lambda \quad (4.11)$$

where

$$E_{ITD} \equiv H(1)H^*(0)$$

The size of the system matrix  $E_{ITD}$  is  $lr \times lr$ . Equation (4.11) is an eigenvalue problem from which the mode shapes and frequencies can be determined. The original Ibrahim Time Domain (ITD) did not use the singular values decomposition to reduce the size of the eigenvalue problem. The ITD method was extended to include the singular value decomposition step and called MRTD and MMRTD.<sup>17</sup>

## 4.2 MRTD Minimal Realization

### 4.2.1 Traditional Development

Like ERA, the traditional development begins with the singular value decomposition of the Hankel matrix  $H(0)$

$$H(0) = P \Sigma Q^T \approx P_n \Sigma_n Q_n^T \quad (4.12)$$

where  $P$  is an orthonormal matrix of order  $lr$ ,  $Q$  is an orthonormal matrix of order  $ms$ , and  $\Sigma$  is a diagonal matrix of the positive singular values of  $H(0)$ . As before,  $P_n$  is the first  $n$  columns of  $P$ ,  $\Sigma_n$  is the upper-square  $n \times n$  submatrix of  $\Sigma$ , and  $Q_n$  is the first  $n$  columns of  $Q$  and this selection defines the order of the system. The Hankel matrix is written in terms of  $\Lambda$ ,  $L$ , and  $\Psi$  instead of  $A$ ,  $B$ , and  $C$ . Therefore,

$$H(0) = \bar{\Psi} \bar{L} \quad \text{and} \quad H(1) = \bar{\Psi} \Lambda \bar{L} \quad (4.13)$$

The MRTD method uses singular value decomposition to reduced the size of the eigenvalue problem in the original ITD formulation. The procedure starts by premultiplying both sides of the two equations in Eq. (4.13) by the matrix  $P_n^T$  yielding

$$P_n^T H(0) = P_n^T \bar{\Psi} \bar{L} \quad (4.14)$$

and

$$P_n^T H(1) = P_n^T \bar{\Psi} \Lambda \bar{L} \quad (4.15)$$

Define the reduced matrix  $\bar{\Psi}_n$  as

$$\bar{\Psi}_n = P_n^T \bar{\Psi} \quad (4.16)$$

The  $i - j$  element of  $\bar{\Psi}_n$  is the projection of the  $j$ -th columns of  $\bar{\Psi}$  projected along the  $i$ -th column of  $P_n$ .  $\bar{\Psi}_n$  is the projection of the columns of  $\bar{\Psi}$  into the  $n$  dimension space spanned by the columns of  $P_n$ . This is similar to a least squares solution. Equations (4.14) and (4.15) become

$$P_n^T H(0) = \bar{\Psi}_n \bar{L} \quad (4.17)$$

$$P_n^T H(1) = \bar{\Psi}_n \Lambda \bar{L} \quad (4.18)$$

To eliminate  $\bar{L}$  between the two Eqs. (4.17) and (4.18), premultiplying Eq. (4.17) by the unknown  $\bar{\Psi}_n^T$

$$\bar{\Psi}_n^T P_n^T H(0) = \bar{\Psi}_n^T \bar{\Psi}_n \bar{L} \quad (4.19)$$

Premultiplying Eq. (4.19) by the inverse of the matrix  $\bar{\Psi}_n^T \bar{\Psi}_n$ , where  $\bar{\Psi}_n^T \bar{\Psi}_n$  is full rank since from Eq. (4.16)  $\bar{\Psi}_n$  is full column rank, gives

$$\left(\bar{\Psi}_n^T \bar{\Psi}_n\right)^{-1} \bar{\Psi}_n^T P_n^T H(0) = \bar{L} \quad (4.20)$$

For a matrix of full column rank, the generalized inverse matrix  $\bar{\Psi}_n^+$  is  $\left(\bar{\Psi}_n^T \bar{\Psi}_n\right)^{-1} \bar{\Psi}_n^T$ , Eq. (4.20) becomes

$$\bar{\Psi}_n^+ P_n^T H(0) = \bar{L} \quad (4.21)$$

So this is a least squares solution for  $\bar{L}$  once  $\bar{\Psi}_n$  is known. To solve for  $\bar{\Psi}_n$ , substituting Eq. (4.21) into Eq. (4.18) yields

$$P_n^T H(1) = \bar{\Psi}_n \Lambda \bar{\Psi}_n^+ P_n^T H(0) \quad (4.22)$$

Define

$$H_{pn}(1) = P_n^T H(1) \quad H_{pn}(0) = P_n^T H(0) \quad (4.23)$$

where  $H_{pn}(1)$  and  $H_{pn}(0)$  will be of full row rank. Then the original Eq. (4.22) becomes

$$H_{pn}(1) = \bar{\Psi}_n \Lambda \bar{\Psi}_n^+ H_{pn}(0) \quad (4.24)$$

Postmultiplying Eq. (4.24) by the transpose of the Hankel matrix  $H_{pn}(0)$  produces

$$H_{pn}(1) H_{pn}^T(0) = \bar{\Psi}_n \Lambda \bar{\Psi}_n^+ H_{pn}(0) H_{pn}^T(0) \quad (4.25)$$

For a system with  $n$  order,  $H_{pn}(0)H_{pn}^T(0)$  is of dimensions  $n \times n$  and is full rank only if  $H_{pn}(0)$  is full row rank. In this case, postmultiplying Eq.(4.25) by the inverse of  $H_{pn}(0)H_{pn}^T(0)$  gives

$$H_{pn}(1)H_{pn}^T(0)[H_{pn}(0)H_{pn}^T(0)]^{-1} = \bar{\Psi}_n \Lambda \bar{\Psi}_n^+ \quad (4.26)$$

Define a  $n \times n$  matrix  $E$

$$\begin{aligned} E &= H_{pn}(1)H_{pn}^T(0)[H_{pn}(0)H_{pn}^T(0)]^{-1} \\ &= H_{pn}(1)H_{pn}^+(0) \end{aligned} \quad (4.27)$$

where  $H_{pn}^+(0) = H_{pn}^T(0)[H_{pn}(0)H_{pn}^T(0)]^{-1}$ . Note that  $E$  is calculated directly from the Hankel matrices. Equation (4.26) becomes

$$E = \bar{\Psi}_n \Lambda \bar{\Psi}_n^+ \quad (4.28)$$

To see that Eq. (4.28) is as an eigenvalue problem, postmultiply Eq. (4.28) by  $\bar{\Psi}_n$ , noting that  $\bar{\Psi}_n^+ \bar{\Psi}_n = I_n$  where  $I_n$  is an identity matrix with order  $n$

$$E \bar{\Psi}_n = \bar{\Psi}_n \Lambda \bar{\Psi}_n^+ \bar{\Psi}_n = \bar{\Psi}_n \Lambda \quad (4.29)$$

where

$$\Lambda = \text{diag}(e^{\lambda_1 \Delta t}, e^{\lambda_2 \Delta t}, \dots, e^{\lambda_n \Delta t}) = \text{diag}(z_1, z_2, \dots, z_n)$$

and  $\lambda_r = \sigma_r + j\omega_r$ ,  $r = 1, 2, \dots, n$ . Solving the eigenvalue-eigenvector problem in Eq. (4.29), the damping factors  $\sigma_r$ , and damped natural frequencies  $\omega_r$  of  $r$ -th mode can be determined as

$$\sigma_r = \frac{\text{Re}(\ln z_r)}{\Delta t} \quad \omega_r = \frac{\text{Im}(\ln z_r)}{\Delta t} \quad (4.30)$$

From Eqs. (4.4) and (4.5), the mode shape and modal participation matrices can be computed as follows

$$\Psi = E_{tr}^T \bar{\Psi} \quad (4.31)$$

and

$$L = \bar{L} E_{ms}$$

Recall that  $\bar{\Psi} = P_n \bar{\Psi}_n$ ,  $\bar{L} = \bar{\Psi}_n^{-1} H_{pn}(0)$ , and  $H_{pn}(0) = P_n^T H(0)$  given in Eqs. (4.16), (4.17), and (4.23), then

$$\Psi = E_{tr}^T P_n \bar{\Psi}_n \quad (4.32)$$

The matrix  $\bar{\Psi}_n$  is determined from the eigenvalue problem as given in Eq. (4.29) and once it is known  $L$  is determined by a least squares method given in Eq. (4.17)

$$L = \bar{\Psi}_n^{-1} P_n^T H(0) E_{ms} \quad (4.33)$$

The procedure of the MRTD method is

- 1) Form the Hankel matrices  $H(0)$  and  $H(1)$
- 2) Obtain the singular value decomposition matrices  $[P, \Sigma, Q]$  of  $H(0)$ .

- 3) Select the order of the system by truncating the decomposition matrices  $[P, \Sigma, Q]$ .
- 4) Premultiply both Hankel matrices by  $P_n^T$  to get  $H_{pn}(0)$  and  $H_{pn}(1)$  and form  $E$ .
- 5) Solve the eigenvalue-eigenvector problem in Eq. (4.29) to obtain the eigenvalues and eigenvectors of  $E$  matrix.
- 6) Calculate the frequencies and damping factors from Eq. (4.30).
- 7) Calculate the mode shapes from Eq. (4.32).
- 8) Calculate the modal participation matrix from Eq. (4.33).

This realization results in complex-valued mode shape and modal participation matrices. In next section, the real-valued realization of the MRTD method will be derived to compare with the output-normal realization of the ERA in Chapter 5.

#### 4.2.2 Real-Valued Realization of MRTD

The combination  $(\Lambda, L, \Psi)$  is a complex-valued realization of the MRTD method in complex modal coordinates. To obtain an equivalent realization where the matrices are real, it will be shown below that the matrix  $E$  can be used as the system matrix. The corresponding input matrix  $F$  and output matrix  $G$  of the MRTD method can then be derived. First, we show that the matrix  $E$  in MRTD can be expressed in terms of singular value decomposition matrices  $[P_n, \Sigma_n, Q_n]$  of  $H(0)$  and the Hankel matrix  $H(1)$ . Recall that from Eq. (4.27), the  $E$  matrix in MRTD is

$$E = H_{pn}(1)H_{pn}^T(0)[H_{pn}(0)H_{pn}^T(0)]^{-1} = H_{pn}(1)H_{pn}^+(0)$$

From Eq. (4.23) the reduced Hankel matrices  $H_{pn}(1)$  and  $H_{pn}(0)$  can be written in terms of by the Hankel matrices  $H(1)$  and  $H(0)$

$$E = P_n^T H(1) (P_n^T H(0))^T \left[ P_n^T H(0) (P_n^T H(0))^T \right]^{-1} \quad (4.34)$$

Note that

$$\begin{aligned} H(0) &= P \Sigma Q^T \\ &= [P_n, P_i] \begin{bmatrix} \Sigma_n & 0 \\ 0 & \Sigma_i \end{bmatrix} \begin{bmatrix} Q_n^T \\ Q_i^T \end{bmatrix} \end{aligned}$$

where

$$P = [P_n, P_i], \quad \Sigma = \begin{bmatrix} \Sigma_n & 0 \\ 0 & \Sigma_i \end{bmatrix}, \quad Q = [Q_n, Q_i]$$

Hence,

$$H(0) = P_n \Sigma_n Q_n^T + P_i \Sigma_i Q_i^T \quad (4.35)$$

$P_i$  is the matrix formed by the remaining columns of  $P$ ,  $\Sigma_i$  is the diagonal matrix of the remaining singular values in  $\Sigma$ , and  $Q_i$  is formed by the remaining columns of  $Q$ . Note that in the absence of noise,  $\Sigma_i$  is a zero matrix identically. In the presence of noise  $\Sigma_i$  is generally non-zero. Premultiplying Eq. (4.35) by  $P_n^T$ , then Eq. (4.35) becomes

$$P_n^T H(0) = P_n^T P_n \Sigma_n Q_n^T + P_n^T P_i \Sigma_i Q_i^T$$

Since the columns of  $P$  are orthonormal,  $P_n^T P_n$  is an identity matrix and  $P_n^T P_i$  is a zero matrix. Therefore,

$$P_n^T H(0) = \Sigma_n Q_n^T \quad (4.36)$$

Note that this result is independent of how the singular values are truncated. In other words, Eq. (4.36) is valid for both noise and noise-free cases. Substituting Eq. (4.36) into Eq. (4.34) yields

$$\begin{aligned} E &= P_n^T H(1) (\Sigma_n Q_n^T)^T \left[ \Sigma_n Q_n^T \quad (\Sigma_n Q_n^T)^T \right]^{-1} \\ &= P_n^T H(1) Q_n \Sigma_n (\Sigma_n^2)^{-1} \end{aligned}$$

Hence,

$$E = P_n^T H(1) Q_n \Sigma_n^{-1} \quad (4.37)$$

Therefore, the matrix  $E$  in MRTD can be written in terms of the singular value decomposition of  $H(0)$ , and  $H(1)$ . From Eq. (4.29), the  $E$  matrix in MRTD can be diagonalized as

$$E = \bar{\Psi}_n \Lambda \bar{\Psi}_n^{-1} \quad (4.38)$$

Therefore,

$$\Lambda = \bar{\Psi}_n^{-1} E \bar{\Psi}_n \quad (4.39)$$

where  $\Lambda$  is a diagonal matrix of eigenvalues of  $E$ ,  $\bar{\Psi}_n$  is an eigenvector matrix of  $E$ . Recall that the pulse response function in the modal space coordinates is expressed as

$$Y(k) = \Psi \Lambda^k L \quad (4.40)$$

Replacing  $\Lambda$  in above Eq. (4.40) by  $\bar{\Psi}_n^{-1} E \bar{\Psi}_n$  in Eq. (4.39) yields

$$Y(k) = (\Psi \bar{\Psi}_n^{-1}) E^k (\bar{\Psi}_n L)$$

To make the realization  $[E, F, G]$  equivalent to the complex valued realization  $[\Lambda, L, \Psi]$  of the MRTD method in modal space coordinates, we must have

$$G = \Psi \bar{\Psi}_n^{-1} \quad (4.41)$$

and

$$F = \bar{\Psi}_n L \quad (4.42)$$

so that  $\Psi \Lambda^k L = G E^k F$ . Since  $\Psi = E_{t'}^T \bar{\Psi}$  and  $L = \bar{L} E_{ms}$  in Eq. (4.31), Eqs. (4.41) and (4.42) become

$$G = E_{t'}^T \bar{\Psi} \bar{\Psi}_n^{-1} \quad (4.43)$$

and

$$F = \bar{\Psi}_n \bar{L} E_{ms} \quad (4.44)$$

From Eq. (4.16),  $\bar{\Psi} = P_n \bar{\Psi}_n$ . Therefore, Eq.(4.43) becomes

$$G = E_{t'}^T P_n \bar{\Psi}_n \bar{\Psi}_n^{-1} = E_{t'}^T P_n$$

which is a real-valued output matrix. Also, from Eq. (4.17),

$$\begin{aligned} \bar{L} &= \bar{\Psi}_n^{-1} P_n^T H(0) \\ &= \bar{\Psi}_n^{-1} \Sigma_n Q_n^T \end{aligned} \quad (4.45)$$

since  $P_n^T H(0) = \Sigma_n Q_n^T$  as given in Eq. (4.36). Substituting Eq. (4.45) into Eq. (4.44) yields

$$F = \Sigma_n Q_n^T E_{ms}$$

which is a real-valued input matrix. In summary, we have found a real-valued realization  $[E, F, G]$  of the MRTD method,

$$\begin{aligned}
 E &= P_n^T H(1) Q_n \Sigma_n^{-1} \\
 F &= \Sigma_n Q_n^T E_{ms} \\
 G &= E_{tr}^T P_n
 \end{aligned} \tag{4.46}$$

Equation (4.46) is the same as Eq. (3.20).

In the original formulation for the MRTD method,<sup>17</sup> the transfer matrix  $P$  is found by solving the following eigenvalue problem

$$H(0)H^T(0)P = P\Sigma^2$$

If the Hankel matrix has more rows than columns, then the size of the matrix  $H(0)H^T(0)$  may become too large to be installed in a small computer.<sup>17</sup> This motivates a modified formulation that does not require solving a large eigenvalue problem. This is known as the Modified Multiple-Reference Time Domain method (MMRTD).<sup>17</sup> In next section, the MMRTD is presented.

## 4.3 Modified Multiple-Reference Time Domain (MMRTD)

### 4.3.1 Traditional Development

In this section, a complex-valued realization  $[\Lambda, L_m, \Psi_m]$  by the Modified Multiple-Reference Time Domain method (MMRTD) in modal space coordinates is derived<sup>17</sup>, and also an equivalent real-valued realization  $[E_m, F_m, G_m]$  of the MMRTD method will be derived. The procedure starts from the singular value decomposition of the Hankel matrix  $H(0)$  in the same way as the MRTD and ERA methods do. The Hankel matrix  $H(0)$  can be written as

$$H(0) = P\Sigma Q^T \approx P_n \Sigma_n Q_n^T \quad (4.47)$$

or

$$H^T(0) = Q\Sigma P^T \approx Q_n \Sigma_n P_n^T \quad (4.48)$$

Recall that the Hankel matrices  $H(0)$  and  $H(1)$  can be written as

$$H(0) = \bar{\Psi} \bar{L} \quad \text{and} \quad H(1) = \bar{\Psi} \Lambda \bar{L}$$

Transposing the above equations yields

$$H^T(0) = \bar{L}^T \bar{\Psi}^T \quad (4.49)$$

$$H^T(1) = \bar{L}^T \Lambda \bar{\Psi}^T \quad (4.50)$$

Premultiplying Eqs. (4.49) and (4.50) by the transfer matrix  $Q_n^T$  produce

$$Q_n^T H^T(0) = Q_n^T \bar{L}^T \bar{\Psi}^T \quad (4.51)$$

and

$$Q_n^T H^T(1) = Q_n^T \bar{L}^T \Lambda \bar{\Psi}^T \quad (4.52)$$

After singular value truncation, define the reduced modal participation matrix  $\bar{L}_n^T$  as

$$\bar{L}_n^T = Q_n^T \bar{L}^T \quad (4.53)$$

Equations (4.51) and (4.52) become

$$Q_n^T H^T(0) = \bar{L}_n^T \bar{\Psi}^T \quad (4.54)$$

$$Q_n^T H^T(1) = \bar{L}_n^T \Lambda \bar{\Psi}^T \quad (4.55)$$

Premultiplying Eq. (4.54) by  $\bar{L}_n$  gives

$$\bar{L}_n Q_n^T H^T(0) = \bar{L}_n \bar{L}_n^T \bar{\Psi}^T \quad (4.56)$$

Define a generalized inverse matrix  $\bar{L}_n^+ = (\bar{L}_n \bar{L}_n^T)^{-1} \bar{L}_n$ ,  $\bar{L}_n$  must have full row rank, Eq. (4.56) becomes

$$\bar{L}_n^+ Q_n^T H^T(0) = \bar{\Psi}^T \quad (4.57)$$

Substituting Eq. (4.57) into Eq. (4.55) yields

$$Q_n^T H^T(1) = \bar{L}_n^T \Lambda \bar{L}_n^+ Q_n^T H^T(0) \quad (4.58)$$

Define the reduced Hankel matrices  $H_{Q_n}(0)$  and  $H_{Q_n}(1)$

$$H_{Q_n}(0) = Q_n^T H^T(0) \quad (4.59)$$

$$H_{Q_n}(1) = Q_n^T H^T(1) \quad (4.60)$$

Equation (4.58) becomes

$$H_{Q_n}(1) = \bar{L}_n^T \Lambda \bar{L}_n^+ H_{Q_n}(0) \quad (4.61)$$

Postmultiplying Eq. (4.61) by the transpose of the Hankel matrix  $H_{Q_n}(0)$  yields

$$H_{Q_n}(1)H_{Q_n}^T(0) = \bar{L}_n^T \Lambda \bar{L}_n^+ H_{Q_n}(0)H_{Q_n}^T(0) \quad (4.62)$$

where  $H_{Q_n}(0)H_{Q_n}^T(0)$  is a  $n \times n$  full rank matrix. Postmultiplying Eq. (4.62) by the inverse of  $H_{Q_n}(0)H_{Q_n}^T(0)$  matrix gives

$$H_{Q_n}(1)H_{Q_n}^T(0)[H_{Q_n}(0)H_{Q_n}^T(0)]^{-1} = \bar{L}_n^T \Lambda \bar{L}_n^+ \quad (4.63)$$

Define

$$E_m^T = H_{Q_n}(1)H_{Q_n}^T(0)[H_{Q_n}(0)H_{Q_n}^T(0)]^{-1} \quad (4.64)$$

Equation (4.63) becomes

$$E_m^T = \bar{L}_n^T \Lambda \bar{L}_n^+ \quad (4.65)$$

Since  $\bar{L}_n^+ \bar{L}_n^T$  is an identity matrix, postmultiplying Eq. (4.65) by  $\bar{L}_n^T$ , one obtains

$$E_m^T \bar{L}_n^T = \bar{L}_n^T \Lambda \bar{L}_n^+ \bar{L}_n^T = \bar{L}_n^T \Lambda (\bar{L}_n \bar{L}_n^T)^{-1} \bar{L}_n \bar{L}_n^T \quad (4.66)$$

Therefore, the eigenvalue problem is

$$E_m^T \bar{L}_n^T = \bar{L}_n^T \Lambda \quad (4.67)$$

or

$$\bar{L}_n E_m = \Lambda \bar{L}_n \quad (4.68)$$

where

$$\Lambda = \text{diag}(e^{\lambda_1 \Delta t}, e^{\lambda_2 \Delta t}, \dots, e^{\lambda_n \Delta t}) = \text{diag}(z_1, z_2, \dots, z_n)$$

and  $\lambda_r = \sigma_r + j\omega_r$ ,  $r = 1, 2, \dots, n$ . Solving the eigenvalue-eigenvector problem in Eq. (4.67), the damping factor  $\sigma_r$ , and damped natural frequency  $\omega_r$  of  $r$ -th mode can be determined as

$$\sigma_r = \frac{\text{Re}(\ln z_r)}{\Delta t} \quad \omega_r = \frac{\text{Im}(\ln z_r)}{\Delta t} \quad (4.69)$$

The mode shape and modal participation matrices given in Eq. (4.31) are

$$\Psi = E_{tr}^T \bar{\Psi}, \quad L = \bar{L} E_{ms}$$

Recall that  $\bar{L} = \bar{L}_n Q_n^T$  and  $\bar{\Psi} = H(0) Q_n (\bar{L}_n)^{-1}$  given in Eqs. (4.53) and (4.54). Therefore,

$$L = \bar{L}_n Q_n^T E_{ms} \quad (4.70)$$

The matrix  $\bar{L}_n$  is determined from the eigenvalue problem as given in Eq. (4.67) and once it is known,  $\Psi$  is determined by a least squares solution

$$\Psi = E_{tr}^T H(0) Q_n (\bar{L}_n)^{-1} \quad (4.71)$$

The procedures of the MMRTD method are

- 1) Form the Hankel matrices  $H(0)$  and  $H(1)$
- 2) Obtain the singular value decomposition matrices  $[P, \Sigma, Q]$  of  $H(0)$ .

- 3) Select the order of the system by truncating the decomposition matrices  $[P, \Sigma, Q]$ .
- 4) Premultiply the transpose of both Hankel matrices given in Eqs. (4.49) and (4.50) by  $Q_n^T$  to get  $H_{Q_n}(0)$  and  $H_{Q_n}(1)$  and form  $E_m^T$ .
- 5) Solve the eigenvalue-eigenvector problem in Eq. (4.67) to obtain the eigenvalues and eigenvectors of  $E_m^T$  matrix.
- 6) Calculate the frequencies and damping factors from Eq. (4.69).
- 7) Calculate the mode shapes from Eq. (4.71).
- 8) Calculate the modal participation matrix from Eq. (4.70).

Therefore, the combination  $[\Lambda, L_m, \Psi_m]$  is a complex-valued realization of the MMRTD method in complex modal coordinates. In the original formulation for MMRTD method, the transfer matrix  $Q$  is found by solving the following eigenvalue problem<sup>17</sup>

$$H^T(0)H(0)Q = Q\Sigma^2$$

In the case  $H(0)$  has more number of rows than columns, the product  $H^T(0)H(0)$  is of smaller dimensions. In the next section, the real-valued realization of the MMRTD method will be derived to compare with the input-normal realization of the ERA in Chapter 5.

### 4.3.2 Real-Valued Realization of MMRTD

Alternately, if the  $E_m$  matrix in Eq. (4.64) is used as the system matrix, the corresponding input matrix  $F_m$  and output matrix  $G_m$  of the MMRTD method can be derived as follows. First, we show that the matrix  $E_m$  in MMRTD can also be expressed in terms of the singular value decomposition matrices  $[P_n, \Sigma_n, Q_n]$  of  $H(0)$  and the

Hankel matrix  $H(1)$  in the same way as the matrix  $E$  does in MRTD. Recall that from Eq. (4.64), the matrix  $E_m^T$  in MMRTD is

$$E_m^T = H_{Q_n}(1)H_{Q_n}^T(0)\left[H_{Q_n}(0)H_{Q_n}^T(0)\right]^{-1}$$

Recall that  $H(0) = P_n \Sigma_n Q_n^T + P_i \Sigma_i Q_i^T$  as given in Eq. (4.35) in Section 4.2.1. Postmultiplying both sides of Eq. (4.35) by  $Q_n$ , then the Eq. (4.35) becomes

$$H(0)Q_n = P_n \Sigma_n Q_n^T Q_n + P_i \Sigma_i Q_i^T Q_n$$

Since the columns of  $Q$  are orthonormal,  $Q_n^T Q_n$  is an identity matrix and  $Q_i^T Q_n$  is a zero matrix. Therefore,

$$H(0)Q_n = P_n \Sigma_n \tag{4.72}$$

Note that this result is independent of how the singular values are truncated. In other words, Eq. (4.72) is valid for both noise and noise-free cases. The reduced Hankel matrices  $H_{Q_n}(0)$  and  $H_{Q_n}(1)$  in Eqs. (4.59) and (4.60) can be replaced by the Hankel matrices  $H(1)$  and  $H(0)$ , respectively with above Eq. (4.72). Therefore, equation (4.64) becomes

$$\begin{aligned} E_m^T &= Q_n^T H^T(1) (Q_n^T H^T(0))^T \left[ Q_n^T H^T(0) (Q_n^T H^T(0))^T \right]^{-1} \\ &= Q_n^T H^T(1) P_n \Sigma_n [\Sigma_n^2]^{-1} = Q_n^T H^T(1) P_n \Sigma_n^{-1} \end{aligned}$$

or

$$E_m = \Sigma_n^{-1} P_n^T H(1) Q_n \tag{4.73}$$

The  $E_m$  matrix in the MMRTD method can be diagonalized with its eigenvector matrix  $\bar{L}_n$  as

$$E_m = \bar{L}_n^{-1} \Lambda \bar{L}_n$$

Therefore,

$$\Lambda = \bar{L}_n E_m \bar{L}_n^{-1} \quad (4.74)$$

where  $\Lambda = \text{diag}(e^{\lambda_1 \Delta t}, e^{\lambda_2 \Delta t}, \dots, e^{\lambda_n \Delta t})$  is a diagonal matrix of the eigenvalues of  $\bar{L}_n$ . Recall that the pulse response function in the modal coordinates is

$$Y(k) = \Psi \Lambda^k L \quad (4.75)$$

Replacing  $\Lambda$  in Eq. (4.75) by  $\bar{L}_n E_m \bar{L}_n^{-1}$  in Eq. (4.70) yields

$$Y(k) = (\Psi \bar{L}_n) E_m^k (\bar{L}_n^{-1} L)$$

To make the realization  $(E_m, F_m, G_m)$  equivalent to the complex realization  $[\Lambda, L_m, \Psi_m]$  of the MMRTD method, one must have

$$G_m = \Psi \bar{L}_n \quad (4.76)$$

and

$$F_m = \bar{L}_n^{-1} L \quad (4.77)$$

where  $\bar{L}_n$  is the eigenvector matrix of  $E_m$ , so that  $\Psi \Lambda^k L = G_m E_m^k F_m$ . Recall that  $\Psi = E_{tr}^T \bar{\Psi}$ , and  $\bar{\Psi} = H(0) Q_n \bar{L}_n^{-1}$  as given in Eqs. (4.31) and (4.54), respectively. Hence,

$$\Psi = E_{tr}^T H(0) Q_n \bar{L}_n^{-1} \quad (4.78)$$

Substituting Eqs. (4.78) and (4.72) into Eq. (4.76) yields

$$G_m = E_{tr}^T P_n \Sigma_n$$

which is a real-valued output matrix. Also, from Eq. (4.70), we know that  $L = \bar{L}_n Q_n^T E_{ms}$ . Therefore, Eq. (4.77) becomes

$$F_m = Q_n^T E_{ms}$$

which is a real-valued input matrix. In summary, we have found a real-valued realization of the MMRTD method,

$$E_m = \Sigma_n^{-1} P_n^T H(1) Q_n$$

$$F_m = Q_n^T E_{ms} \quad (4.79)$$

$$G_m = E_{tr}^T P_n \Sigma_n$$

Equation (4.79) is the same as Eq. (3.10).

## **Chapter 5**

# **Coordinate Transformation Matrices between Different Equivalent Realizations**

In this chapter, the coordinate transformation matrices between different equivalent realizations presented in previous chapters will be derived. Section 5.1 describes the relationship between output-normal form of the ERA and MRTD methods. Section 5.2 describes the relationship between input-normal form of the ERA and MMRTD methods. In Section 5.3, the coordinate transformation matrices between three different equivalent realizations, input-normal, internally balanced, and output-normal realizations, are derived.

### **5.1 Relationship between ERA and MRTD Realizations**

For convenience, the output-normal realization of the ERA and the real realization of the MRTD method are summarized below. With  $H(0) = P_n \Sigma_n Q_n^T$  in the noise free case and  $H(0) = P_n \Sigma_n Q_n^T$  in the noise case, recall that the output-normal minimal realization of the ERA given in Eq. (3.20) is

$$\begin{aligned}
A_o &= P_n^T H(1) Q_n \Sigma_n^{-1} \\
B_o &= \Sigma_n Q_n^T E_{ms}
\end{aligned} \tag{5.1}$$

$$C_o = E_{tr}^T P_n$$

Recall also that the real valued realization of the MRTD method given in Section 4.2.2 is

$$\begin{aligned}
E &= H_{pn}(1) H_{pn}^T(0) [H_{pn}(0) H_{pn}^T(0)]^{-1} \\
F &= \Sigma_n Q_n^T E_{ms}
\end{aligned} \tag{5.2}$$

$$G = E_{tr}^T P_n$$

where we have used the formula for  $E$  as derived in the original MRTD formulation. However, it is shown in Eq. (4.37) that the expression for  $E$  in Eq. (5.2) is the same as

$$E = P_n^T H(1) Q_n \Sigma_n^{-1}$$

Comparing Eq. (5.1) to Eq. (5.2) reveals that *the real-valued realization* ( $E$ ,  $F$ ,  $G$ ) of *the MRTD method is exactly the same as the output-normal realization* ( $A_o$ ,  $B_o$ ,  $C_o$ ) of the ERA, *ie.*,

$$E = A_o$$

$$F = B_o$$

$$G = C_o$$

## 5.2 Relationship between ERA and MMRTD Realizations

In this section, the relationship between the real realization  $[E_m, F_m, G_m]$  of the MMRTD method and the input-normal realization  $[A_i, B_i, C_i]$  of the ERA is shown. Recall that the input-normal minimal realization of the ERA given in Eq. (3.10) is

$$\begin{aligned}
 A_i &= \Sigma_n^{-1} P_n^T H(1) Q_n \\
 B_i &= Q_n^T E_{ms} \\
 C_i &= E_{tr}^T P_n \Sigma_n
 \end{aligned} \tag{5.3}$$

Recall also that the real realization of the MMRTD method given in Section 4.3.2 is

$$\begin{aligned}
 E_m^T &= H_{Q_n}(1) H_{Q_n}^T(0) \left( H_{Q_n}(0) H_{Q_n}^T(0) \right)^{-1} \\
 F_m &= Q_n^T E_{ms} \\
 G_m &= E_{tr}^T P_n \Sigma_n
 \end{aligned} \tag{5.4}$$

where again, we have used the formula for  $E_m^T$  as in the original MMRTD formulation. However, it is shown in Eq. (4.73) that the expression for  $E_m$  in Eq. (5.4) is the same as

$$E_m = \Sigma_n^{-1} P_n^T H(1) Q_n$$

Comparing Eq. (5.3) to Eq. (5.4) shows that *the real realization*  $(E_m, F_m, G_m)$  of the MMRTD method is the same as the *input-normal realization*  $(A_i, B_i, C_i)$  of the ERA, ie.,

$$\begin{aligned} E_m &= A_i \\ F_m &= B_i \\ G_m &= C_i \end{aligned}$$

### 5.3 Transformation Matrices between three Realizations of the ERA

In this section, the transformation matrices between three different realizations, input-normal, internally balanced, and output-normal realizations of the ERA, are derived. Recall that the internally balanced minimal realization of the ERA given in Eq. (3.15) is

$$\begin{aligned} A_b &= \Sigma_n^{-1/2} P_n^T H(1) Q_n \Sigma_n^{-1/2} \\ B_b &= \Sigma_n^{1/2} Q_n^T E_{ms} \\ C_b &= E_{ls}^T P_n \Sigma_n^{1/2} \end{aligned} \tag{5.5}$$

Comparing Eq. (5.1) to Eq. (5.3) reveals that the output-normal and the input-normal realizations of the ERA are related by the transformation matrix  $\Sigma_n$ , ie.,

$$\begin{aligned} A_o &= \Sigma_n A_i \Sigma_n^{-1} & A_i &= \Sigma_n^{-1} A_o \Sigma_n \\ B_o &= \Sigma_n B_i & \text{or} & B_i &= \Sigma_n^{-1} B_o \\ C_o &= C_i \Sigma_n^{-1} & C_i &= C_o \Sigma_n \end{aligned} \tag{5.6}$$

Similarly, comparing Eq. (5.1) to Eq. (5.5) reveals that the output-normal and internally balanced realizations of the ERA are related by the transformation matrix  $\Sigma_n^{1/2}$ , ie.,

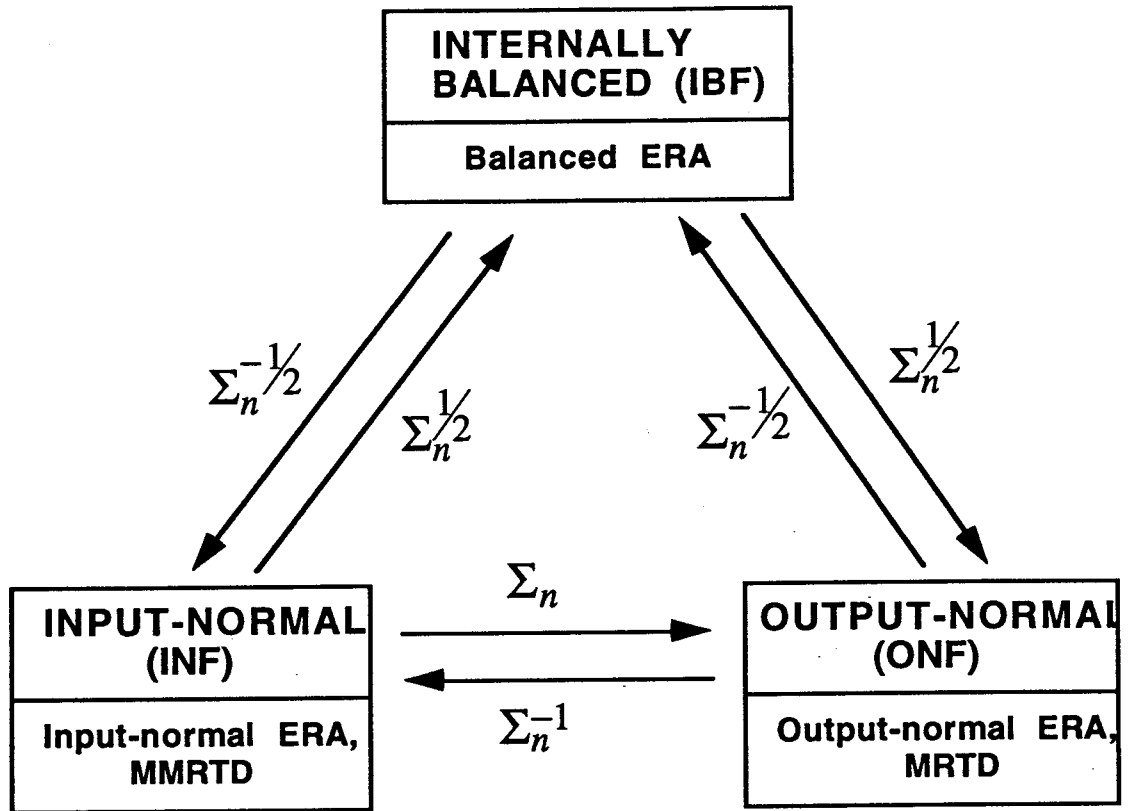
$$\begin{aligned}
 A_o &= \Sigma_n^{1/2} A_b \Sigma_n^{-1/2} & A_b &= \Sigma_n^{-1/2} A_o \Sigma_n^{1/2} \\
 B_o &= \Sigma_n^{1/2} B_b & \text{or} & & B_b &= \Sigma_n^{-1/2} B_o \\
 C_o &= C_b \Sigma_n^{-1/2} & & & C_b &= C_o \Sigma_n^{1/2}
 \end{aligned} \tag{5.7}$$

Finally, comparing Eq. (5.3) to Eq. (5.5) reveals that the input-normal and internally balanced realizations of the ERA are related by the transformation matrix  $\Sigma_n^{-1/2}$ , ie.,

$$\begin{aligned}
 A_i &= \Sigma_n^{-1/2} A_b \Sigma_n^{1/2} & A_b &= \Sigma_n^{1/2} A_i \Sigma_n^{-1/2} \\
 B_i &= \Sigma_n^{-1/2} B_b & \text{or} & & B_b &= \Sigma_n^{1/2} B_i \\
 C_i &= C_b \Sigma_n^{1/2} & & & C_b &= C_i \Sigma_n^{-1/2}
 \end{aligned} \tag{5.8}$$

## 5.4 Summary Graphics

In previous sections, the transformation matrices between the three different equivalent realizations of the ERA are presented. Recall that the real realization of the MRTD method is the same as the output-normal realization of the ERA, and the real realization of the MMRTD method is the same as the input-normal realization of the ERA. These transformation matrices are summarized in the following graphics.



## Chapter 6

### **Numerical Results**

The three realizations of the ERA and the realizations of the MRTD and MMRTD methods are theoretically identical and would give the same mode shapes and complex frequencies when there are no numerical errors. The purpose of this chapter is to determine the difference for computer implementation. The theoretical results presented in Chapters 3-5 are now illustrated by a set of examples using both simulated and actual experimental data. The simulated system has closely spaced frequencies and mode shapes. The test example is performed using data from an actual structure (HMB-2R). The following example will show that from the Hankel matrix, the input-normal, output-normal, and internally balanced realizations of the ERA are equivalent to 11 decimal places. Furthermore, the real-valued realization of the MRTD method is numerically the same as the output-normal realization of the ERA and the real-valued realization of the MMRTD method is numerically the same as the input-normal realization of the ERA. The calculation is performed using double precision 386 MATLAB<sup>24</sup> on an IBM 386 personal computer.

## 6.1 Simulation Results

In the simulation example, the data is generated from an eight-order, four-output, and one-input system with the following modal characteristics. The real-valued mode shape matrix is taken to be

$$\Psi_r = \begin{bmatrix} 1.00 & 0.00 & 2.00 & 0.00 & 2.002 & 0.00 & 3.00 & 0.00 \\ 2.00 & 0.00 & 3.00 & 0.00 & 3.003 & 0.00 & 4.00 & 0.00 \\ 1.00 & 0.00 & 3.00 & 0.00 & 3.003 & 0.00 & 4.00 & 0.00 \\ 0.00 & 0.00 & 2.00 & 0.00 & 2.002 & 0.00 & 4.00 & 0.00 \end{bmatrix} \quad (6.1)$$

with damping factors and damped frequencies given in Table 2.

Table 2: Damped frequencies and damping factors of model used in simulation

Mode No.	Damped Frequencies $\omega_{dr}$ (Hz)	Damping Factor $\zeta_r$
1	1.000	0.0025
2	9.000	0.0022
3	9.003	0.0022
4	20.000	0.0499

The real-valued modal participation vector  $L_r$  is given in Eq. (C.4) where

$$l = \begin{bmatrix} l_1 \\ l_2 \\ l_3 \\ l_4 \end{bmatrix} = \begin{bmatrix} 1.0 \\ 3.0 \\ 3.5 \\ 4.0 \end{bmatrix}, \quad \varphi = \begin{bmatrix} \varphi_{11} \\ \varphi_{12} \\ \varphi_{13} \\ \varphi_{14} \end{bmatrix} = \begin{bmatrix} 0 \\ \pi/3 \\ 0 \\ \pi/4 \end{bmatrix}, \quad \theta = \begin{bmatrix} \theta_1 \\ \theta_2 \\ \theta_3 \\ \theta_4 \end{bmatrix} = \begin{bmatrix} \pi/4 \\ \pi \\ \pi/3 \\ 0 \end{bmatrix} \quad (6.2)$$

The real system matrix  $\Lambda_r$  is given in Eq. (C.2) with the damped frequencies and damping factors given in Table 2. Note that the second and the third modes have closely spaced frequencies and specially similar mode shapes. The Markov parameters of the system described by  $\Lambda_r$ ,  $\Psi_r$ , and  $L_r$  are computed from (see Appendix C)

$$Y(k) = \Psi_r(\Lambda_r)^k L_r \quad (6.3)$$

With the simulated data computed from Eq. (6.3), the Hankel matrix is formed with 127 row shifts and 31 column shifts. The Hankel matrix size is  $512 \times 32$ . This Hankel matrix is used to compute all the realizations shown below. The 127 row shifts were selected to produce about 1 cycle of the lowest frequency. The data span does not cover a beating period of the closely spaced frequencies which would require a  $42721 \times 32$  matrix.

### 6.1.1 Noise-free Results

In this section, results from the three realizations of the ERA method will be presented. It will be showed that three realizations of the ERA produce the same Markov parameters. These three different realizations can be transformed from one to the other by transformation matrices. The damping factors, damped frequencies, and mode shapes of the MRTD and MMRTD methods are verified to be the same as results from three realizations of the ERA. In the following examples, only three decimal places are shown.

For the noise-free case, the three realizations of the ERA are

(1) Input-normal realization

$$A_i = \begin{bmatrix} 0.551 & 0.828 & 0.000 & 0.000 & -0.000 & 0.000 & -0.000 & 0.000 \\ -0.829 & 0.556 & -0.000 & -0.000 & -0.000 & 0.000 & 0.000 & -0.000 \\ 0.012 & 0.008 & 0.972 & -0.037 & 0.184 & -0.033 & 0.000 & -0.000 \\ 0.014 & 0.009 & -0.047 & 0.929 & 0.351 & -0.016 & 0.000 & -0.000 \\ 0.062 & 0.042 & -0.247 & -0.377 & 0.905 & 0.009 & 0.000 & -0.000 \\ -0.149 & -0.102 & 0.180 & 0.073 & 0.034 & 0.990 & -0.000 & 0.000 \\ -0.053 & -0.036 & 0.048 & 0.015 & 0.032 & -0.058 & 0.902 & -0.378 \\ -0.031 & -0.021 & 0.050 & 0.034 & -0.097 & 0.246 & 0.479 & 0.904 \end{bmatrix}$$

$$B_i = \begin{bmatrix} 0.240 \\ -0.097 \\ -0.220 \\ -0.107 \\ -0.103 \\ 0.326 \\ 0.188 \\ -0.259 \end{bmatrix} \quad (6.4)$$

$$C_i = \begin{bmatrix} 85.375 & 34.197 & -0.023 & 0.533 & -6.074 & 4.969 & 0.000 & -0.003 \\ 113.911 & 44.960 & -0.196 & 0.863 & -8.373 & 9.629 & 0.000 & -0.004 \\ 113.831 & 45.682 & 0.126 & 0.736 & -9.846 & 5.283 & 0.000 & -0.004 \\ 113.677 & 46.869 & 0.300 & 0.406 & -7.549 & 0.620 & 0.000 & -0.003 \end{bmatrix}$$

(2) Output-normal realization

$$A_o = \begin{bmatrix} 0.551 & 0.829 & 0.001 & 0.002 & -0.002 & 0.000 & -0.003 & 0.044 \\ -0.828 & 0.556 & -0.000 & -0.001 & -0.000 & 0.001 & 0.002 & -0.032 \\ 0.001 & 0.000 & 0.972 & -0.042 & 0.213 & -0.077 & 0.000 & -0.012 \\ 0.001 & 0.000 & -0.042 & 0.929 & 0.363 & -0.033 & 0.001 & -0.012 \\ 0.005 & 0.003 & -0.214 & -0.365 & 0.965 & 0.018 & 0.002 & -0.042 \\ -0.006 & -0.004 & 0.079 & 0.036 & 0.017 & 0.990 & -0.004 & 0.054 \\ -0.000 & -0.000 & 0.000 & 0.000 & 0.000 & -0.000 & 0.902 & -0.422 \\ -0.000 & -0.000 & 0.000 & 0.000 & -0.000 & 0.000 & 0.429 & 0.904 \end{bmatrix}$$

$$B_o = \begin{bmatrix} 386.144 \\ -156.163 \\ -37.671 \\ -16.403 \\ -15.349 \\ 24.397 \\ 0.008 \\ -0.010 \end{bmatrix} \quad (6.5)$$

$$C_o = \begin{bmatrix} 0.053 & 0.021 & -0.000 & 0.003 & -0.041 & 0.066 & 0.012 & -0.081 \\ 0.070 & 0.028 & -0.001 & 0.005 & -0.056 & 0.128 & 0.022 & -0.122 \\ 0.070 & 0.028 & 0.000 & 0.004 & -0.066 & 0.070 & 0.015 & -0.123 \\ 0.070 & 0.029 & 0.001 & 0.002 & -0.051 & 0.008 & 0.005 & -0.083 \end{bmatrix}$$

(3) Internally balanced realization

$$A_b = \begin{bmatrix} 0.551 & 0.829 & 0.000 & 0.000 & -0.000 & 0.000 & -0.000 & 0.000 \\ -0.829 & 0.556 & -0.000 & -0.000 & -0.000 & 0.000 & 0.000 & -0.000 \\ 0.003 & 0.002 & 0.972 & -0.039 & 0.198 & -0.050 & 0.000 & -0.000 \\ 0.004 & 0.003 & -0.045 & 0.929 & 0.357 & -0.023 & 0.000 & -0.000 \\ 0.018 & 0.012 & -0.230 & -0.371 & 0.905 & 0.012 & 0.000 & -0.000 \\ -0.032 & -0.022 & 0.119 & 0.051 & 0.024 & 0.990 & -0.000 & 0.001 \\ -0.000 & -0.000 & 0.000 & 0.000 & 0.000 & -0.001 & 0.902 & -0.400 \\ -0.000 & -0.000 & 0.000 & 0.000 & -0.001 & 0.005 & 0.454 & 0.904 \end{bmatrix}$$

$$B_b = \begin{bmatrix} 9.632 \\ -3.898 \\ -2.884 \\ -1.327 \\ -1.263 \\ 2.823 \\ 0.039 \\ 0.051 \end{bmatrix} \quad (6.6)$$

$$C_b = \begin{bmatrix} 2.129 & 0.853 & -0.001 & 0.043 & -0.499 & 0.575 & 0.002 & -0.016 \\ 2.841 & 1.122 & -0.015 & 0.069 & -0.689 & 1.114 & 0.004 & -0.024 \\ 2.839 & 1.140 & 0.009 & 0.059 & -0.810 & 0.611 & 0.003 & -0.024 \\ 2.835 & 1.169 & 0.023 & 0.032 & -0.621 & 0.071 & 0.001 & -0.016 \end{bmatrix}$$

Note that in the input-normal realization, the elements of the input matrix  $B_i$  range from  $-0.097$  to  $0.326$ , a ratio of less than four while the elements of the output matrix  $C_i$  have values ranging from  $2.401 \times 10^{-4}$  to  $113.911$ , a ratio of about  $10^6$ . Similarly, in the output-normal realization, the elements of the output matrix  $C_o$  range from  $-0.0001$  to  $0.128$ , a ratio of 1280 while the elements of the input matrix  $B_o$  have values ranging from  $0.008$  to  $386.144$ , a ratio of 48000. However, in the internally balanced realization, the elements of the input matrix  $B_b$  range from  $0.039$  to  $9.632$ , a ratio of 250, and the elements of the output matrix  $C_b$  range from  $0.001$  to  $2.841$ , a ratio of less than 2800. From this, we might expect the internally balanced realization to be better conditioned numerically. Numerical test shows that the realizations of the ERA produce the same Markov parameters to 11 significant digits. That is

$$C_i B_i = C_o B_o = C_b B_b$$

$$C_i A_i B_i = C_o A_o B_o = C_b A_b B_b$$

and

$$C_i A_i^2 B_i = C_o A_o^2 B_o = C_b A_b^2 B_b$$

$$\vdots$$

$$C_i A_i^{640} B_i = C_o A_o^{640} B_o = C_b A_b^{640} B_b$$

to 11 significant digits.

Comparing Eqs. (6.4), (6.5), and (6.6), transformation matrices between three realizations of the ERA can be obtained

(1) The transformation matrix from input-normal realization to internally balanced realization is

$$T_{ib} = \Sigma_n^{1/2} = \begin{bmatrix} 40.086 & 0 & 0 & 0 & 0 & 0 & 0 & 0 \\ 0 & 40.062 & 0 & 0 & 0 & 0 & 0 & 0 \\ 0 & 0 & 13.062 & 0 & 0 & 0 & 0 & 0 \\ 0 & 0 & 0 & 12.357 & 0 & 0 & 0 & 0 \\ 0 & 0 & 0 & 0 & 12.150 & 0 & 0 & 0 \\ 0 & 0 & 0 & 0 & 0 & 8.642 & 0 & 0 \\ 0 & 0 & 0 & 0 & 0 & 0 & 0.210 & 0 \\ 0 & 0 & 0 & 0 & 0 & 0 & 0 & 0.199 \end{bmatrix}$$

i.e.,

$$T_{ib}A_iT_{ib}^{-1} = \begin{bmatrix} 0.551 & 0.829 & 0.000 & 0.000 & -0.000 & 0.000 & -0.000 & 0.000 \\ -0.829 & 0.556 & -0.000 & -0.000 & -0.000 & 0.000 & 0.000 & -0.000 \\ 0.003 & 0.002 & 0.972 & -0.039 & 0.198 & -0.050 & 0.000 & -0.000 \\ 0.004 & 0.003 & -0.045 & 0.929 & 0.357 & -0.023 & 0.000 & -0.000 \\ 0.018 & 0.012 & -0.230 & -0.371 & 0.905 & 0.012 & 0.000 & -0.000 \\ -0.032 & -0.022 & 0.119 & 0.051 & 0.024 & 0.990 & -0.000 & 0.001 \\ -0.000 & -0.000 & 0.000 & 0.000 & 0.000 & -0.001 & 0.902 & -0.400 \\ -0.000 & -0.000 & 0.000 & 0.000 & -0.001 & 0.005 & 0.454 & 0.904 \end{bmatrix}$$

The values of the elements in  $T_{ib}A_iT_{ib}^{-1}$  and  $A_b$  given in Eq. (6.6) agree up to 14 decimal places except for 8 values that agree up to 12 decimal places. Likewise,  $T_{ib}B_i = B_b$  to 14 decimal places and  $C_iT_{ib}^{-1} = C_b$  to 14 decimal places.

(2) The transformation matrix from output-normal realization to internally balanced realization of the ERA is

$$T_{ob} = \Sigma_n^{-1/2} = \begin{bmatrix} 0.024 & 0 & 0 & 0 & 0 & 0 & 0 & 0 \\ 0 & 0.024 & 0 & 0 & 0 & 0 & 0 & 0 \\ 0 & 0 & 0.076 & 0 & 0 & 0 & 0 & 0 \\ 0 & 0 & 0 & 0.080 & 0 & 0 & 0 & 0 \\ 0 & 0 & 0 & 0 & 0.082 & 0 & 0 & 0 \\ 0 & 0 & 0 & 0 & 0 & 0.115 & 0 & 0 \\ 0 & 0 & 0 & 0 & 0 & 0 & 4.747 & 0 \\ 0 & 0 & 0 & 0 & 0 & 0 & 0 & 5.014 \end{bmatrix}$$

The values of the elements in  $T_{ob}A_oT_{ob}^{-1}$  and  $A_b$  given in Eq. (6.6) agree up to 14 decimal places except for 7 values that agree up to 12 decimal places,  $T_{ob}B_o = B_b$  to 14 decimal places, and  $C_oT_{ob}^{-1} = C_b$  to 14 decimal places.

(3) Similarly, the transformation matrix from input-normal realization to output-normal realization of the ERA is

$$T_{io} = \Sigma_n = \begin{bmatrix} 1606.942 & 0 & 0 & 0 & 0 & 0 & 0 & 0 \\ 0 & 1604.974 & 0 & 0 & 0 & 0 & 0 & 0 \\ 0 & 0 & 170.622 & 0 & 0 & 0 & 0 & 0 \\ 0 & 0 & 0 & 152.718 & 0 & 0 & 0 & 0 \\ 0 & 0 & 0 & 0 & 147.630 & 0 & 0 & 0 \\ 0 & 0 & 0 & 0 & 0 & 74.688 & 0 & 0 \\ 0 & 0 & 0 & 0 & 0 & 0 & 0.044 & 0 \\ 0 & 0 & 0 & 0 & 0 & 0 & 0 & 0.039 \end{bmatrix}$$

The values of the elements in  $T_{io}A_iT_{io}^{-1}$  and  $A_o$  given in Eq. (6.5) agree up to 14 decimal places except for 6 values that agree up to 11 decimal places. Likewise,  $T_{io}B_i = B_o$  to 14 decimal places, and  $C_iT_{io}^{-1} = C_o$  to 14 decimal places. The real realization of the MRTD method given in Eq. (5.2) is found to be the same as the output-normal realization of the ERA given in Eq. (5.1) to 12 significant digits. Also, the real realization of the MMRTD

method given in Eq. (5.4) is found to be the same as the input-normal realization of the ERA given in Eq. (5.3) to 12 significant digits. From a practical standpoint, the particular form of the realization will have no influence on the results.

### 6.1.2 Noise-contaminated Results

In this section, results with noise from three realizations of the ERA method will be presented in terms of damping factors, damped frequencies, and mode shapes. In the presence of noise, the results will not be exact. However, it will be shown that three realizations of the ERA still produce the same Markov parameters to 12 significant digits. It will be shown that even in the presence of noise, the real realization of the MRTD method is still the same as the output-normal realization of the ERA to 14 decimal places and the real realization of the MMRTD method is still the same as the output-normal realization of the ERA to 13 decimal places. The transformation matrix between MRTD and MMRTD will be shown. In the following results only three decimal places are shown.

To examine the case with noise, noise are added in the data which are then used in the different algorithms. Eq. (6.3) is replaced by

$$Y(k) = \Psi_r(\Lambda_r)^k L_r + \varepsilon(k) \quad (6.7)$$

where  $\varepsilon(k)$  is zero-mean Gaussian noise with a standard deviation of 5% of the response. For the noise case, the three realizations of the ERA are

(1) Input-normal realization

$$A_i = \begin{bmatrix} 0.551 & 0.828 & -0.000 & 0.000 & 0.000 & -0.000 & 0.000 & -0.000 \\ -0.829 & 0.556 & 0.000 & -0.000 & -0.000 & -0.000 & -0.000 & 0.000 \\ -0.013 & -0.009 & 0.966 & 0.038 & 0.207 & -0.033 & 0.000 & -0.000 \\ 0.014 & 0.009 & 0.052 & 0.934 & -0.339 & 0.011 & -0.000 & 0.000 \\ -0.063 & -0.043 & -0.272 & 0.361 & 0.905 & 0.008 & 0.000 & -0.000 \\ 0.147 & 0.100 & 0.180 & -0.057 & 0.033 & 0.985 & 0.002 & 0.001 \\ 0.038 & 0.026 & 0.034 & -0.007 & 0.028 & -0.055 & -0.242 & -0.923 \\ -0.011 & -0.007 & -0.012 & 0.004 & 0.004 & -0.014 & 0.934 & -0.282 \end{bmatrix}$$

$$B_i = \begin{bmatrix} 0.240 \\ -0.096 \\ 0.227 \\ -0.092 \\ 0.105 \\ -0.329 \\ -0.151 \\ 0.003 \end{bmatrix}$$

(6.8)

$$C_i = \begin{bmatrix} 86.208 & 33.661 & 0.233 & 6.794 & 6.099 & -5.137 & 0.373 & 0.487 \\ 113.194 & 46.383 & 0.411 & 1.088 & 7.427 & -9.722 & 0.274 & 1.039 \\ 114.069 & 44.782 & -1.560 & -1.849 & 10.304 & -4.769 & -0.772 & 0.541 \\ 113.050 & 47.856 & 0.728 & -6.164 & 7.432 & -0.334 & -0.284 & 0.729 \end{bmatrix}$$

(2) Output-normal realization

$$A_o = \begin{bmatrix} 0.551 & 0.829 & -0.001 & 0.003 & 0.002 & -0.000 & 0.007 & -0.006 \\ -0.828 & 0.556 & 0.000 & -0.001 & -0.000 & -0.002 & -0.005 & 0.004 \\ -0.001 & -0.000 & 0.966 & 0.043 & 0.237 & -0.076 & 0.005 & -0.000 \\ 0.001 & 0.000 & 0.047 & 0.934 & -0.348 & 0.024 & -0.002 & 0.002 \\ -0.005 & -0.004 & -0.237 & 0.351 & 0.905 & 0.018 & 0.003 & -0.003 \\ 0.006 & 0.004 & 0.078 & -0.027 & 0.016 & 0.985 & 0.011 & 0.005 \\ 0.000 & 0.000 & 0.003 & -0.000 & 0.003 & -0.011 & -0.242 & -0.929 \\ -0.000 & -0.000 & -0.001 & 0.000 & 0.000 & -0.003 & 0.928 & -0.282 \end{bmatrix}$$

$$B_o = \begin{bmatrix} 386.389 \\ -155.714 \\ 38.879 \\ -14.171 \\ 15.784 \\ -24.427 \\ -2.395 \\ 0.058 \end{bmatrix} \quad (6.9)$$

$$C_o = \begin{bmatrix} 0.053 & 0.020 & 0.001 & 0.004 & 0.040 & -0.069 & 0.023 & 0.031 \\ 0.070 & 0.028 & 0.002 & 0.000 & 0.049 & -0.131 & 0.017 & 0.066 \\ 0.070 & 0.027 & -0.009 & -0.001 & 0.068 & -0.064 & -0.048 & 0.034 \\ 0.070 & 0.029 & 0.004 & -0.004 & 0.049 & -0.004 & -0.017 & 0.046 \end{bmatrix}$$

(3) Internally balanced realization

$$A_b = \begin{bmatrix} 0.551 & 0.829 & -0.000 & 0.001 & 0.000 & -0.000 & 0.000 & -0.000 \\ -0.829 & 0.556 & 0.000 & -0.000 & -0.000 & -0.000 & -0.000 & 0.000 \\ -0.004 & -0.002 & 0.966 & 0.041 & 0.222 & -0.050 & 0.001 & -0.000 \\ 0.004 & 0.002 & 0.049 & 0.934 & -0.344 & 0.017 & -0.000 & 0.000 \\ -0.019 & -0.013 & -0.254 & 0.356 & 0.905 & 0.012 & 0.001 & -0.001 \\ 0.031 & 0.021 & 0.118 & -0.040 & 0.023 & 0.985 & 0.005 & 0.002 \\ 0.003 & 0.002 & 0.010 & -0.002 & 0.009 & -0.025 & -0.242 & -0.926 \\ -0.001 & -0.000 & -0.003 & 0.001 & 0.001 & -0.006 & 0.931 & -0.282 \end{bmatrix}$$

$$B_b = \begin{bmatrix} 9.633 \\ -3.884 \\ 2.971 \\ -1.143 \\ 1.291 \\ -2.837 \\ -0.602 \\ 0.014 \end{bmatrix} \quad (6.10)$$

$$C_b = \begin{bmatrix} 2.149 & 0.839 & 0.017 & 0.054 & 0.498 & -0.596 & 0.093 & 0.123 \\ 2.822 & 1.157 & 0.031 & 0.008 & 0.607 & -1.129 & 0.069 & 0.262 \\ 2.844 & 1.117 & -0.119 & -0.014 & 0.842 & -0.554 & -0.194 & 0.136 \\ 2.818 & 1.193 & 0.055 & -0.049 & 0.607 & -0.038 & -0.071 & 0.184 \end{bmatrix}$$

The deviation caused by the noise can be seen by comparing Eqs. (6.4) to (6.8), Eqs. (6.5) to (6.9), and Eqs. (6.6) to (6.10). The differences are in the second or third decimal places. It was verified that the three realizations of the ERA produce numerically the same Markov parameters. By this, we mean that the Markov parameters computed from the three realizations agree to 12 significant digits. For example

$$C_i B_i = C_o B_o = C_b B_b$$

$$C_i A_i B_i = C_o A_o B_o = C_b A_b B_b$$

and

$$C_i A_i^2 B_i = C_o A_o^2 B_o = C_b A_b^2 B_b$$

$$\vdots$$

$$C_i A_i^{640} B_i = C_o A_o^{640} B_o = C_b A_b^{640} B_b$$

to 12 significant digits. They also produce numerically the same damping factors, and damped frequencies which are given in Table 3. The closely spaced frequency that is not identified is marked with the symbol “\_” in Table 3 because the data length is not long enough to include the beating period. The true answers are given in Table 2.

Table 3: ERA identified damping factors and damped frequencies with noise

Mode No.	Damped Frequencies ( $\omega_{dr}$ (Hz))	Damping Factor ( $\zeta_r$ )
1	0.990	0.099
2	9.030	0.002
3	—	—
4	20.000	0.002

and the real mode shape matrix is found to be

$$\Psi_r = \begin{bmatrix} 1.000 & 0.000 & 2.000 & 0.000 & 2.002 & 0.000 & 3.000 & 0.000 \\ 1.958 & -0.080 & 2.716 & 0.170 & 2.650 & -0.054 & 4.834 & 1.914 \\ 0.855 & -0.178 & 3.045 & 0.005 & 2.648 & -0.001 & -0.116 & 4.420 \\ -0.046 & 0.026 & 1.915 & 0.342 & 2.649 & -0.045 & 1.996 & 3.175 \end{bmatrix} \quad (6.11)$$

Comparing Eqs. (6.8), (6.9), and (6.10), the transformation matrices between three realizations of the ERA can be obtained in the following.

(1) The transformation matrix from input-normal realization to output-normal realization of the ERA is given in Eq. (5.6),  $T_{io} = \Sigma_n$ . Similarly, the matrix  $T_{io}A_iT_{io}^{-1} = A_o$  to 13 decimal places,  $T_{io}B_i = B_o$  to 14 decimal places, and  $C_iT_{io}^{-1} = C_o$  to 14 decimal places.

(2) The transformation matrix from output-normal realization to internally balanced realization of the ERA is given in Eq. (5.7),  $T_{ob} = \Sigma_n^{-1/2}$ . The matrix  $T_{ob}A_oT_{ob}^{-1}$  is the same as  $A_b$  to 13 decimal places,  $T_{ob}B_o = B_b$  to 14 decimal places, and  $C_oT_{ob}^{-1} = C_b$  to 14 decimal places.

(3) The transformation matrix from input-normal realization to internally balanced realization of the ERA is given in Eq. (5.8),  $T_{ib} = \Sigma_n^{1/2}$ . The matrix  $T_{ib}A_iT_{ib}^{-1}$  is the same as  $A_b$  given in Eq. (6.10) to 13 decimal places. Likewise,  $T_{ib}B_i = B_b$  to 14 decimal places, and  $C_iT_{ib}^{-1} = C_b$  to 14 decimal places.

*For the simulated data which has a closely spaced frequencies and mode shapes, there is no significant numerical difference for identification of frequencies, damping factors, and mode shapes between input-normal, output-normal, and internally balanced realizations of the ERA.*

## 6.2 Test Data

The methods are tested using one set of the Hybrid Model Build 2 Rigid (HMB-2R) random pulse input data<sup>18</sup>. A schematic of the structure is shown in Fig. 1. There are 93 accelerometers on the structure of which 8 sensors on the main truss were selected (1003x+, 1003z-, 1007x+, 1007z+, 1083x+, 1083z-, 1087x+, and 1087z+). The notation x+ implies that the accelerometer measures positive acceleration in positive x direction and the notation x- implies that the positive acceleration is in negative x direction, etc. The system has 8 outputs. Free decay response from three separate tests (Tests A, B, and C) are used in the computation using the ERA, MRTD, and MMRTD methods. The response at output locations 1003z- and 1087x+ of the HMB-2R structure are shown in Fig. 2 and Fig. 3, respectively for Test A. The output of each accelerometer has been passed through a low pass filter with a cut off at 40 Hz. Responses at other output locations (1003x+, 1007x+, 1007z+, 1083x+, 1083z-, and 1087z+) are similar, and not shown here. The power spectral densities of the data are shown in Figs. 4, 5, and 6 for Tests A, B, and C, respectively. The identified frequencies and damping factors are shown in Table 4 in Case 1 and Case 2. The data used in Case 1 has a sampling rate of 128 Hz, and the data used in Case 2 has a sampling rate of 64 Hz so that a longer time record can be used. This also helps identify the lower frequency mode of the system since a longer time history and a lower sampling rate are used in the second test. There is no unique way to select the size of the Hankel matrix. In both cases, the Hankel matrix used to obtain the results shown here has 128 row shifts and 32 column shifts. Therefore, the size of the Hankel matrix is  $1032 \times 99$ . Note that in this case, the data that are used to make the data matrix are not the Markov parameters but free decay data samples. However, for convenience, we still refer this matrix as a Hankel matrix. The results obtained from Case 1 and Case 2 are close to the results obtained from a more complete study as shown in Cases 3-5.<sup>18</sup> In both Cases, the total number of the singular values is

99. The damped frequencies and damping factors shown in Table 4 are obtained by keeping 96 singular values. Therefore, the size of the identified system matrix  $A$  in the ERA (or  $E$  in the MRTD method or  $E_m$  in the MMRTD method) is  $96 \times 96$ .

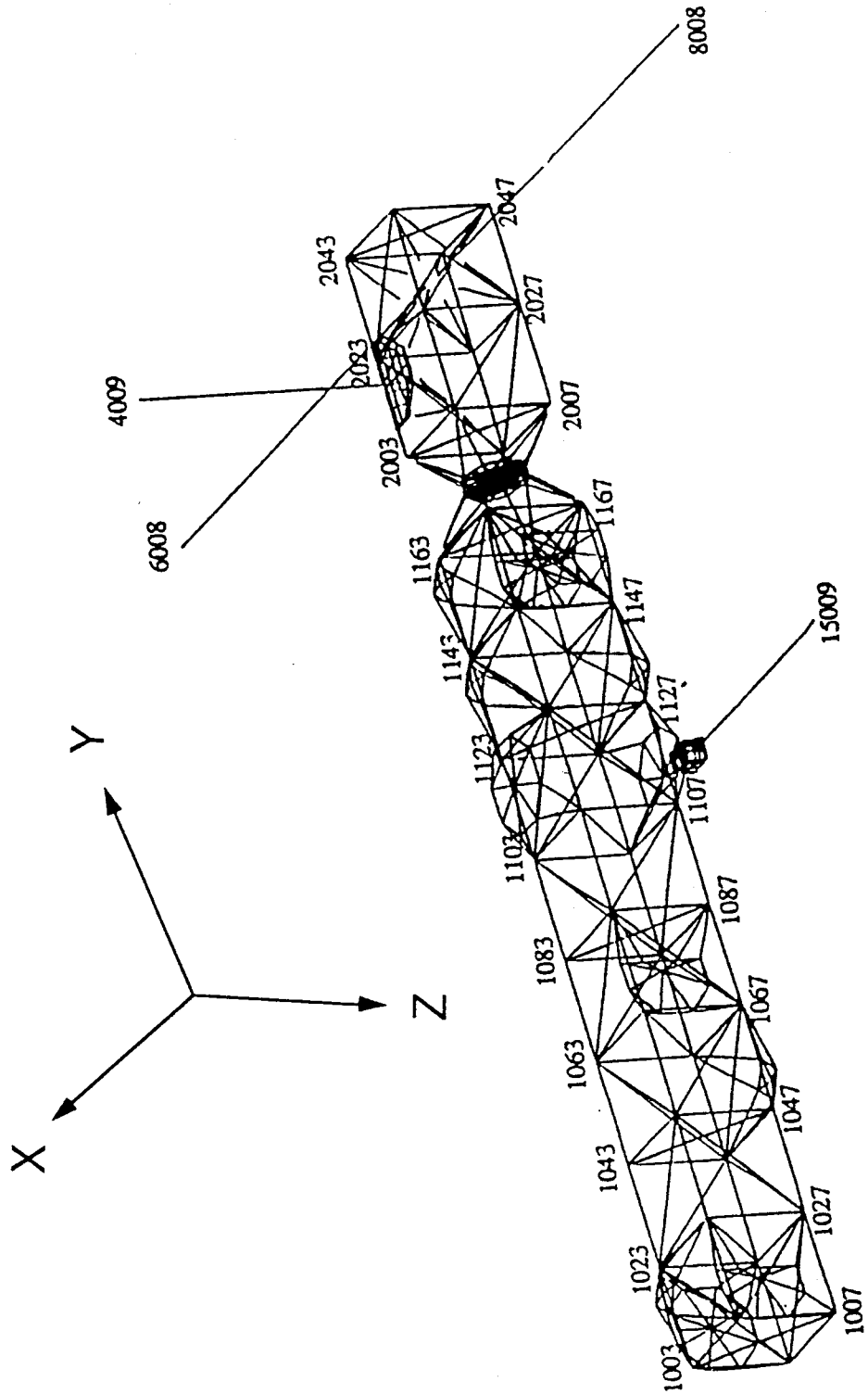


Fig.1: NASTRAN  $\{\}$  points for HMB-2R structure

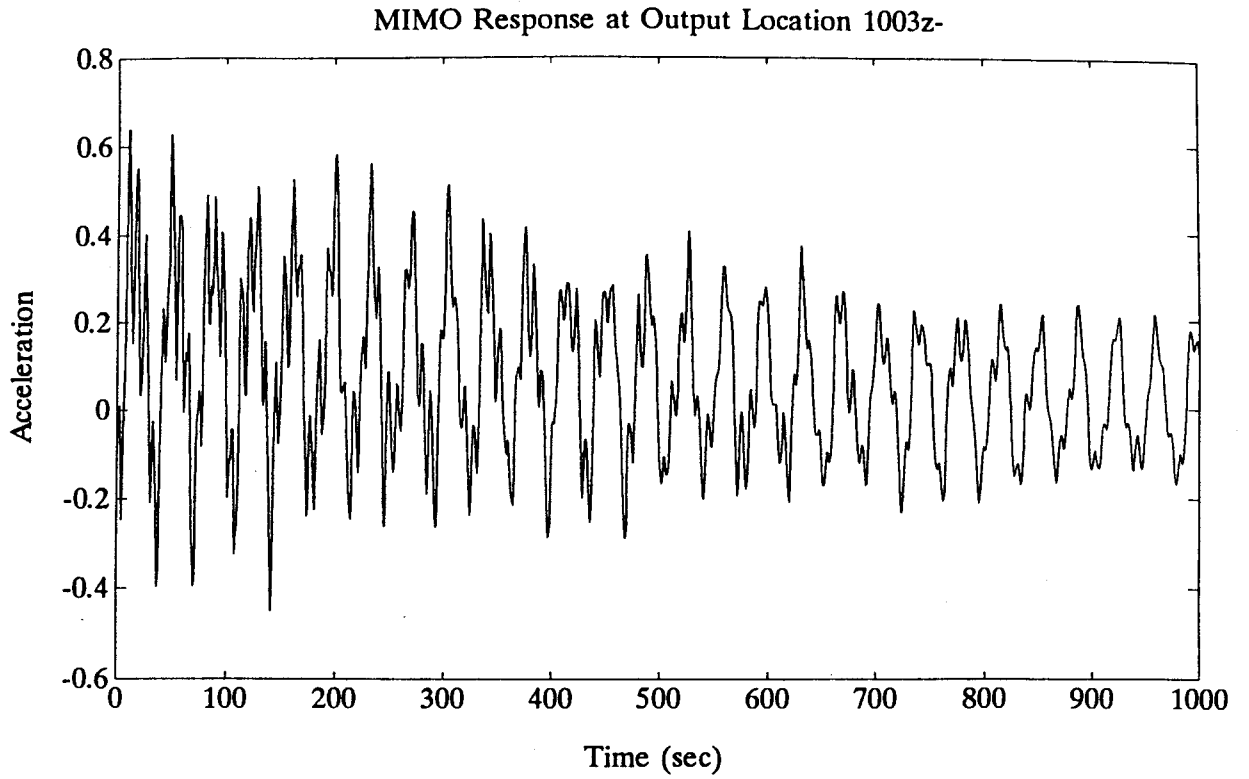


Fig. 2: Free decay response at output location 1003z- of the HMB-2R structure (Test A)

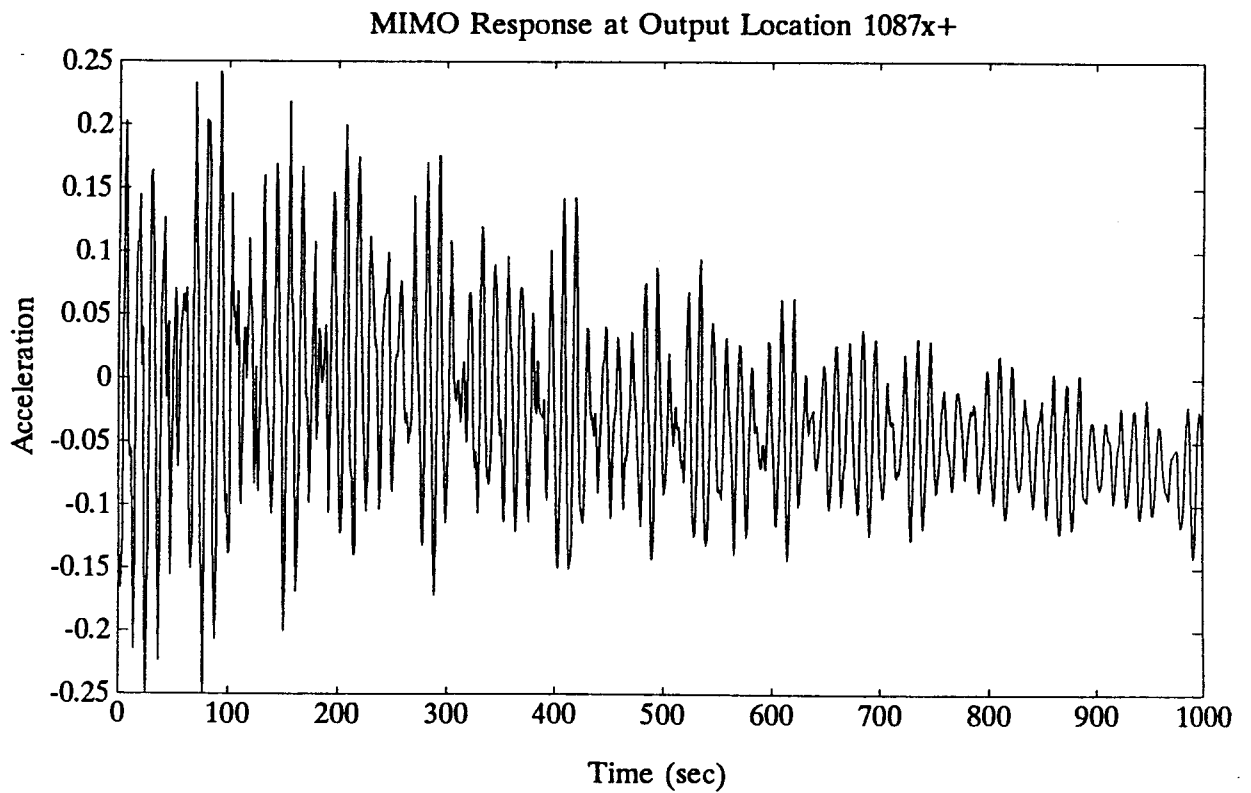


Fig. 3: Free decay response at output location 1087x+ of the HMB-2R structure (Test A)

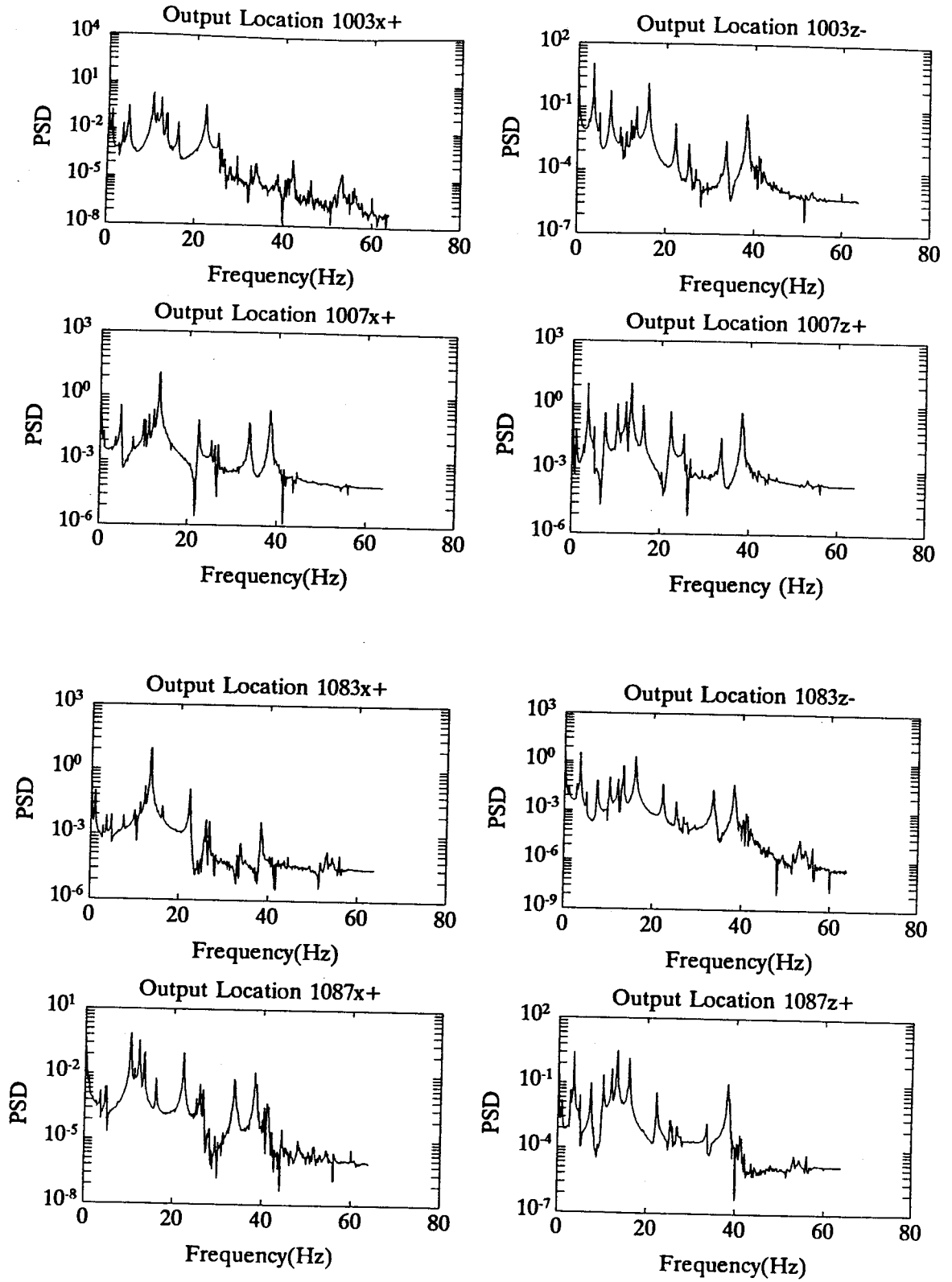


Fig. 4: Power spectral densities of 8 responses for the HMB-2R structure (Test A)

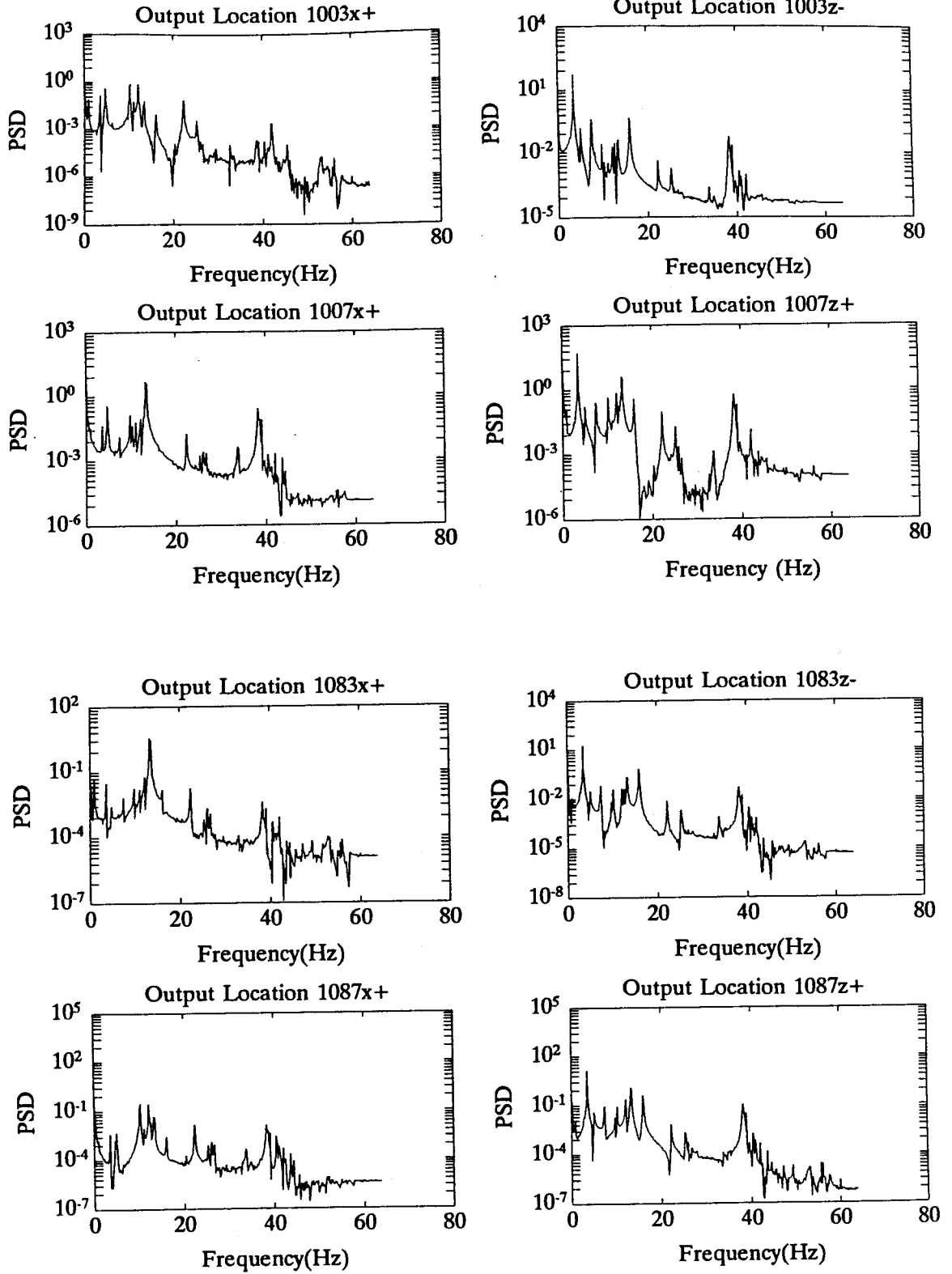


Fig. 5: Power spectral densities of 8 responses for the HMB-2R structure (Test B)

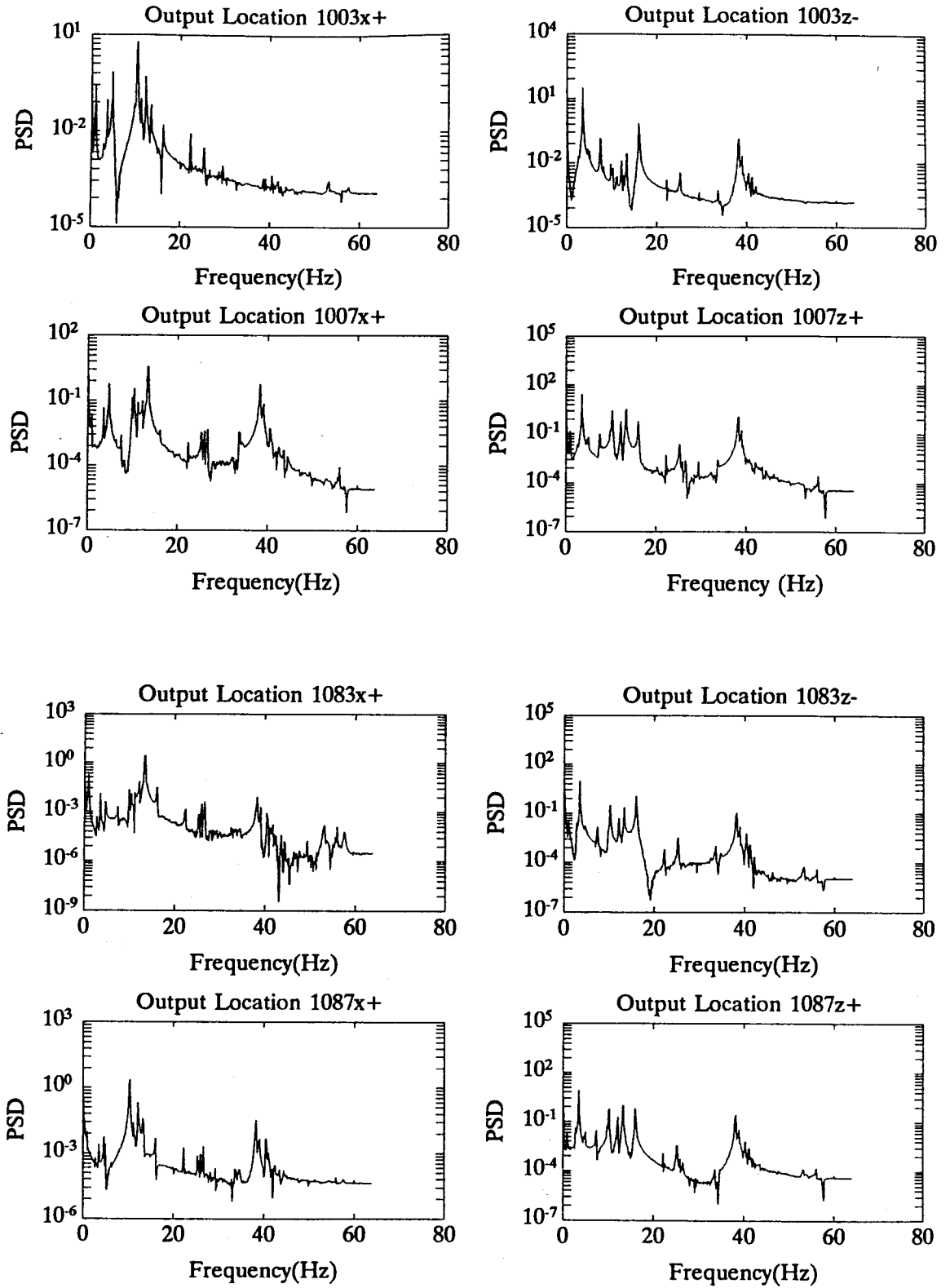


Fig. 6: Power spectral densities of 8 responses for the HMB-2R structure (Test C)

Table 4: Identified frequencies and damping factors using test data from the HMB-2R structure by keeping 96 singular values

	Case 1 $\Delta t = \frac{1}{128}$ (sec)		Case 2 $\Delta t = \frac{1}{64}$ (sec)		Case 3	Case 4	Case 5
Mode No.	Freq. (Hz)	Damping Factor	Freq. (Hz)	Damping Factor	Freq. (Hz)	Freq. (Hz)	Freq. (Hz)
1	-	-	0.91	0.018	0.91	0.91	0.91
2	3.01	0.887	2.79	0.160	2.72	2.72	2.72
3	3.51	0.67	3.51	0.005	3.52	3.51	3.52
4	4.65	0.004	4.66	0.005	4.66	4.66	4.66
5	4.96	0.007	5.02	0.004	5.03	5.02	5.02
6	7.42	0.871	7.42	0.003	7.43	7.42	7.43
7	-	-	9.75	0.003	9.76	9.75	9.76
8	10.19	0.008	10.19	0.002	10.20	10.20	10.20
9	11.82	0.032	11.05	0.002	11.06	11.06	11.06
10	12.11	0.034	12.13	0.004	12.14	12.14	12.14
11	-	-	12.6	0.007	12.65	12.65	12.65
12	13.30	0.001	13.30	0.002	13.27	13.30	13.22
13	13.52	0.002	13.49	0.001	-	13.44	13.30
14	16.03	0.273	16.04	0.002	16.05	16.04	16.05
15	-	-	16.58	0.062	-	-	16.05
16	22.28	0.026	22.27	0.002	22.28	22.28	-
17	25.28	0.005	25.37	0.003	-	25.13	25.29
18	25.96	0.006	25.79	0.003			
19	38.21	0.081	-	-			
20	38.69	0.0002	-	-			

The modes that are not identified in each case are marked with the symbol "-" in Table 4. Because the signal is filtered at 40 Hz, modes above 40 Hz are not presented. The power spectral densities in Figs. 4-6 of course show that there is little information in

the signals beyond 40 Hz. From the power spectral density plots in Figs. 4-6, the stronger modes are at about 5 Hz, 7 Hz, 16 Hz, and 38 Hz. The identified frequencies shown in Table 4 are in agreement with the power spectral density plots in Figs. 4-6. An overlay of the power spectral density plots from actual data and from the identified model is shown in Figs. 7-12 for Case 1 and in Figs. 13-18 for Case 2. The solid curves are obtained from test data, and the dashed curves are obtained from identified model. Table 4 shows that the system has several sets of closely spaced frequencies at about 5 Hz (modes number 4 and 5), 10 Hz (modes number 7 and 8), 12 Hz (modes number 10 and 11), 13 Hz (modes number 12 and 13), 16 Hz (modes number 14 and 15), 25 Hz (modes number 17 and 18), and 38 Hz (modes number 19 and 20). Note that Case 1 can not distinguish modes 7 and 8, modes 10 and 11, and modes 14 and 15. Also, the lowest frequency mode can not be identified in Case 1. Furthermore, one can not show that the system has closely spaced frequencies by examining the power spectral density plots in Figs. 4-18 alone. By comparing the power spectral density plots from test and reconstructed data, one can easily see that the model in Case 1 does not identified modes number 1, 7, 11, and 15. This is because the data used is too short (about 1.2 second). We are limited by the size of the Hankel matrix which can be handled by the computer. When the sampling rate is decreased to 64 Hz, a longer data record can be used (about 2.4 second). In this case, the modes number 1, 7, 11, and 15 can be identified. It should be recalled that the objective here is not to perform the "best" modal identification of the HMB-2R structure, but rather to compare various system identification methods, the ERA, MRTD, and MMRTD methods, using real data.

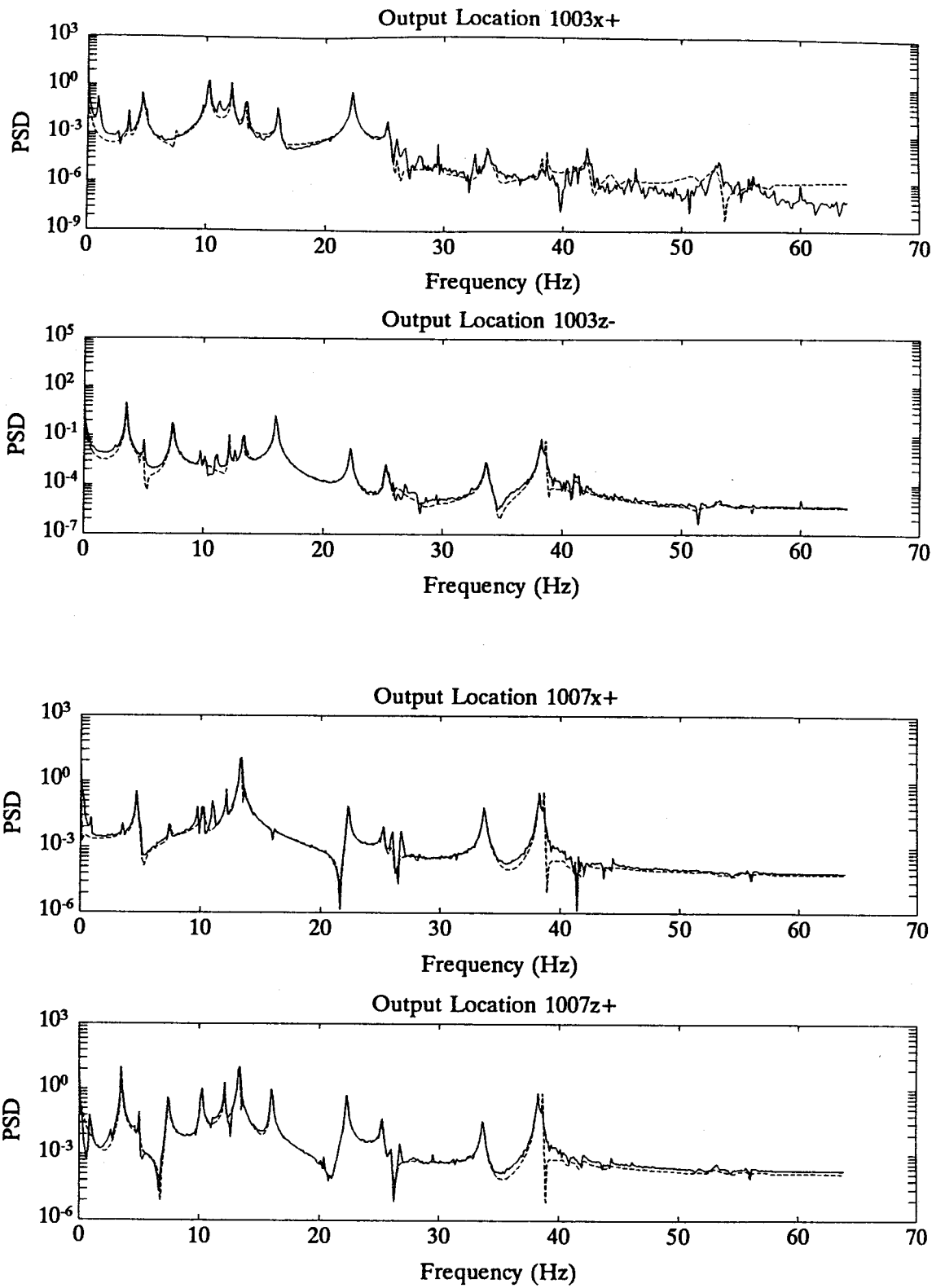


Fig. 7: Comparison of power spectral density plots between test data and reconstructed data (Test A, sampling frequency = 128 Hz)  
 — : Test  
 - - - : Reconstructed from identified model



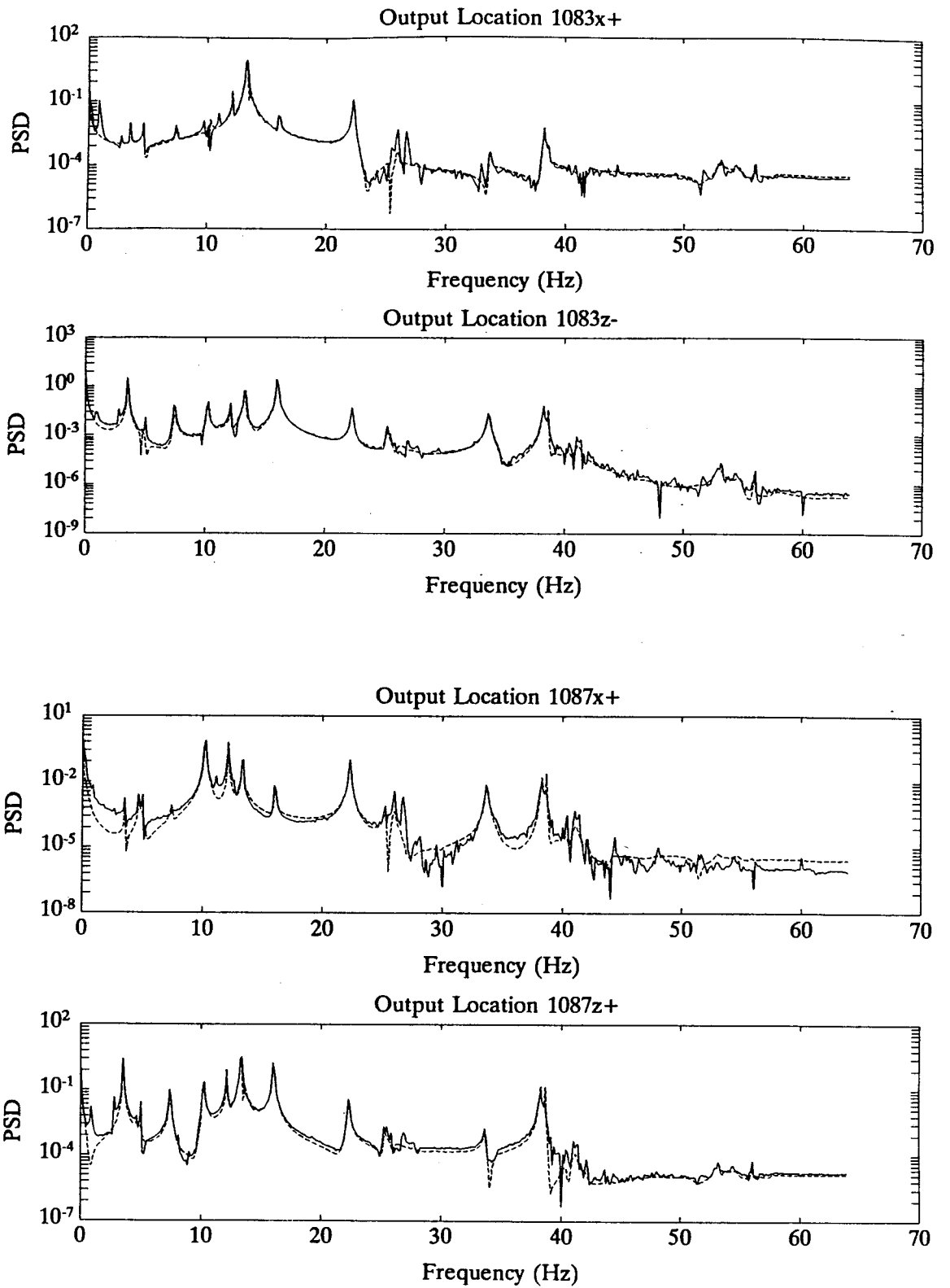


Fig. 8: Comparison of power spectral density plots between test data and reconstructed data (Test A , sampling frequency = 128 Hz)  
 \_\_\_\_\_ : Test  
 - - - - - : Reconstructed from identified model

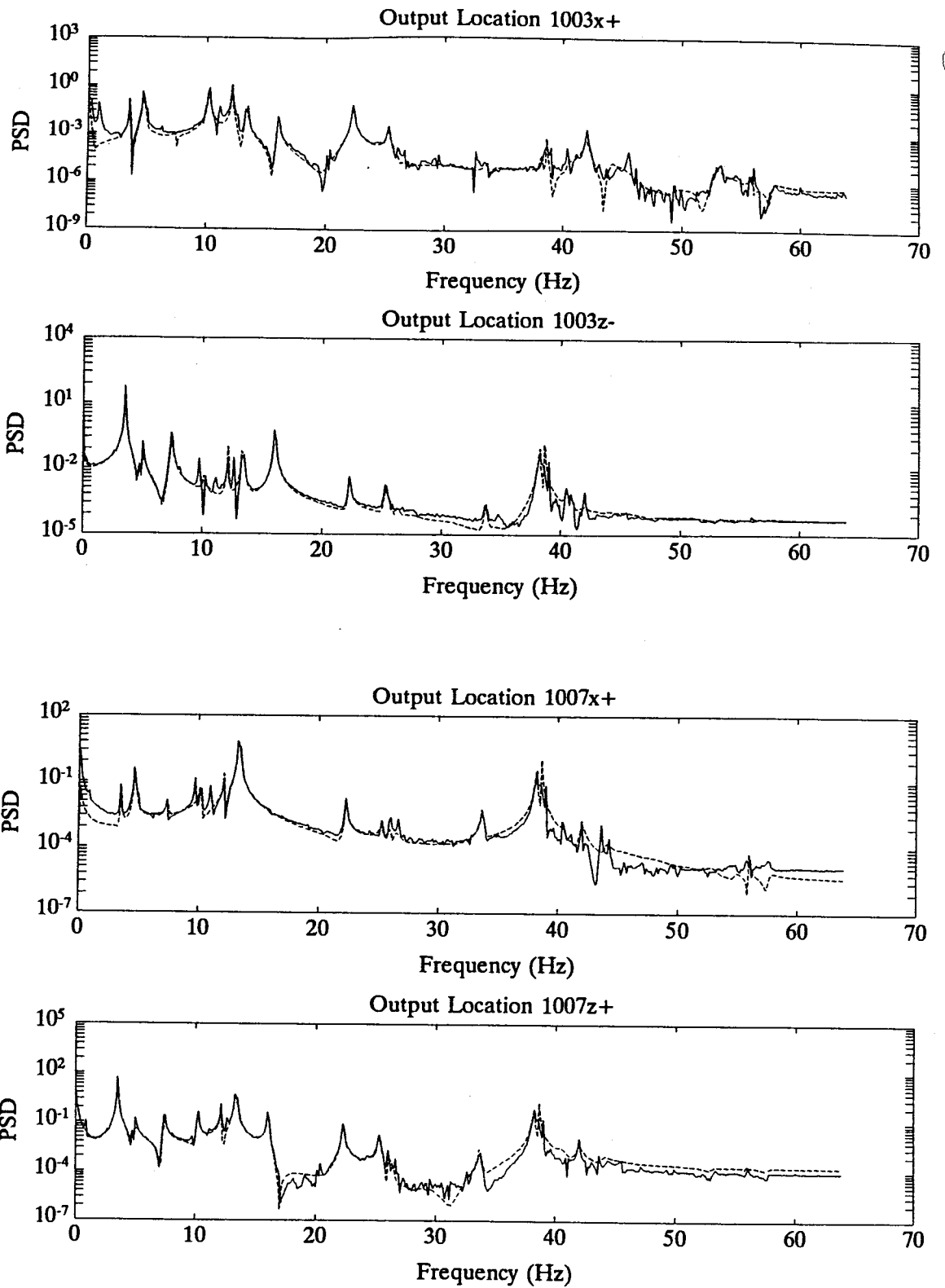


Fig. 9: Comparison of power spectral density plots between test data and reconstructed data (Test B, sampling frequency = 128 Hz)  
 \_\_\_\_\_ : Test  
 ----- : Reconstructed from identified model

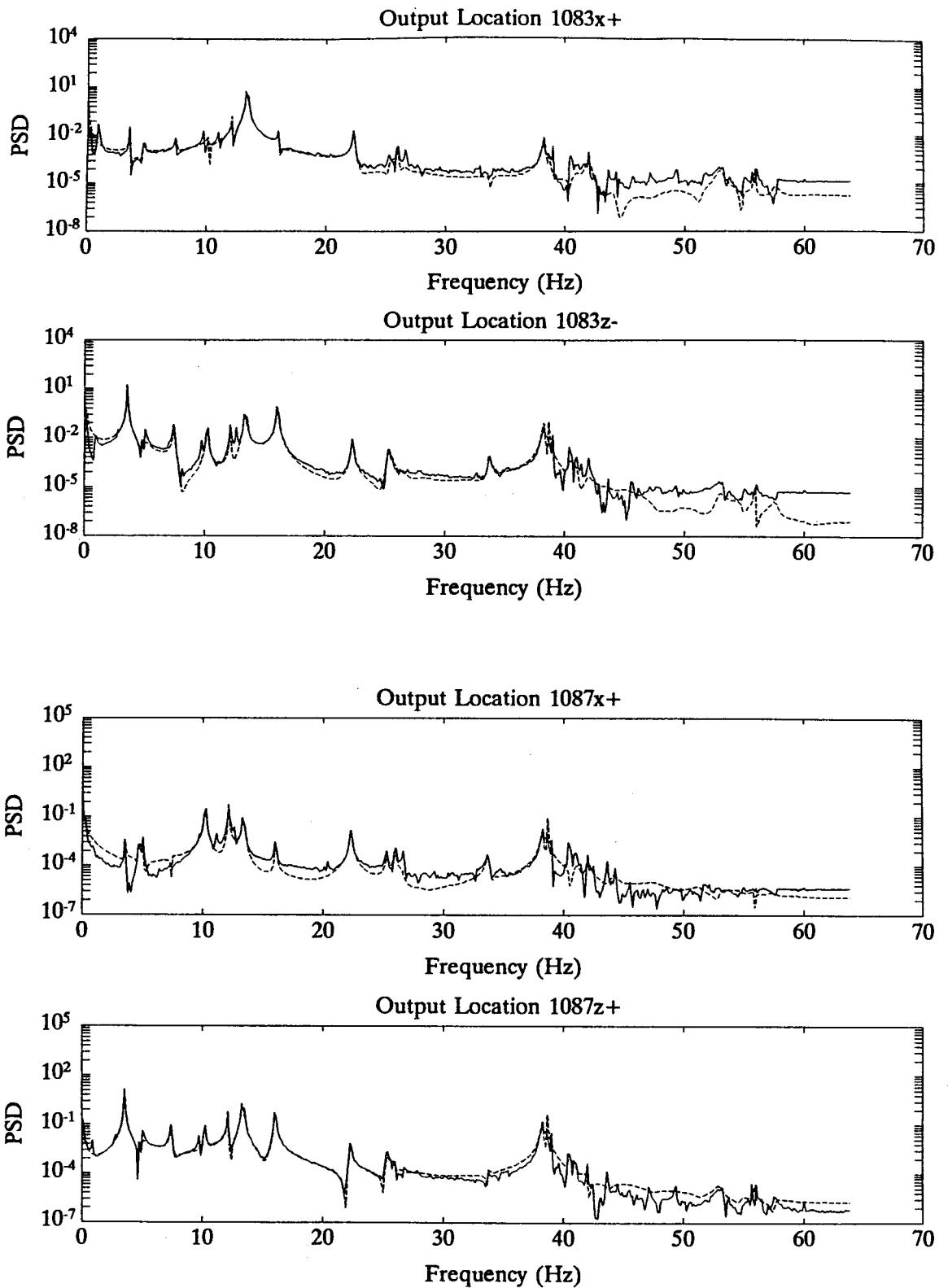


Fig. 10: Comparison of power spectral density plots between test data and reconstructed data (Test B, sampling frequency = 128 Hz)  
 — : Test  
 - - - : Reconstructed from identified model

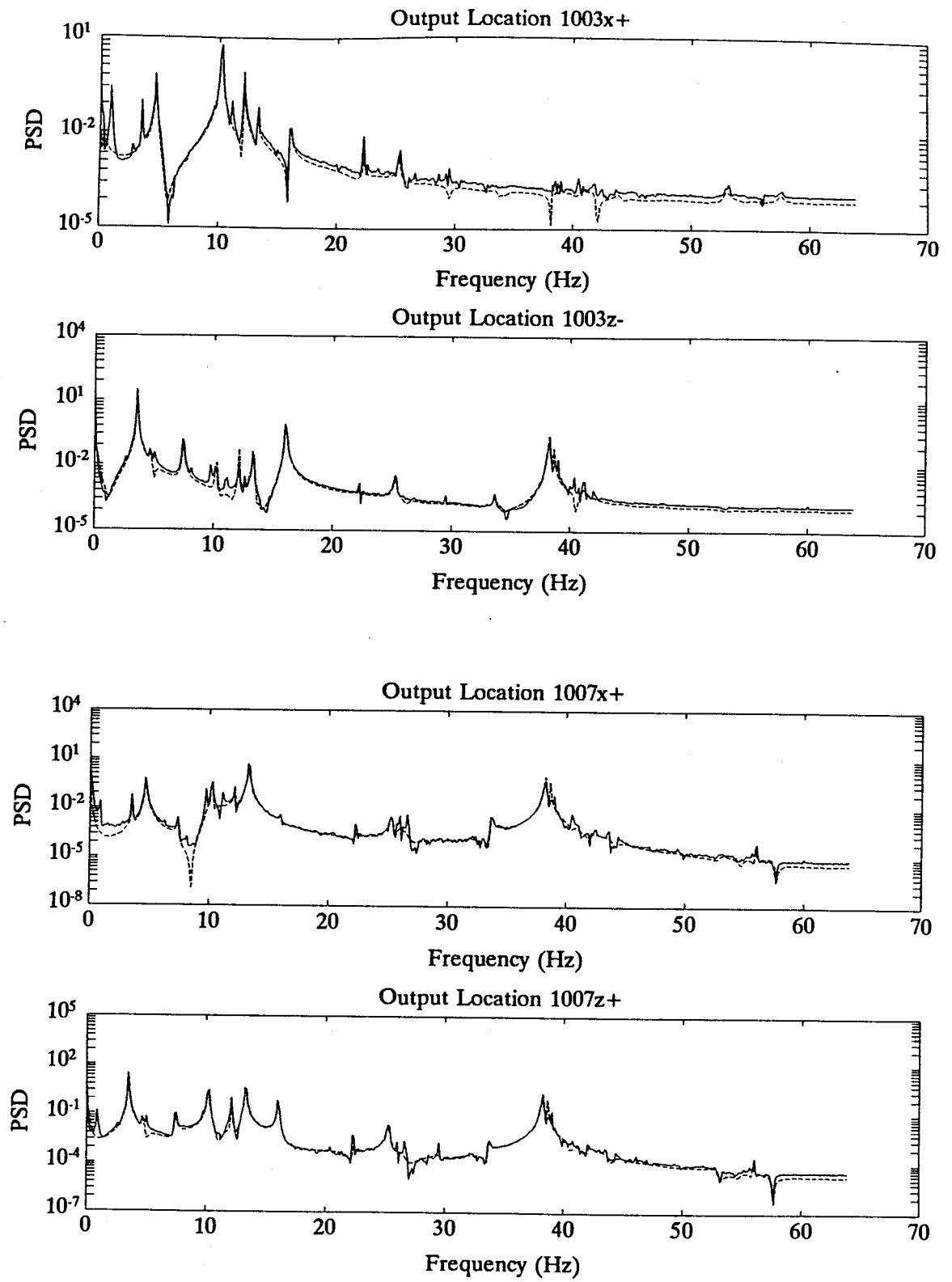


Fig. 11: Comparison of power spectral density plots between test data and reconstructed data (Test C, sampling frequency = 128 Hz)  
 \_\_\_\_\_ : Test  
 ----- : Reconstructed from identified model

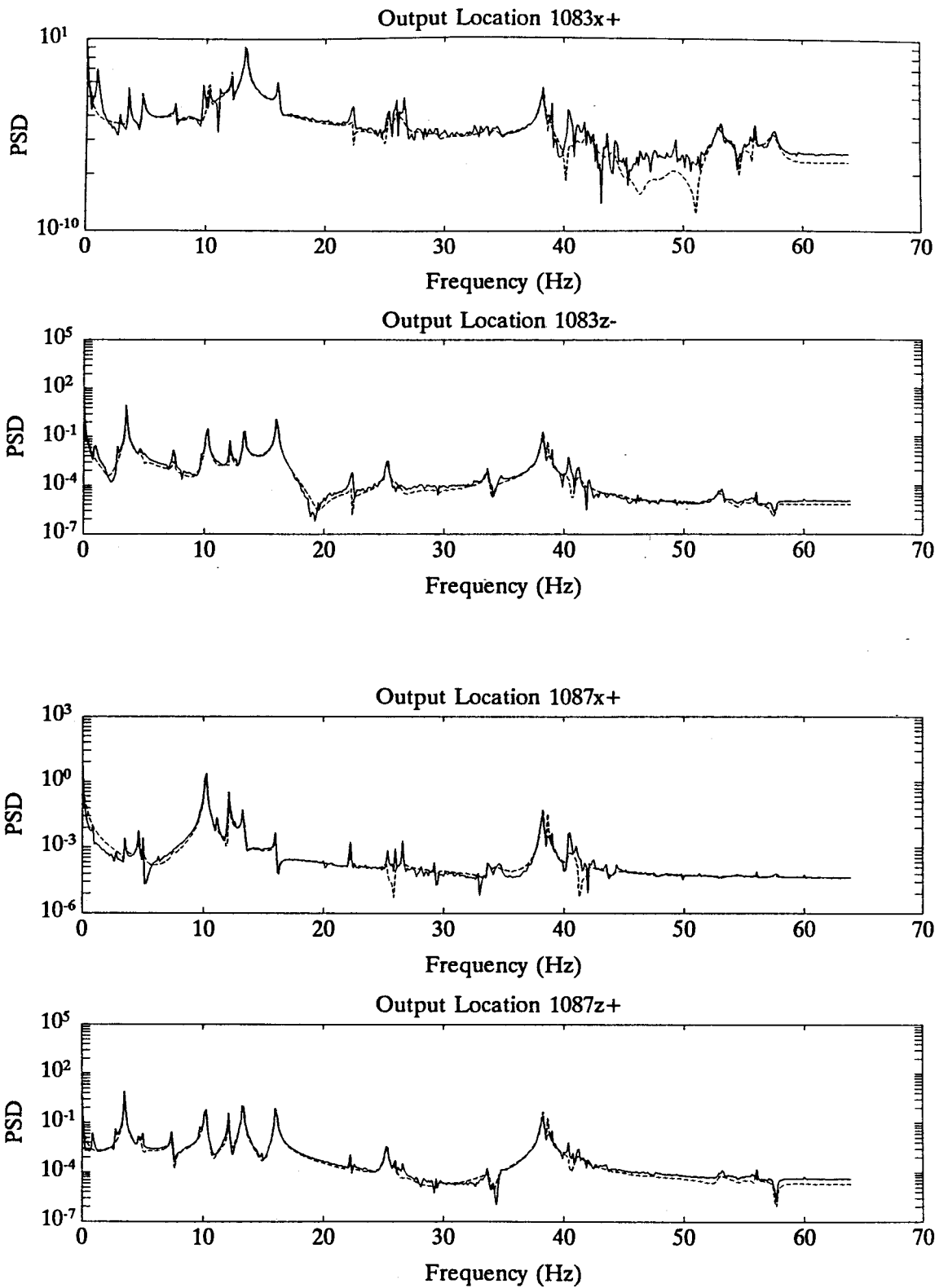


Fig. 12: Comparison of power spectral density plots between test data and reconstructed data (Test C , sampling frequency = 128 Hz)  
 \_\_\_\_\_ : Test  
 ----- : Reconstructed from identified model

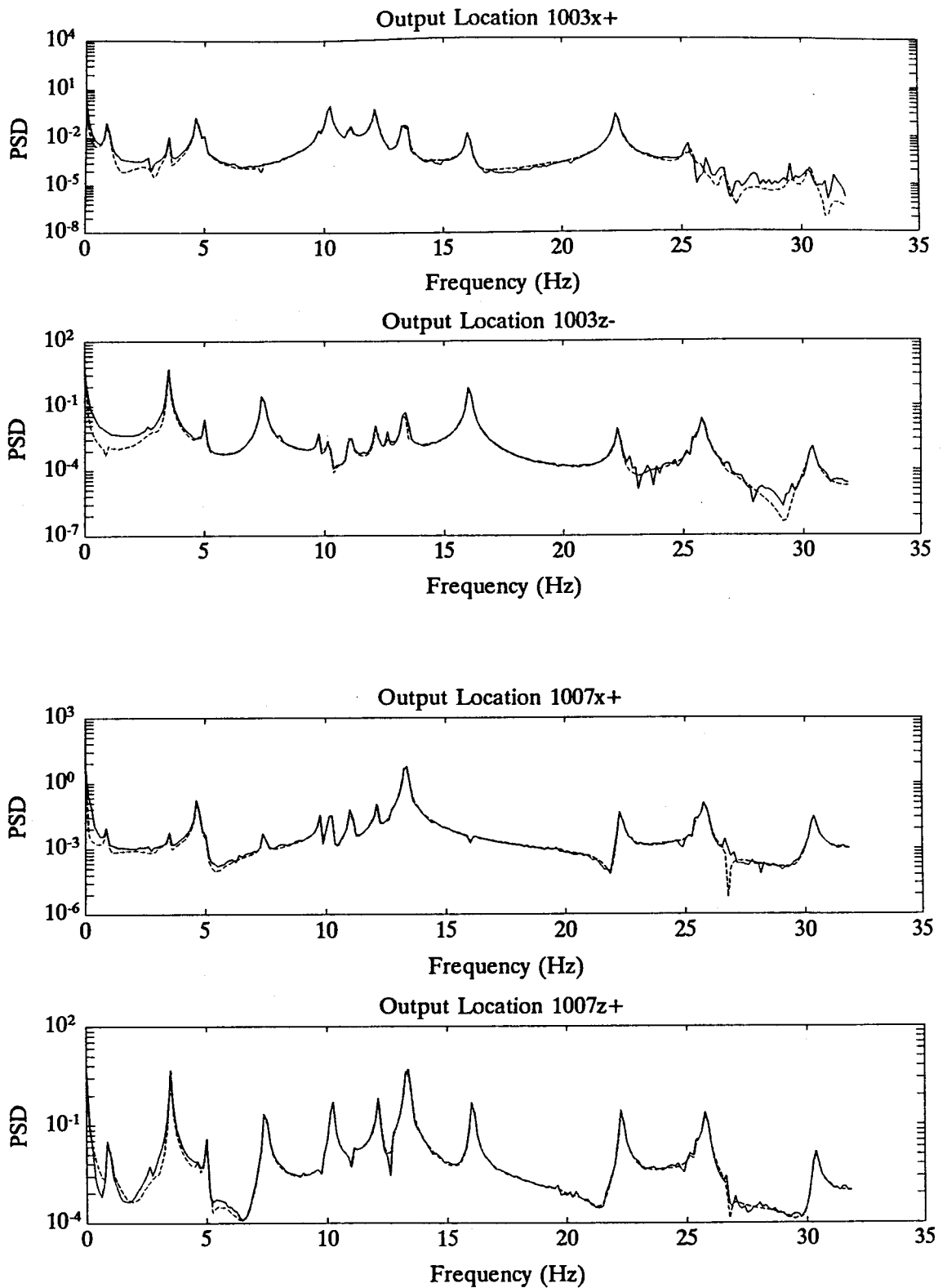


Fig. 13: Comparison of power spectral density plots between test data and reconstructed data (Test A , sampling frequency = 64Hz)  
 — : Test  
 - - - : Reconstructed from identified model

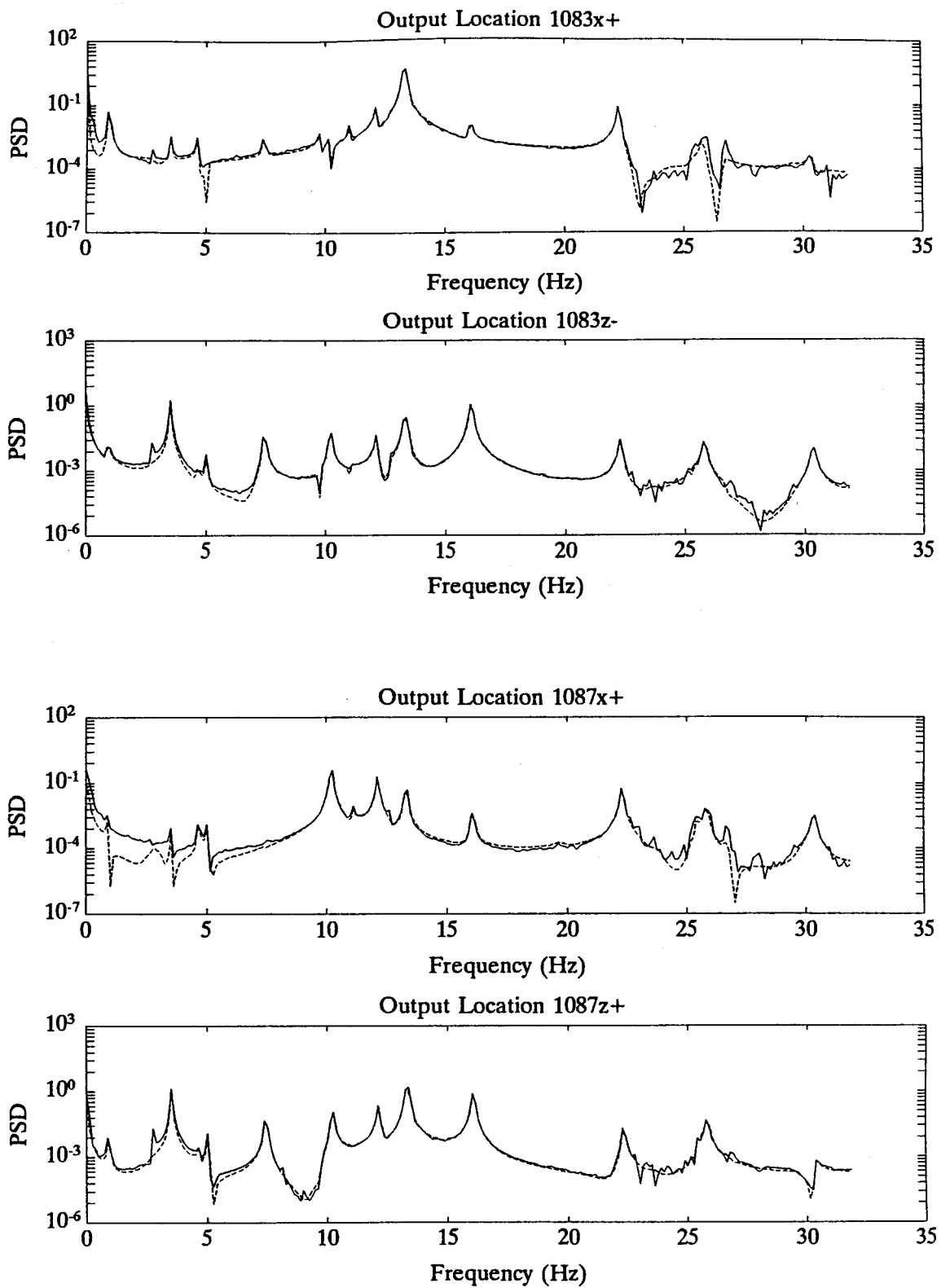


Fig. 14: Comparison of power spectral density plots between test data and reconstructed data (Test A , sampling frequency = 64Hz)

\_\_\_\_\_ : Test  
 - - - - - : Reconstructed from identified model

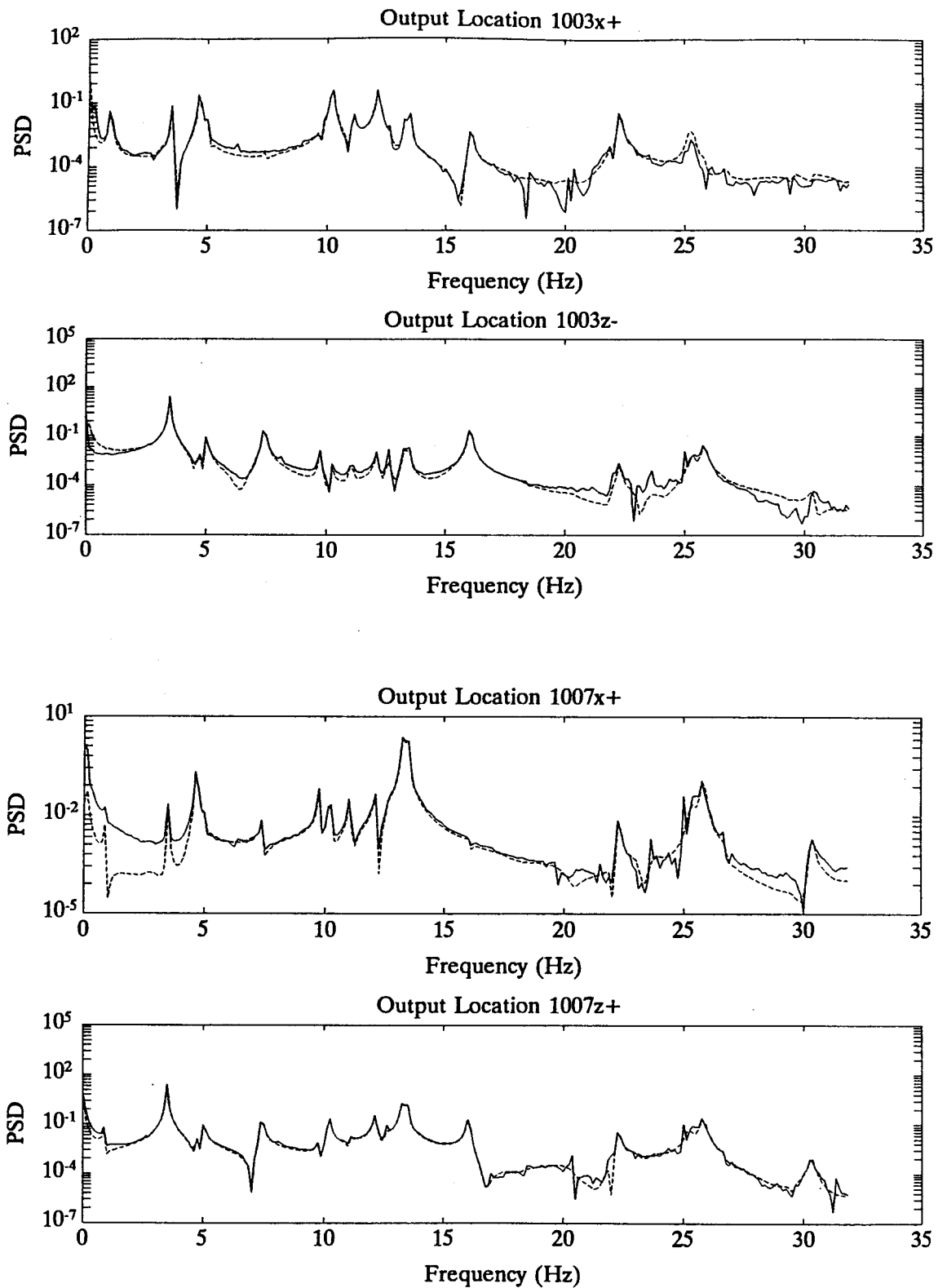


Fig. 15: Comparison of power spectral density plots between test data and reconstructed data (Test B , sampling frequency = 64Hz)

— : Test

- - - : Reconstructed from identified model

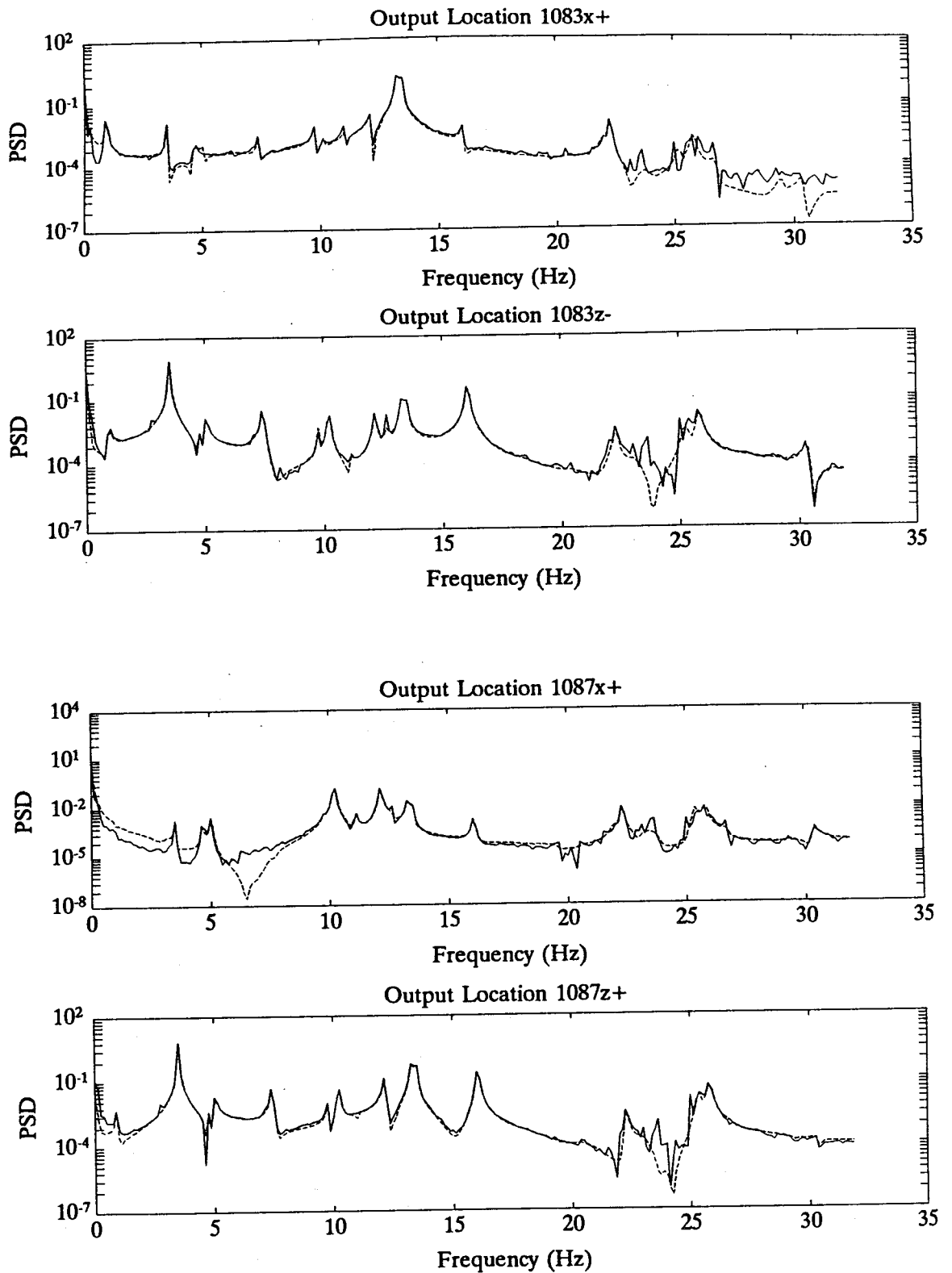


Fig. 16: Comparison of power spectral density plots between test data and reconstructed data (Test B, sampling frequency = 64Hz)

— : Test  
 - - - : Reconstructed from identified model

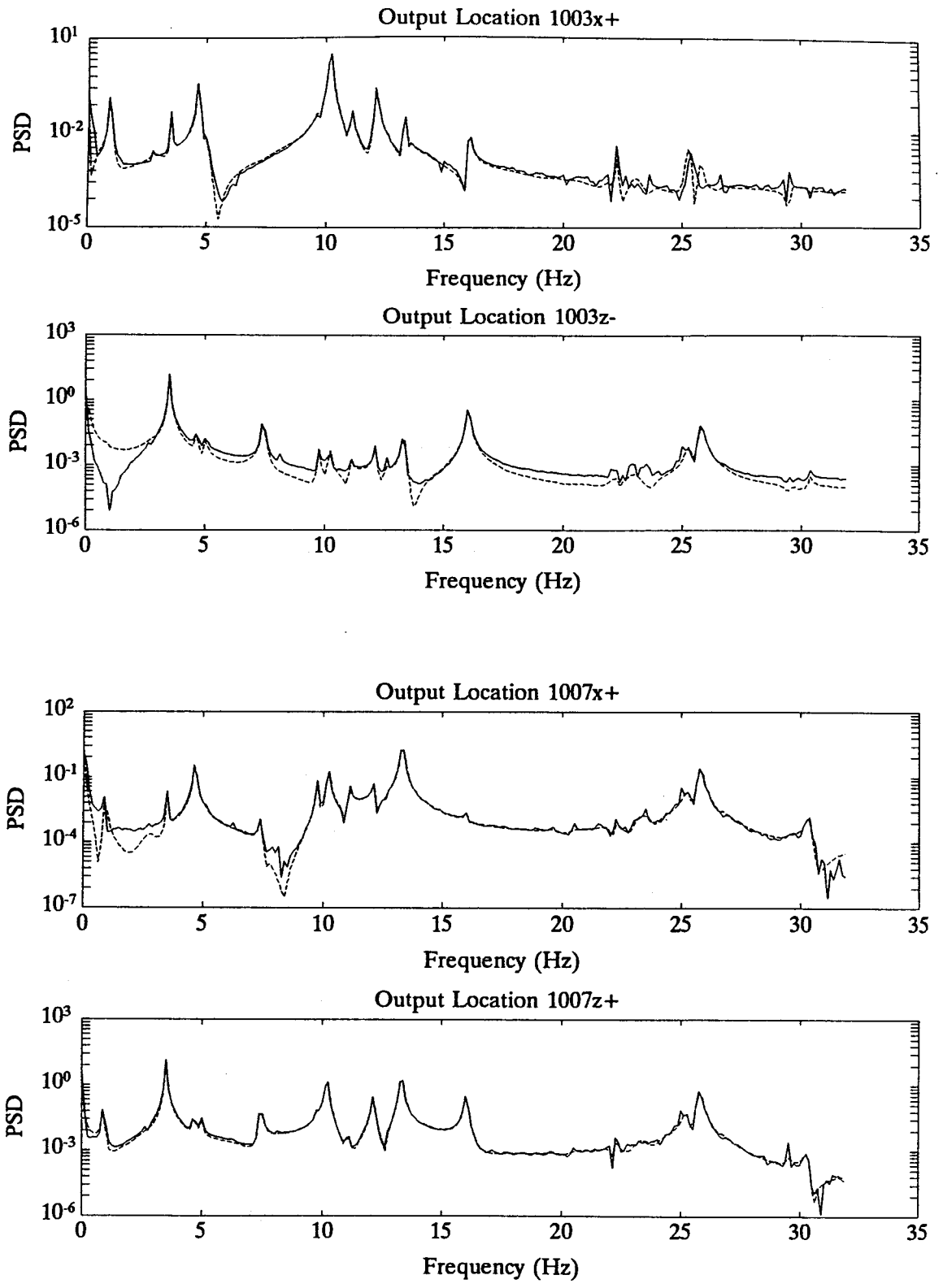


Fig. 17: Comparison of power spectral density plots between test data and reconstructed data (Test C, sampling frequency = 64Hz)  
 \_\_\_\_\_ : Test  
 - - - - - : Reconstructed from identified model

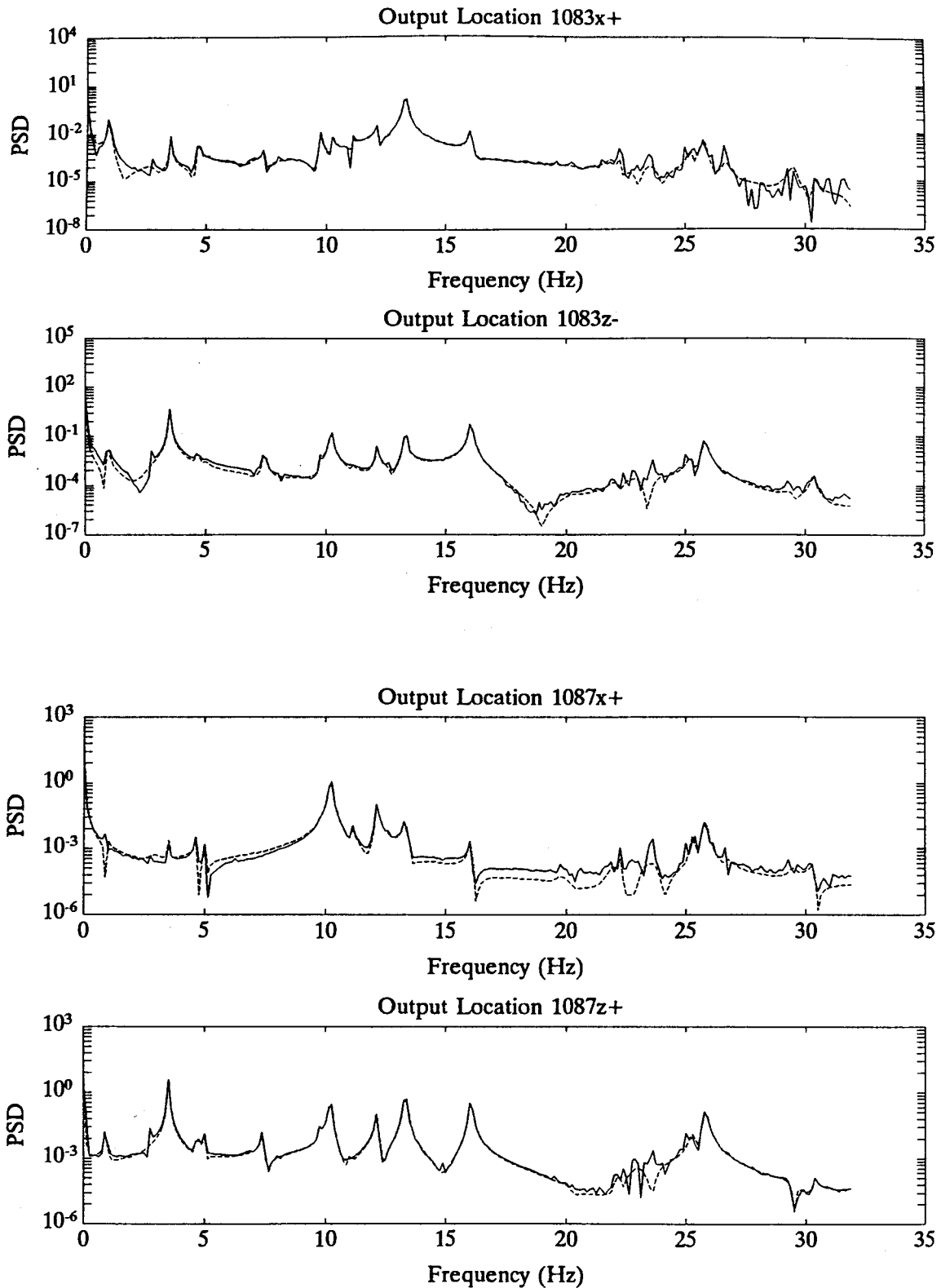


Fig. 18: Comparison of power spectral density plots between test data and reconstructed data (Test C , sampling frequency = 64Hz)

— : Test  
 - - - : Reconstructed from identified model

In this study using experimental data, the realization methods of the ERA, MRTD, and MMRTD produce the same frequencies, damping factors, and mode shapes as established in the theoretical sections and the simulation examples presented in this thesis. The MRTD and MMRTD formulation are simply special versions of the ERA. There is no additional information about the system that can be found by using the MRTD or MMRTD methods, or using input-normal, output-normal, or internally balanced realization of the ERA. Specifically, the following findings are made

- 1) The real-valued realization of the MMRTD method gives the same system matrix as the output-normal realization the ERA to 11 decimal places.
- 2) The real-valued realization of the MMRTD method gives the same system matrix as the input-normal realization of the ERA to 11 decimal places.
- 3) The input-normal, output-normal, and internally balanced forms produce the same Markov parameters to 12 decimal places.
- 4) The frequencies, damping factors, and mode shapes computed from input-normal, output-normal, and internally balanced realizations are the same to 11 decimal places.
- 5) In the input-normal realization, the ratio between the largest and the smallest values in the input matrix  $B_i$  is 2200 while the ratio between the largest and smallest values in the output matrix  $C_i$  is about 1000000. In the output-normal realization, the ratio between the largest and the smallest values in the output matrix  $C_o$  is less than 2000 while the ratio between the largest and smallest values in the input matrix  $B_o$  is about 100000. However, in the internally balanced realization, the ratio between the largest and the smallest values in input matrix  $B_b$  is about 23000, and the ratio between the largest and the smallest values in output matrix  $C_b$  is about 80000. Even though the internally balanced realization appears to be better conditioned, the numerical results are essentially equivalent. For this data set there appears to be no advantage in selecting one realization from another for purpose of modal parameters identification.

In the results presented so far, 96 out of 99 singular values are kept resulting in a state space model of order 96. If more singular values are truncated, then the identified state space model will have smaller order. However, this will introduce larger error due to the truncated singular values. Table 5 shows the identified frequencies and damping factors for the case where only 36 singular values are kept. The data used in Case 6 has a sampling rate of 128 Hz, and the data used in Case 7 has a sampling rate of 64 Hz. The modes that are not identified in each case are marked with the symbol "\_" in Table 5. In Case 6, the lower frequency modes 1 and 2 can not be identified. Because of additional error introduced by the truncated singular values, when compared with the results in Cases 1 and 2, several modes can not be identified. These are modes number 2 and 18 in Case 6 and modes number 2, 11, and 15 in Case 7. In this case, the real-valued realizations of the MRTD and MMRTD methods also give the same system matrices as the output-normal and input-normal realizations of the ERA to 12 decimal places, respectively. The input-normal, output-normal, and internally balanced are equivalent to 11 decimal places.

Table 5: Identified frequencies and damping factors using test data from the HMB-2R structure by keeping 36 singular values

Mode No.	Case 6 $\Delta t = \frac{1}{128}(\text{sec})$		Case 7 $\Delta t = \frac{1}{64}(\text{sec})$	
	Freq. (Hz)	Damping Factor	Freq. (Hz)	Damping Factor
1	-	-	0.85	0.051
2	-	-	-	-
3	3.51	0.004	3.51	0.004
4	4.64	0.006	4.65	0.005
5	4.85	0.013	5.01	0.008
6	7.43	0.004	7.42	0.004
7	-	-	9.79	0.006
8	10.18	0.003	10.19	0.002
9	10.48	0.022	11.06	0.003
10	12.12	0.002	12.14	0.004
11	-	-	-	-
12	13.24	0.011	13.30	0.002
13	13.33	0.004	13.48	0.0002
14	16.04	0.002	16.04	0.002
15	-	-	-	-
16	22.26	0.002	22.28	0.002
17	25.35	0.003	25.31	0.001
18	-	-	25.78	0.003
19	38.21	0.001		
20	38.62	0.009		

## **Chapter 7**

### **Summary and Conclusions**

#### **7.1 Summary**

Chapter 2 presents a review of basic mathematical preliminaries in connection with the system identification problem presented in this thesis. The state space model description for linear system is reviewed. Relationships between discrete and continuous-time models are derived. The Markov parameters and various ways of determining the Markov parameters are explained. The Hankel matrix often used in several minimal realization techniques is simply a matrix of Markov parameters. The concept of controllability and observability grammians, which are later used to relate various different realizations, is explained.

Chapter 3 presents three system realizations of the Eigensystem Realization Algorithm using finite Hankel matrices. The Eigensystem Realization Algorithm uses the singular value decomposition of the Hankel matrix to determine a minimal realization. There are several ways to factor the Hankel matrix into controllability and observability matrices. Different choices of controllability and observability matrices results in different but equivalent realizations. When the number of columns and rows of the Hankel matrix

tend to infinity, for an asymptotically stable system, the three realizations of the Eigensystem Realization Algorithm converge to the input-normal, output-normal, and internally balanced forms.

Chapter 4 presents the original Ibrahim time domain method which did not use the singular values decomposition to reduce the size of the eigenvalue problem. The Multiple-Reference Time Domain and Modified Multiple-Reference Time Domain methods are also presented. Both methods are traditionally formulated in the complex modal space and used to determine the modal parameters of the system such as damping factors, frequencies, mode shapes, and modal participation factor matrix. These methods also use the singular value decomposition to compute the minimal order realizations. Equivalent real-valued realizations of the Multiple-Reference Time Domain and the Modified Multiple-Reference Time Domain methods are derived.

Chapter 5 presents the transformation matrices between different equivalent realizations in previous chapters. We show that the real-valued realizations of the Multiple-Reference Time Domain and the Modified Multiple-Reference Time Domain methods are the same as the output-normal and input-normal realizations of the Eigensystem Realization Algorithm, respectively. We also show that the realizations can be transformed from one to the other by transformation matrices.

In Chapter 6, the theoretical comparisons are verified by examples using both simulated and actual test data. From the same Hankel matrix, the three realizations, which are input-normal, output-normal, and internally balanced, are equivalent because they produce the same Markov parameters. The simulation examples use a system with the closely spaced frequencies and mode shapes. The test example uses experimental data obtained from a large flexible structure (HMB-2R).

## 7.2 Conclusions

Based on this thesis, the following conclusions are made:

- (1) Three realizations of the Eigensystem Realization Algorithm converge to the input-normal, output-normal, and internally balanced forms in the limit as the size of the Hankel matrix tends to infinity. Consequently, in the case of the finite Hankel matrix, these realizations are mathematically equivalent in the sense that they produce the same Markov parameters. As a result, they produce the same damping factors, frequencies, and mode shapes.
- (2) The real-valued realization of the Multiple-Reference Time Domain is mathematically the same as the output-normal realization of the Eigensystem Realization Algorithm. In the examples using simulated data and test data shown in this thesis, the real-valued realization of the Multiple-Reference Time Domain is numerically the same as the output-normal realization of the Eigensystem Realization Algorithm up to 12 significant digits.
- (3) The real-valued realization of the Modified Multiple-Reference Time Domain method is mathematically the same as the input-normal realization of the Eigensystem Realization Algorithm. In the examples using simulated data and test data shown in this thesis, the real-valued realization of the Modified Multiple-Reference Time Domain method is numerically the same as the input-normal realization of the Eigensystem Realization Algorithm up to 12 significant digits.
- (4) The singular value decomposition is an important step in obtaining a minimal order realization. In fact, the Multiple-Reference Time Domain, Modified Multiple-

Reference Time Domain, and Eigensystem Realization Algorithm realizations are equivalent because all of them use the Hankel matrix and the singular value decomposition in obtaining a state space realization. In fact, the singular value decomposition was previously used in realization theory on which the Eigensystem Realization Algorithm formulation is based.

- (5) The state space model of the internally balanced realization is better conditioned numerically and is the recommended approach .

## Appendix A

### General Response of Linear System by Modal Analysis

This appendix is adapted from Ref. 25. The second order equation of motion for a linear time-invariant dynamic system is

$$m\ddot{q}(t) + c_d\dot{q}(t) + kq(t) = F_f u(t) \quad (\text{A.1})$$

where  $m$ ,  $c_d$ , and  $k$  are the mass, damping, and stiffness matrices, respectively. The vectors  $q(t)$  and  $F_f u(t)$  are the generalized coordinates and forces, respectively. First, consider the undamped case,

$$m\ddot{q}(t) + kq(t) = F_f u(t) \quad (\text{A.2})$$

Equation. (A.2) is a set of simultaneous linear second-order ordinary differential equations with constant coefficients. The  $m$  and  $k$  matrices are symmetric, non-negative definite and usually not diagonal matrices. For a given mass matrix  $m$ , and stiffness matrix  $k$ , there exists a linear transformation

$$q(t) = V\eta(t) \quad (\text{A.3})$$

where  $V$  is a constant nonsingular square transformation matrix such that the equations of motion in Eq. (A.2) become uncoupled in the new coordinates  $\eta(t)$ . Since  $V$  is a constant matrix, we also have

$$\dot{q}(t) = V\dot{\eta}(t) \quad , \quad \ddot{q}(t) = V\ddot{\eta}(t) \quad (\text{A.4})$$

Substituting Eqs. (A.3) and (A.4) into Eq. (A.2) yields

$$mV\ddot{\eta}(t) + kV\eta(t) = F_f u(t) \quad (\text{A.5})$$

Premultiplying both sides of Eq. (A.5) by  $V^T$ , one obtains

$$M\ddot{\eta}(t) + K\eta(t) = N(t) \quad (\text{A.6})$$

where

$$M = V^T m V = M^T \quad , \quad K = V^T k V = K^T$$

The matrices  $M$  and  $K$  are diagonal and symmetric.  $N(t) = V^T F_f u(t)$  is an  $N$ -dimensional vector whose elements are the forces  $N_i$  associated with the coordinates  $\eta_i$ . Equation (A.6) presents a set of  $N$  independent equations of motion. The transformation matrix  $V$  is found by solving an eigenvalue problem corresponding to the free vibration case of Eq. (A.2). The eigenvalue problem in the matrix form is

$$k v = \omega^2 m v$$

where  $\omega^2$  and  $v$  are eigenvalues and eigenvectors, respectively. The eigenvalues  $\omega^2$  are determined from the following characteristic equation or frequency equation

$$\Delta(\omega^2) = |k - \omega^2 m| = 0$$

It has roots  $\omega_1^2, \omega_2^2, \dots, \omega_N^2$ . The square roots of these eigenvalues are the system natural frequencies  $\omega_r$  ( $r = 1, 2, \dots, N$ ). Assuming that the eigenvalue problem is non-defective, i. e., every eigenvalue has an independent eigenvector, corresponding to each eigenvalue  $\omega_r$  is an eigenvector  $v_r$ ,

$$k v_r = \omega_r^2 m v_r \quad r = 1, 2, \dots, N$$

The vector  $v_r$  is also called modal vector or natural mode. The shape of the natural mode is unique, but the amplitude is not. The modal vector  $v_r$  is usually normalized, such that

$$\bar{v}_r^T m \bar{v}_r = 1, \quad \bar{v}_r^T k \bar{v}_r = \omega_r^2$$

or

$$\bar{V}^T m \bar{V} = I, \quad \bar{V}^T k \bar{V} = \Omega$$

where  $\Omega = \text{diag}(\omega_1^2, \omega_2^2, \dots, \omega_N^2)$ , and the matrix  $\bar{V}$  is made up of the normalized modal vectors  $\bar{v}_r$ ,  $r = 1, 2, \dots, N$ . After normalization, the vectors  $\bar{v}_r$  are called normal modes and  $\bar{V}$  is a constant non-singular square transformation matrix. Consider the linear transformation

$$q(t) = \bar{V} \eta(t) \tag{A.7}$$

Because  $\bar{V}$  is a constant matrix, we also have  $\ddot{q}(t) = \bar{V} \ddot{\eta}(t)$ . Therefore, Eq. (A.2) can be expressed as

$$\ddot{\eta}(t) + \Omega \eta(t) = N(t) \tag{A.8}$$

where  $N(t) = \bar{V}^T F_f u(t)$  is an  $N$ -dimensional vector of generalized forces associated with the vector of generalized coordinates  $\eta(t)$ . Equation (A.8) can be rewritten with normal modes as

$$\ddot{\eta}_r(t) + \omega_r^2 \eta_r(t) = N_r(t) \quad r = 1, 2, \dots, N \quad (\text{A.9})$$

where  $\eta_r(t)$  are the system normal coordinates and  $N_r(t)$  are generalized forces in the normal coordinates. The solution of the Eq. (A.9) is

$$\begin{aligned} \eta_r(t) = & \frac{1}{\omega_r} \int_0^t N_r(\tau) \sin \omega_r(t - \tau) d\tau + \eta_r(0) \cos \omega_r t \\ & + \frac{\dot{\eta}_r(0)}{\omega_r} \sin \omega_r t \quad r = 1, 2, \dots, N \end{aligned} \quad (\text{A.10})$$

where  $\eta_r(0)$  and  $\dot{\eta}_r(0)$  are the initial generalized displacements and velocities, respectively.

We now return to the damped dynamic system given in Eq. (A.8). Using the same transformation matrix in Eq. (A.7), Eq. (A.8) becomes

$$\ddot{\eta}(t) + [C_d] \dot{\eta}(t) + \Omega \eta(t) = N(t) \quad (\text{A.11})$$

where

$$[C_d] = \bar{V}^T C_d \bar{V}$$

is an  $N \times N$  symmetric matrix, generally nondiagonal. In the special case in which  $c_d$  is a linear combination of the matrix  $m$  and  $k$ , i.e.,

$$c_d = \alpha m + \beta k \quad (\text{A.12})$$

where  $\alpha$  and  $\beta$  are constants, the matrix  $[C_d]$  becomes diagonal

$$C_d = \alpha I + \beta \Omega$$

Therefore, Eq. (A.11) becomes an uncoupled set of equations. The case given in Eq. (A.12) is known as proportional damping. Let

$$C_d = \text{diag}(2\zeta_1\omega_1, 2\zeta_2\omega_2, \dots, 2\zeta_N\omega_N)$$

then the independent set of equations can be rewritten as

$$\ddot{\eta}_r(t) + 2\zeta_r\omega_r\dot{\eta}_r(t) + \omega_r^2\eta_r(t) = N_r(t) \quad r=1, 2, \dots, N$$

which has a solution of the form

$$\eta_r(t) = \frac{1}{\omega_{dr}} \int_0^t N_r(\tau) e^{-\zeta_r\omega_r(t-\tau)} \sin \omega_{dr}(t-\tau) d\tau + e^{-\zeta_r\omega_r t} \left[ \frac{\eta_r(0)}{(1-\zeta_r^2)^{1/2}} \cos(\omega_{dr} - \varphi_r) + \frac{\dot{\eta}_r(0)}{\omega_{dr}} \sin \omega_{dr} t \right]$$

where

$$\omega_{dr} = (1 - \zeta_r^2)^{1/2} \omega_r \quad \varphi_r = \tan^{-1} \frac{\zeta_r}{(1 - \zeta_r^2)^{1/2}}$$

$\omega_{dr}$  and  $\varphi_r$  are the damped frequency and a phase angle of the the  $r$ -th mode, respectively.

## Appendix B

### The Generalized Inverse

#### B.1. Definition of the (Moore-Penrose) Generalized Inverse

Let  $M$  be an  $m \times n$  matrix. Then there exists a unique  $n \times m$  matrix  $M^+$  is called the (Moore-Penrose) generalized inverse of  $M$  if and only if the following three statements are true<sup>26</sup>:

- (i)  $MM^+M = M$ ;
- (ii)  $M^+MM^+ = M^+$ ;
- (iii)  $MM^+$  and  $M^+M$  are hermitian.

#### B.2 The Singular Value Decomposition as a Method to Calculate the Generalized Inverse

This appendix is adapted from Ref. 27. Let  $M$  be an arbitrary real matrix of dimension  $m \times n$ . Then there exist the orthonormal matrices  $P$  and  $Q$  of dimensions  $m \times m$  and  $n \times n$ , respectively such that

$$M = P \begin{bmatrix} \Sigma_1 & 0 \\ 0 & 0 \end{bmatrix}_{m \times n} Q^T$$

where

$$\Sigma_1 = \text{diagonal}[\sigma_1, \sigma_2, \dots, \sigma_r]$$

is a diagonal matrix of the positive singular values,  $\sigma_i, i = 1, 2, \dots, r$ . Furthermore,

$$P^T = P^{-1}, \quad Q^T = Q^{-1}$$

The orthogonal column vectors of  $P$ ,

$$P = [p_1, p_2, \dots, p_m]_{m \times m}$$

are called the left singular vectors of  $M$ . The orthogonal column vectors of  $Q$ ,

$$Q = [q_1, q_2, \dots, q_n]_{n \times n}$$

are called the right singular vectors of  $M$ . If  $P$  is partitioned such that  $P_1$  has  $r$  orthogonal columns  $p_1, p_2, \dots, p_r$ , and  $P_2$  has  $(m-r)$  orthogonal columns  $p_{r+1}, \dots, p_m$ , and  $Q$  is partitioned such that  $Q_1$  has  $r$  orthogonal columns  $q_1, q_2, \dots, q_r$ , and  $Q_2$  has  $(n-r)$  orthogonal columns  $q_{r+1}, \dots, q_n$ , i. e.,

$$P = [P_1, P_2], \quad Q = [Q_1, Q_2]$$

then

$$\begin{aligned} M &= P \Sigma Q^T = [P_1, P_2] \begin{bmatrix} \Sigma_1 & 0 \\ 0 & 0 \end{bmatrix} \begin{bmatrix} Q_1^T \\ Q_2^T \end{bmatrix} \\ &= P_1 \Sigma_1 Q_1^T \end{aligned}$$

### B.3. Least Squares Solution and the Generalized Inverse

Consider the problem of finding  $x$  from the equation

$$Mx = d$$

where  $M$  and  $d$  are given. The solution  $\hat{x}$  that minimizes the norm-squared error

$$\|M\hat{x} - d\|^2$$

is called the least squares solution of equation  $Mx = d$ . The solution

$$x^* = Q\Sigma_1^{-1}P_1^T d$$

will minimize the norm-squared error and also is the solution  $\hat{x}$  of minimum norm itself; that is,  $\|x^*\| < \|\hat{x}\|$  for all  $\hat{x} \neq x^*$ . The solution  $x^*$  is also called the generalized or pseudoinverse solution of the linear equation  $Mx = d$ , and the quantity  $M^+$ ,

$$M^+ = Q\Sigma_1^{-1}P_1^T$$

is the generalized or pseudoinverse solution of the matrix  $M$ . If  $M$  is of full column rank, i.e., its rank is equal to the number of columns, then

$$M = P\Sigma Q^T = [P_1, P_2] \begin{bmatrix} \Sigma_1 \\ 0 \end{bmatrix} Q^T = P_1 \Sigma_1 Q^T$$

and

$$M^+ = Q\Sigma_1^{-1}P_1^T$$

Since  $P_1^T P_1 = I$  and  $Q^T = Q^{-1}$ , we obtain

$$M^+M = I$$

Similarly, If  $M$  is of full row rank, i.e., its rank is equal to the number of rows, then

$$M = P\Sigma Q^T = P[\Sigma_1, 0] \begin{bmatrix} Q_1^T \\ Q_2^T \end{bmatrix} = P\Sigma_1 Q_1^T$$

and

$$M^+ = Q_1 \Sigma_1^{-1} P^T$$

Since  $Q_1^T Q_1 = I$  and  $P^T = P^{-1}$ , we have

$$MM^+ = I$$

## Appendix C

### Real Realization from Complex Realization

In some time domain modal identification methods, the recovered models are complex. It is sometimes of interest to convert the complex model to an equivalent real model. To develop the necessary transformation, consider first the simple case of a single-input two-output system with two modes. The general case for a multiple-input multiple-output system with several modes follows similarly.

#### C.1. Single Input Two Output System with Two Modes

For a single-input, two-output, two-mode system, the complex mode shapes  $\Psi_c$ , and modal participation matrix  $L_c$  take the form

$$\Psi_c = \begin{bmatrix} \psi_{11} & \psi_{11}^* & \psi_{12} & \psi_{12}^* \\ \psi_{21} & \psi_{21}^* & \psi_{22} & \psi_{22}^* \end{bmatrix}, \quad L_c = \begin{bmatrix} \ell_{c1} \\ \ell_{c1}^* \\ \ell_{c2} \\ \ell_{c2}^* \end{bmatrix}$$

where  $\psi_{jk} = r_{jk} e^{i\varphi_{jk}}$ . The integer  $j$  and  $k$  denote the  $j$ -th output and  $k$ -th mode of the system, respectively. The subscript  $c$  denotes complex matrix. The superscript  $*$  denotes the complex conjugate and  $\varphi_{jk}$  is the phase angle of the complex number  $\psi_{jk}$ .

and the complex system matrix  $\Lambda_c$  is

$$\Lambda_c = \begin{bmatrix} e^{\lambda_1 \Delta t} & 0 & 0 & 0 \\ 0 & e^{\lambda_1^* \Delta t} & 0 & 0 \\ 0 & 0 & e^{\lambda_2 \Delta t} & 0 \\ 0 & 0 & 0 & e^{\lambda_2^* \Delta t} \end{bmatrix}$$

where

$$\lambda_k = \left( -\zeta_k \pm j\sqrt{1 - \zeta_k^2} \right) \omega_k$$

and  $\omega_k$  is the natural frequency of the  $k$ -th mode. To convert the above complex realization to a real realization, the following transformation matrix can be used

$$T = \begin{bmatrix} T_1 & 0 \\ 0 & T_2 \end{bmatrix}, \quad T_k = \begin{bmatrix} e^{i\varphi_k} & e^{-i\varphi_k} \\ -ie^{i\varphi_k} & ie^{-i\varphi_k} \end{bmatrix}, \quad k = 1, 2$$

Straight forward algebra leads to the real representation  $\Psi_r, \Lambda_r, L_r$

$$\Psi_r = \Psi_c T^{-1}$$

$$= \begin{bmatrix} r_{11} & 0 & r_{12} & 0 \\ r_{21} \cos(\varphi_{21} - \varphi_{11}) & -r_{21} \sin(\varphi_{21} - \varphi_{11}) & r_{22} \cos(\varphi_{22} - \varphi_{12}) & -r_{22} \sin(\varphi_{22} - \varphi_{12}) \end{bmatrix}$$

and

$$\Lambda_r = T \Lambda_c T^{-1}$$

$$= \begin{bmatrix} e^{\sigma_1 \Delta t} \cos \omega_{d1} \Delta t & -e^{\sigma_1 \Delta t} \sin \omega_{d1} \Delta t & 0 & 0 \\ e^{\sigma_1 \Delta t} \sin \omega_{d1} \Delta t & e^{\sigma_1 \Delta t} \cos \omega_{d1} \Delta t & 0 & 0 \\ 0 & 0 & e^{\sigma_2 \Delta t} \cos \omega_{d2} \Delta t & -e^{\sigma_2 \Delta t} \sin \omega_{d2} \Delta t \\ 0 & 0 & e^{\sigma_2 \Delta t} \sin \omega_{d2} \Delta t & e^{\sigma_2 \Delta t} \cos \omega_{d2} \Delta t \end{bmatrix}$$

where  $\Lambda_r$  is a real matrix,  $\sigma_k = -\zeta_k \omega_k$ , and  $\omega_{dk} = (\sqrt{1 - \zeta_k^2}) \omega_k$ . Define  $\ell_{ck} = \ell_k e^{i\theta_k}$ ,  $k = 1, 2$ , where  $\theta_k$  is the phase angle of the complex number  $\ell_{ck}$ . Hence, the real participation matrix  $L_r$  is

$$L_r = TL_c = \begin{bmatrix} 2\ell_1 \cos(\varphi_{11} + \theta_1) \\ 2\ell_1 \sin(\varphi_{11} + \theta_1) \\ 2\ell_2 \cos(\varphi_{12} + \theta_2) \\ 2\ell_2 \sin(\varphi_{12} + \theta_2) \end{bmatrix}$$

The Markov parameters can be expressed in terms of the real state space representation  $(\Lambda_r, L_r, \Psi_r)$  as

$$Y(k) = \Psi_r (\Lambda_r)^k L_r \quad (\text{C.1})$$

If the mode shapes are normal modes, then  $\varphi_{21} = \varphi_{11}$  and  $\varphi_{22} = \varphi_{12}$ . The mode shape matrix in Eq. (C.1) becomes

$$\Psi_r = \begin{bmatrix} r_{11} & 0 & r_{12} & 0 \\ r_{21} & 0 & r_{22} & 0 \end{bmatrix}$$

## C.2. Single-Input Multiple-Output (SIMO) System with Multiple Modes

For the single-input multiple-output system with several modes, the conversion from the complex realization to a real realization can be derived similarly. The complex system matrix  $\Lambda_c$ , mode shapes matrix  $\Psi_c$ , and modal participation matrix  $L_c$  are

$$\Lambda_c = \begin{bmatrix} \begin{bmatrix} e^{\lambda_1 \Delta t} & 0 \\ 0 & e^{\lambda_1^* \Delta t} \end{bmatrix} & & & \\ & \begin{bmatrix} e^{\lambda_2 \Delta t} & 0 \\ 0 & e^{\lambda_2^* \Delta t} \end{bmatrix} & & \\ & & \begin{bmatrix} e^{\lambda_3 \Delta t} & 0 \\ 0 & e^{\lambda_3^* \Delta t} \end{bmatrix} & \\ & & & \ddots \end{bmatrix}$$

and

$$\Psi_c = \begin{bmatrix} \psi_{11}, & \psi_{11}^*, & \psi_{12}, & \psi_{12}^*, & \dots \\ \psi_{21}, & \psi_{21}^*, & \psi_{22}, & \psi_{22}^*, & \dots \\ \psi_{31}, & \psi_{31}^*, & \psi_{32}, & \psi_{32}^*, & \dots \\ \vdots & \vdots & \vdots & \vdots & \vdots \end{bmatrix}, \quad L_c = \begin{bmatrix} \ell_{c1} \\ \ell_{c1}^* \\ \ell_{c2} \\ \ell_{c2}^* \\ \vdots \end{bmatrix}$$

Define the transformation matrix  $T$

$$T = \begin{bmatrix} T_1 & 0 & 0 & & \\ 0 & T_2 & 0 & & \\ 0 & 0 & T_3 & & \\ & & & \ddots & \end{bmatrix} \quad \text{where} \quad T_k = \begin{bmatrix} e^{i\varphi_{1k}} & e^{-i\varphi_{1k}} \\ -ie^{i\varphi_{1k}} & ie^{-i\varphi_{1k}} \end{bmatrix}$$

where  $\psi_{jk} = r_{jk} e^{i\varphi_{jk}}$  with  $j$ -th output and  $k$ -th mode,  $T_k$  is a  $2 \times 2$  transformation matrix with  $k$ -th mode,  $\ell_{ck}$  is the complex modal participation with  $k$ -th mode. Similarly, straight forward algebra leads to the real system matrix, real mode shapes matrix, and real modal participation matrix,

$$\Lambda_r = T\Lambda_c T^{-1}$$

$$= \begin{bmatrix} \begin{bmatrix} e^{\sigma_1 \Delta t} \cos \omega_{d1} \Delta t & -e^{\sigma_1 \Delta t} \sin \omega_{d1} \Delta t \\ e^{\sigma_1 \Delta t} \sin \omega_{d1} \Delta t & e^{\sigma_1 \Delta t} \cos \omega_{d1} \Delta t \end{bmatrix} & & & \\ & \begin{bmatrix} e^{\sigma_2 \Delta t} \cos \omega_{d2} \Delta t & -e^{\sigma_2 \Delta t} \sin \omega_{d2} \Delta t \\ e^{\sigma_2 \Delta t} \sin \omega_{d2} \Delta t & e^{\sigma_2 \Delta t} \cos \omega_{d2} \Delta t \end{bmatrix} & & \\ & & \ddots & \\ & & & \ddots \end{bmatrix} \quad (\text{C.2})$$

$$\Psi_r = \Psi_c T^{-1}$$

$$= \begin{bmatrix} r_{11} & 0 & r_{12} & 0 & \cdots \\ r_{21} \cos(\varphi_{21} - \varphi_{11}) & -r_{21} \sin(\varphi_{21} - \varphi_{11}) & r_{22} \cos(\varphi_{22} - \varphi_{12}) & -r_{22} \sin(\varphi_{22} - \varphi_{12}) & \cdots \\ r_{31} \cos(\varphi_{31} - \varphi_{11}) & -r_{31} \sin(\varphi_{31} - \varphi_{11}) & r_{32} \cos(\varphi_{32} - \varphi_{12}) & -r_{32} \sin(\varphi_{32} - \varphi_{12}) & \cdots \\ \vdots & \vdots & \vdots & \vdots & \cdots \end{bmatrix} \quad (\text{C.3})$$

and

$$L_r = TL_c = \begin{bmatrix} 2l_1 \cos(\varphi_{11} + \theta_1) \\ 2l_1 \sin(\varphi_{11} + \theta_1) \\ 2l_2 \cos(\varphi_{12} + \theta_2) \\ 2l_2 \sin(\varphi_{12} + \theta_2) \\ 2l_3 \cos(\varphi_{13} + \theta_3) \\ 2l_3 \sin(\varphi_{13} + \theta_3) \\ \vdots \end{bmatrix} \quad (\text{C.4})$$

### C.3. Multiple-Input Multiple-Output (MIMO) System with Multiple Modes

For a system with many inputs, the modal participation matrix is of the form

$$L_c = \begin{bmatrix} l_{c11} & l_{c12} & \cdots \\ l_{c11}^* & l_{c12}^* & \cdots \\ l_{c21} & l_{c22} & \cdots \\ l_{c21}^* & l_{c22}^* & \cdots \\ \vdots & \vdots & \vdots \end{bmatrix}$$

The same procedure can be applied for each column of  $L_c$  corresponding to each input. The results are then combined to obtain a real modal participation matrix for the multiple-input system. Note that the system matrix and the mode shape matrix are not affected by this procedure.

## References

- [1] Chen, C. T., Introduction to Linear System Theory, Holt, Rienhart and Winston, Inc., New York, 1970.
- [2] Gilbert, E. G., "Controllability and Observability in Multi-Variable Control Systems," *SIAM J. Control*, Vol. 1, No. 1, pp. 128-151, 1963.
- [3] Kalman, R. E., "Mathematical Description of Linear Dynamical Systems," *SIAM J. Control*, Vol. 1, pp. 152-192, 1963.
- [4] Ho, B. L. and Kalman, R. E., "Effective Construction of Linear State-Variable Models From Input/Output Data," *Proc. 3rd Ann. Allerton Conf. Circuit and System Theory*, 1965, pp. 449-459; also *Regelungstech*, Vol. 14, pp. 545-548, 1966.
- [5] Tether, A., "Constructions of Minimum Linear State Variable Models From Input / Output Data," *IEEE Trans. on Auto. Contr.*, Vol. AC-15, No. 4, pp. 427-436, Aug. 1970.
- [6] Silverman, L. M., "Realization of Linear Dynamical Systems," *IEEE Trans. on Auto. Contr.*, 16, 554, 1971.
- [7] Rossen, R. H. and Lapidus, L., "Minimum Realizations and System Modeling. I. Fundamental Theory and Algorithms," *AICHE Journal*, Vol. 18, No. 4, pp. 673-684, July 1972.
- [8] Zeiger, H. P. and McEwen, A. J., "Approximate Linear Realizations of Given Dimension Via Ho's Algorithm," *IEEE Trans. Automatic Contr.*, Vol. 19, 153, 1974.
- [9] Kung, S., "A New Identification and Model Reduction Algorithm Via Singular Value Decomposition," *12th Asilomar Conf., Circuits, Systems and Computers*, Nov. 6-8, 1978.
- [10] Golub, G. H. and Reinsch, C., "Singular Value Decomposition and Least Squares Solutions," *Numer. Math*, Vol. 14, pp. 403-420.
- [11] Kelma, V. C. and Laub, A. J., "The Singular Value Decomposition: Its Computation and Some Application," *IEEE Trans. on Auto. Contr.*, Vol. AC-25, No. 2, pp. 164-176, April 1980.
- [12] Juang, J. N. and Pappa, R. S., "An Eigensystem Realization Algorithm (ERA) for Modal Parameter Identification and Model Reduction," *Journal of Guidance, Control, and Dynamics*, Vol. 8, No. 5, pp. 620-627, Sept. - Oct. 1985.
- [13] Juang, J. N. and Lew, J. S., "Integration of System Identification and Robust Controller Designs for Flexible Structures in Space," *AIAA Guidance, Control and Navigation Conference*, Aug. 1990.

- [14] Juang, J. N., "Mathematical Correlation of Modal-Parameter-Identification Methods Via System-Realization Theory." Journal of Modal Analysis, Nov. 1986.
- [15] Graupe, D., Identification of System, R.E. Krieger Publishing Co., Malabar, FL., 1976
- [16] Ibrahim, S. R. and Mikulcik, E. C., "A Method for the Direct Identification of Vibration Parameters from the Free Response," Shock and Vibration Bulletin, Vol. 47, Part 4, pp. 183-198, Sep. 1977.
- [17] Allemang, R. J. and Brown, D. L., "Experimental Modal Analysis and Dynamic Component Synthesis," AFWAU-TR-87-3069, Vol. III., Dec. 1987.
- [18] Gold, R. R. and Friedman, I. P., "MIE Ground Test Simulations, Methods Development," Dynamic Engineering, Inc., Report No. D444, To be Published June 1992.
- [19] Wiberg, D. M., State Space and Linear Systems, McGraw-Hill Book Company, 1971.
- [20] Herber, P. Neff, Jr., Continuous and Discrete Linear Systems, Harper and Row, Publishers, Inc., New York, pp. 81-83, 1984.
- [21] Longman, R. W., Juang, J. N., and Phan, M., "Input and Output Matrices in Modal Identification," Society for Experimental Mechanics, Proceedings of the 9th International Modal Analysis Conference, Florence, Italy, April 1991.
- [22] Moore, B. C., "Singular Value Analysis of Linear Systems, parts I, II," Dep. Elec. Eng., Univ. Toronto, Toronto, Ont., Syst. Contr. Rep. 7801 and 7802, July 1978; also in Proc. IEEE Conf. Dec. Contr., pp. 66-73.
- [23] Moore, B. C., "Principal Component Analysis in Linear Systems: Controllability, Observability, and Model Reduction," IEEE Trans. on Automatic Control, Vol., AC-26, No. 1, Feb. 1981.
- [24] Laub, A. J. and Little, J. N., Control System Toolbox for use with PC-MATLAB, User's Guide, The MathWorks, Inc.
- [25] Meirovitch, L., Elements of Vibration Analysis, McGraw-Hill Book Company, pp. 145-199.
- [26] Noble, B. and Daniel, J. W., Applied Linear Algebra, Prentic-Hall, Inc., pp. 338-340, 1969.
- [27] Reid, J. G., Linear System Fundamentals Continuous and Discrete, Classic and Modern, McGraw-Hill Book Company, pp. 451-456, 1983.

